PeV Scale Dark Skyrmions

A Thesis Submitted to the
College of Graduate and Postdoctoral Studies
in Partial Fulfillment of the Requirements
for the degree of Master of Science
in the Department of Physics and Engineering Physics
University of Saskatchewan
Saskatoon

By
Madeline Berezowski

Permission to Use

In presenting this thesis in partial fulfillment of the requirements for a Postgraduate degree from the University of Saskatchewan, I agree that the Libraries of the University may make it freely available for inspection. I further agree that permission for copying of this thesis in any manner, in whole or in part, for scholarly purposes may be granted by the professor or professors who supervised my thesis work or, in their absence, by the Head of the Department or the Dean of the College in which my thesis work was done. It is understood that any copying or publication or use of this thesis or parts thereof for financial gain shall not be allowed without my written permission. It is also understood that due recognition shall be given to me and to the University of Saskatchewan in any scholarly use which may be made of any material in my thesis.

Requests for permission to copy or to make other use of material in this thesis in whole or in part should be addressed to:

Head of the Department of Physics and Engineering Physics
162 Physics Building
116 Science Place
University of Saskatchewan
Saskatoon, Saskatchewan
Canada
S7N 5E2

Dean
College of Graduate and Postdoctoral Studies
116 Thorvaldson Building
110 Science Place
University of Saskatchewan
Saskatoon, Saskatchewan
Canada
S7N 5C9

Abstract

The background information relevant to understanding skyrmions and dark matter is first reviewed. PeV scale skyrmions as a coherent state of dark heavy mesons with an Anderson-Higgs portal coupling to the Standard Model are analyzed as dark matter. Their creation would have been non-thermal via a chiral phase transition in the early universe. It turns out that it does not matter whether the transition is First Order or Second Order. Constraints are put on the skyrmion parameter $g_V^2 M_S$, where g_V is the Skyrme coupling and M_S is the skyrmion mass, which indicate that it is possible for the skyrmions to be PeV scale and for $g_V \lesssim 1$. For the dark mesons to not contribute significantly to dark matter they must be TeV scale if g_{wh}, their coupling to the Anderson-Higgs field, is to be perturbative. Considering the dark skyrmions as coherent states of the dark mesons gives an expression for the skyrmion-nucleon scattering cross section in terms of g_V, g_{wh}, and M_S. Direct dark matter detection experiment results are used to constrain g_V in terms of g_{wh} for $100\text{TeV} \leq M_S \leq 10\text{PeV}$. It is possible for g_V to be of perturbative strength, especially for skyrmion masses closer to 10PeV. Future direct detection experiments will yield even more stringent constraints.

Acknowledgements

I would like to thank

- My supervisor, Professor Rainer Dick.
- The Department of Physics and Engineering Physics Secretaries, Debbie Gjertsen and Marj Granrude.
- My advisory committee, Professor Kaori Tanaka, Professor Masoud Ghezelbash, Professor Robert Green, and Professor Steven Rayan.
- My fiancé, Ryan Cooney.
- My parents, Mary and Bill Berezowski.

Contents

Permission to Use i

Abstract ii

Acknowledgements iii

Contents iv

List of Figures vi

Conventions and Notation vii

1 Introduction 1

2 Continuous Symmetry and Field Theory 2
- 2.1 Lie Groups . . . 2
  - 2.1.1 SU(2) . . . 3
- 2.2 Lagrangian Field Theory . . . 3
  - 2.2.1 Noether's Theorem . . . 3
  - 2.2.2 Quantum Field Theory . . . 4
- 2.3 Local Symmetry Transformations . . . 6

3 Spontaneous Symmetry Breaking and σ-Models 8
- 3.1 Global Spontaneous Symmetry Breaking . . . 8
- 3.2 Gauged Symmetry Breaking . . . 9
  - 3.2.1 Electroweak Symmetry Breaking . . . 10
- 3.3 Topological Defects . . . 10
  - 3.3.1 Homotopy . . . 10
  - 3.3.2 Types of Topological Defects . . . 11
- 3.4 The Linear σ-Model . . . 11
  - 3.4.1 Spontaneous Chiral Symmetry Breaking . . . 12
  - 3.4.2 Explicit Chiral Symmetry Breaking . . . 13
- 3.5 The Nonlinear σ-Model . . . 14
  - 3.5.1 Chiral Symmetry Breaking . . . 15
- 3.6 Gauged Nonlinear σ-Model . . . 16

4 Skyrmions 20
- 4.1 Stability . . . 20
- 4.2 Hedgehog Skyrmions . . . 21

5 Phase Transitions **25**
5.1 Effective Potential . . . 25
5.2 First and Second Order Phase Transitions . . . 26
5.3 First Order Phase Transitions . . . 26
5.3.1 Summary of Derivation . . . 26
5.3.2 Thin Wall Approximation . . . 28
5.3.3 Finite Temperature . . . 29
5.4 Second Order Phase Transitions . . . 30

6 Dark Matter **32**
6.1 Cosmology . . . 32
6.2 Evidence for Dark Matter . . . 35
6.3 Freeze-Out Thermodynamics . . . 37
6.4 Dark Matter Detection . . . 39

7 PeV Scale Dark Skyrmions **41**
7.1 Anderson-Higgs Portal Model . . . 41
7.2 Relic Skyrmion Density . . . 42
7.3 Constraints on the Heavy Dark Mesons . . . 45
7.4 Direct Signals from the Dark Skyrmions . . . 47

8 Conclusion **52**

Appendix A Nucleon-Dark Meson Scattering Cross Section **53**
A.1 First Order S Matrix . . . 54
A.2 Scattering Cross Section . . . 56

List of Figures

3.1 The linear σ-model potential $V(\phi_\alpha)$ . . . 12
3.2 The linear σ-model potential $V(\phi_\alpha)$, shifted coordinates . . . 13

4.1 The hedgehog skyrmion profile function . . . 24

5.1 Temperature-dependent effective potential for a few temperatures . . . 26
5.2 Relaxation time of Second Order phase transition . . . 31

6.1 X-ray image and matter distribution of the bullet cluster over visible light image (NASA/CXC/M. Weiss). . . . 36

7.1 Possible values of the skyrmion parameter for $5 \leq x_c \leq 10$. . . . 45
7.2 Constraints on dark meson mass and Anderson-Higgs portal coupling strength . . . 46
7.3 The hedgehog skyrmion profile function in k space. . . . 47
7.4 The $\boldsymbol{w}$ meson number in the coherent skyrmion state . . . 49
7.5 The skyrmion-nucleon recoil cross section for $1\text{TeV} \leq g_V^2 m_w g_{wh}^{-1} \leq 1\text{PeV}$ . . . 49
7.6 The skyrmion-nucleon recoil cross section for $100\text{TeV} \leq g_V^4 M_S g_{wh}^{-1} \leq 100\text{PeV}$ . . . 50
7.7 The XENON1T 1 ton year results [46] . . . 50
7.8 XENON1T constraints on PeV scale dark skyrmions . . . 51

Conventions and Notation

The following natural unit convention will be used,

$$\hbar = c = k_B = 1, \tag{1}$$

except in circumstances where it is noted otherwise.

Unless otherwise stated, Latin indices run from 1 to 3 and Greek indices run from 0 to 3. Indices that appear twice in a term are implicitly summed over, unless otherwise stated. In particular, a pair of repeated lower indices indicate the Euclidean inner product while a pair of upper and lower repeated indices indicate the Minkowskian inner product. A 3-vector $v^i = (v^1, v^2, v^3)$ may also be written using boldface as $\boldsymbol{v}$.

The Minkowski metric is written here as

$$\eta_{\mu\nu} = \eta^{\mu\nu} = \begin{pmatrix} 1 & 0 & 0 & 0 \\ 0 & -1 & 0 & 0 \\ 0 & 0 & -1 & 0 \\ 0 & 0 & 0 & -1 \end{pmatrix} \tag{2}$$

A contravariant 4-vector v^μ in Minkowski space is

$$v^\mu = (v^0, \boldsymbol{v}), \tag{3}$$

meaning that it transforms under a Lorentz transformation $\Lambda^\mu{}_\nu$ as

$$v^\mu \to v'^\mu = \Lambda^\mu{}_\nu v^\nu. \tag{4}$$

A covariant vector

$$v_\mu = (v^0, -\boldsymbol{v}) \tag{5}$$

transforms under the same Lorentz transformation as

$$v_\mu \to v'_\mu = (\Lambda^{-1})^\nu{}_\mu v_\nu \tag{6}$$

The inner product of two 4-vectors v^μ and w^μ in Minkowski space is

$$v^\mu w_\mu = \eta_{\mu\nu} v^\mu w^\nu. \tag{7}$$

The partial derivative is sometimes written as

$$\frac{\partial}{\partial x^\mu} = \partial_\mu. \tag{8}$$

Any other notational conventions used will be noted and explained when they first appear.

Chapter 1

Introduction

Dark matter is a mysterious cosmological phenomenon which interacts only gravitationally. The term "dunkle Materie", or in English "dark matter", was coined in 1933 by F. Zwicky when he found that the Coma Cluster must have a mass much larger than the mass accounted for by only its visible components [1]. Since then, much compelling evidence for dark matter has been found in observations of the motion of and gravitational lensing due to galaxies and galaxy clusters.

Skyrmions were originally proposed as a nucleon model by T.H.R. Skyrme in 1962 [2], [3]. They are stable topological defects created from chiral symmetry breaking in the nonlinear σ-model. They are also a possible candidate for dark matter.

First a review of symmetry and symmetry breaking, especially in σ-models, is given. This leads naturally to a discussion of skyrmions themselves. As skyrmions are a type of topological defect, the phase transitions from which these defects can arise are reviewed. The nature of dark matter is then discussed.

With the relevant background information laid out, the aim of this thesis is to analyze non-thermally created PeV (peta-electron volt, or 10^{15}eV) scale skyrmions with an Anderson-Higgs portal coupling to Standard Model particles as dark matter. In comparison to the skyrmion mass scale of interest here, note that the most recent LHC run reached a maximal center of mass energy of 13TeV (or 1.3×10^{13}eV) in 2015 [4]. In this analysis, direct dark matter experimental search results are referred to in order to place constraints on these very heavy dark skyrmions.

Chapter 2

Continuous Symmetry and Field Theory

Invariance under a transformation is called symmetry. Symmetry in the Lagrangian density provides valuable information about the system in question, especially symmetry under the action of a Lie group G. If G does not depend on the spacetime location, it is called a global symmetry group. If the elements of G are spacetime-dependent, then G is a local symmetry group, and a gauge field must be introduced.

2.1 Lie Groups

A continuous transformation is one which can be written as a composition of infinitesimal transformations. A Lie group [5], [6](pp.495-504), [7](pp.49-69) G is a group of continuous transformations $U(\xi)$ which are determined by a finite set of N parameters ξ_a, $a = (1, 2, ..., N)$, and are differentiable with respect to said parameters.

An infinitesimal group element is one that is very close to the identity. Suppose, for the Lie group G, that ξ_0 is the set of parameters that determines the identity element, meaning $U(\xi_0) = 1$. Taking an infinitesimal group element $U(\delta\xi) \in G$ and Taylor expanding it about $\xi = \xi_0$ yields

$$U(\delta\xi) = U(\xi_0) + \Big(\partial_a U(\xi)\Big|_{\xi=\xi_0}\Big)\delta\xi^a + \mathcal{O}(\delta\xi^2). \tag{2.1}$$

The generators T_μ of the Lie group are defined by

$$-iT_a = \partial_a U(\xi)\Big|_{\xi=\xi_0}, \tag{2.2}$$

so that

$$U(\delta\xi) = U(\xi_0) - iT_a\delta\xi^a + \mathcal{O}(\delta\xi^2). \tag{2.3}$$

A finite group element $U(\xi)$ is obtain by taking n successive infinitesimal elements where $\delta\xi = \xi/n$ as $n \to \infty$. Ignoring the higher order terms,

$$\begin{aligned} U(\xi) &= \lim_{n\to\infty} U(\delta\xi) \\ &= \lim_{n\to\infty} \Big(1 - iT_a\frac{\xi^a}{n}\Big)^n \\ &= e^{-iT_a\xi^a}. \end{aligned} \tag{2.4}$$

Every Lie group has an associated Lie algebra which gives the generators necessary commutation relations,

$$[T_a, T_b] = if_{abc}T_c, \tag{2.5}$$

where f_{abc} is the structure constant of the Lie algebra. This means the generators also satisfy the Jacobi identity,

$$[[T_a, T_b], T_c] + [[T_b, T_c], T_a] + [[T_c, T_a], T_b] = 0. \tag{2.6}$$

2.1.1 SU(2)

The group of special (unit determinant) unitary $N \times N$ matrices, $SU(N)$, is an example of a Lie group. $SU(N)$ has $N^2 - 1$ degrees of freedom. Of particular importance here is $SU(2)$. It has $2^2 - 1 = 3$ degrees of freedom which means it has three generators T_a, $a = 1, 2, 3$. The generators must obey

$$[T_a, T_b] = i\epsilon_{abc}T^c, \tag{2.7}$$

where the structure constant ϵ_{abc} is the Levi-Civita symbol. The Pauli matrices,

$$\tau_1 = \begin{pmatrix} 0 & 1 \\ 1 & 0 \end{pmatrix}, \quad \tau_2 = \begin{pmatrix} 0 & -i \\ i & 0 \end{pmatrix}, \quad \tau_3 = \begin{pmatrix} 1 & 0 \\ 0 & -1 \end{pmatrix}, \tag{2.8}$$

satisfy this and therefore provide a basis for the corresponding Lie algebra. Note that this Lie algebra has the same structure as $SO(3)$, the group of special orthogonal matrices, which describes three-dimensional rotations.

2.2 Lagrangian Field Theory

Lagrangian field theory [7](pp.23-48) is like Lagrangian mechanics for fields. Recall that the Lagrangian, L, is the difference between the kinetic energy and the potential energy of the system which it describes. It is a function of N generalized coordinates $q_i(t)$, $i = 1, ..., N$, and their velocities, $\dot{q}_i(t)$. For field theory, the q_i are replaced by fields $\phi_i(x)$ and the $\dot{q}_i(t)$ are replaced by $\partial_\mu\phi_i(x)$, $\mu = 0, 1, 2, 3$. The Lagrangian density, $\mathcal{L}(\phi_i, \partial_\mu\phi_i)$, is defined by

$$L = \int \mathcal{L}d^3x. \tag{2.9}$$

The action is given by

$$S = \int \mathcal{L}d^3xdt = \int \mathcal{L}d^4x. \tag{2.10}$$

The principle of least action requires that the variance of the action with respect to the ϕ_i be minimized. That is,

$$\begin{aligned} 0 &= \delta S \\ &= \int \delta\mathcal{L}d^4x \\ &= \int \left(\frac{\partial\mathcal{L}}{\partial\phi_i}\delta\phi_i + \frac{\partial\mathcal{L}}{\partial(\partial_\mu\phi_i)}\delta(\partial_\mu\phi_i) \right) d^4x \\ &= \int \left(\frac{\partial\mathcal{L}}{\partial\phi_i} - \partial_\mu\Big(\frac{\partial\mathcal{L}}{\partial(\partial_\mu\phi_i)}\Big) \right) \delta\phi_i d^4x, \end{aligned} \tag{2.11}$$

where the last step used $\delta(\partial_\mu\phi_i) = \partial_\mu(\delta\phi_i)$ and integration by parts. The variation in ϕ_i is non-zero, $\delta\phi_i \neq 0$, so the other factor in the integrand must be equal to 0. This gives the equations of motion,

$$\frac{\partial\mathcal{L}}{\partial\phi_i} - \partial_\mu\Big(\frac{\partial\mathcal{L}}{\partial(\partial_\mu\phi_i)}\Big) = 0. \tag{2.12}$$

In field theories, the equations of motion are often called the field equations or the Euler-Lagrange equations.

2.2.1 Noether's Theorem

Noether's theorem says that for every continuous symmetry, there is an associated conserved current (and charge). Substituting the equations of motion, Eq. (2.12), into the variation of the Lagrangian density, it is easy to see that

$$\delta\mathcal{L} = \partial_\mu\Big(\frac{\partial\mathcal{L}}{\partial(\partial_\mu\phi_i)}\delta\phi_i\Big). \tag{2.13}$$

Recall that this is equal to zero in order to satisfy the principle of least action. Therefore there exists the conserved current

$$j^\mu = \frac{\partial \mathcal{L}}{\partial(\partial_\mu \phi_i)} \delta\phi_i, \tag{2.14}$$

so-called because $\partial_\mu j^\mu = 0$. Every conserved current also has an associated conserved charge,

$$Q = \int j^0 d^3x. \tag{2.15}$$

As an important example, consider an infinitesimal continuous transformation $x \to x + \epsilon$, for which the field $\phi(x)$ transforms via a Taylor expansion approximation as $\phi \to \phi + \epsilon^\mu \partial_\mu \phi$. The variation in the field therefore is

$$\delta\phi = \epsilon^\mu \partial_\mu \phi. \tag{2.16}$$

Substituting this into Equation (2.13) gives

$$\delta\mathcal{L} = \epsilon^\mu \partial_\nu \Big(\frac{\partial \mathcal{L}}{\partial(\partial_\nu \phi_i)} \partial_\mu \phi_i \Big). \tag{2.17}$$

The variation in the Lagrangian density can also be expressed using a Taylor expansion,

$$\delta\mathcal{L} = \epsilon^\mu \partial_\mu \mathcal{L} = \epsilon^\mu g^\nu_\mu \partial_\nu \mathcal{L}, \tag{2.18}$$

where $g_{\mu\nu}$ is the metric. Putting this all together yields

$$\delta\mathcal{L} = \partial_\mu \Big(\frac{\partial \mathcal{L}}{\partial(\partial_\mu \phi_i)} \partial_\nu \phi_i - g^\mu_\nu \mathcal{L} \Big) \epsilon^\nu. \tag{2.19}$$

This gives the definition of the energy-momentum tensor,

$$T^\mu_\nu = \frac{\partial \mathcal{L}}{\partial(\partial_\mu \phi_i)} \partial_\nu \phi_i - g^\mu_\nu \mathcal{L}. \tag{2.20}$$

Noether's theorem tells us this is a conserved quantity,

$$\partial_\mu T^\mu_\nu = 0, \tag{2.21}$$

corresponding to the conservation of energy and momentum. The fan-favourite component of $T^{\mu\nu}$ is T^{00}, the energy density.

2.2.2 Quantum Field Theory

This is a good point to briefly discuss quantum field theory [6](pp.13-76), [7](pp.109-138), [8](pp.495-515). In quantum mechanics, dynamical variables such as position and momentum are quantized and therefore are operators. For the canonical formalism of quantum field theory, the fields themselves are the quantized operators, and this is referred to as second quantization.

Klein-Gordon Fields

A spin-0 field $\phi(x) = \phi(\boldsymbol{x}, t)$ with mass m is a scalar field which satisfies the Klein-Gordon equation

$$(\partial_\mu \partial^\mu + m^2)\phi(x) = 0. \tag{2.22}$$

The field is an operator and is written as the Fourier transform of annihilation and creation operators. A real Klein-Gordon field looks like

$$\phi(x) = \int \frac{d^3k}{(2\pi)^{3/2}\sqrt{2\omega(\boldsymbol{k})}} \Big(a(\boldsymbol{k}) e^{-ikx} + a^\dagger(\boldsymbol{k}) e^{ikx} \Big), \tag{2.23}$$

where

$$\omega^2(\boldsymbol{k}) = \boldsymbol{k}^2 + m^2. \tag{2.24}$$

Note that for brevity, $kx = k_\mu x^\mu$. The creation operator $a^\dagger(\boldsymbol{k})$ creates a ϕ particle with momentum $\boldsymbol{k}$ and acts on the vacuum $|0\rangle$ as

$$a^\dagger(\boldsymbol{k})\,|0\rangle = |\boldsymbol{k}\rangle\,. \tag{2.25}$$

The annihilation operator $a(\boldsymbol{k})$ destroys a ϕ particle with momentum $\boldsymbol{k}$. It annihilates the vacuum, and it also annihilates any state that has no ϕ particle with momentum $\boldsymbol{k}$ so that

$$a(\boldsymbol{k})\,|\boldsymbol{k'}\rangle = \delta(\boldsymbol{k} - \boldsymbol{k'})\,|0\rangle\,. \tag{2.26}$$

The only non-vanishing commutation relation for the annihilation and creation operators is

$$[a(\boldsymbol{k}), a^\dagger(\boldsymbol{k'})] = \delta(\boldsymbol{k} - \boldsymbol{k'}). \tag{2.27}$$

The Hamiltonian operator is

$$H = \int d^3k\omega(\boldsymbol{k})a^\dagger(\boldsymbol{k})a(\boldsymbol{k}). \tag{2.28}$$

If the field $\phi(x)$ is a complex Klein-Gordon field then it is expressed as

$$\phi(x) = \int \frac{d^3k}{(2\pi)^{3/2}\sqrt{2\omega(\boldsymbol{k})}}\Big(a(\boldsymbol{k})e^{-ikx} + b^\dagger(\boldsymbol{k})e^{ikx}\Big), \tag{2.29}$$

where the operator $b^\dagger(\boldsymbol{k})$ creates an antiparticle with momentum $\boldsymbol{k}$ (and $b(\boldsymbol{k})$ destroys one). The antiparticle ladder operators $b(\boldsymbol{k})$ and $b^\dagger(\boldsymbol{k})$ obey the same commutation relations as the particle ladder operators with the additions

$$[a(\boldsymbol{k}), b(\boldsymbol{k'})] = [a^\dagger(\boldsymbol{k}), b(\boldsymbol{k'})] = 0. \tag{2.30}$$

The Hamiltonian operator in this case is

$$H = \int d^3k\omega(\boldsymbol{k})(a^\dagger(\boldsymbol{k})a(\boldsymbol{k}) + b^\dagger(\boldsymbol{k})b(\boldsymbol{k})). \tag{2.31}$$

Dirac Fields

A spin-1/2 field $\psi(x)$ with mass m obeys the Dirac equation

$$(i\gamma_\mu\partial^\mu - m)\psi(x) = 0, \tag{2.32}$$

where the γ_μ are 4×4 matrices known as the Dirac matrices which obey the anti-commutation relation

$$\{\gamma_\mu, \gamma_\nu\} = 2\eta_{\mu\nu}. \tag{2.33}$$

In the basis known as the Dirac basis, these matrices are

$$\gamma_0 = \begin{pmatrix} -1 & 0 \\ 0 & 1 \end{pmatrix}, \qquad \gamma_i = \begin{pmatrix} 0 & \sigma_i \\ -\sigma_i & 0 \end{pmatrix}, \tag{2.34}$$

noting that each entry is a 2×2 matrix and the σ_i are the Pauli matrices. A Dirac field takes the form

$$\psi(x) = \sum_{s=\uparrow,\downarrow} \int \frac{d^3p}{(2\pi)^{3/2}\sqrt{2\omega(\boldsymbol{p})}}\Big(a(\boldsymbol{p}, s)u(\boldsymbol{p}, s)e^{-ipx} + b^\dagger(\boldsymbol{p}, s)v(\boldsymbol{p}, s)e^{ipx}\Big), \tag{2.35}$$

where $a(\boldsymbol{p}, s)$ destroys a particle with spin s, $b^\dagger(\boldsymbol{p}, s)$ creates an antiparticle with spin s, and $u(\boldsymbol{p}, s)$ and $v(\boldsymbol{p}, s)$ can be written as

$$u(\boldsymbol{p}, 1/2) = \frac{1}{\sqrt{\omega(\boldsymbol{p}) + m}} \begin{pmatrix} \omega(\boldsymbol{p}) + m \\ 0 \\ p_3 \\ p_1 + ip_2 \end{pmatrix}, \tag{2.36}$$

$$u(\boldsymbol{p},-1/2)=\frac{1}{\sqrt{\omega(\boldsymbol{p})+m}}\begin{pmatrix}0\\ \omega(\boldsymbol{p})+m\\ p_1-ip_2\\ -p_3\end{pmatrix}, \tag{2.37}$$

$$v(\boldsymbol{p},1/2)=\frac{1}{\sqrt{\omega(\boldsymbol{p})+m}}\begin{pmatrix}p_1-ip_2\\ -p_3\\ 0\\ \omega(\boldsymbol{p})+m\end{pmatrix}, \tag{2.38}$$

$$v(\boldsymbol{p},-1/2)=\frac{1}{\sqrt{\omega(\boldsymbol{p})+m}}\begin{pmatrix}p_3\\ p_1+ip_2\\ \omega(\boldsymbol{p})+m\\ 0\end{pmatrix}. \tag{2.39}$$

Note that the adjoint of $\psi(x)$ is $\overline{\psi}(x)=\psi^\dagger(x)\gamma^0$.

The non-vanishing anti-commutation relations that the creation and annihilation operators obey are

$$\{a(\boldsymbol{p},s),a^\dagger(\boldsymbol{p}',s')\}=\{b(\boldsymbol{p},s),b^\dagger(\boldsymbol{p}',s')\}=\delta_{s,s'}\delta(\boldsymbol{p}-\boldsymbol{p}'). \tag{2.40}$$

The spinors $u(\boldsymbol{p},s)$ and $v(\boldsymbol{p},s)$ follow some helpful properties including

$$\overline{u}(\boldsymbol{p},s)u(\boldsymbol{p},s')=-\overline{v}(\boldsymbol{p},s)v(\boldsymbol{p},s')=2m\delta_{s,s'}, \tag{2.41}$$

$$\sum_s u(\boldsymbol{p},s)\overline{u}(\boldsymbol{p},s)=m1+\gamma^\mu p_\mu, \tag{2.42}$$

$$\sum_s v(\boldsymbol{p},s)\overline{v}(\boldsymbol{p},s)=-m1+\gamma^\mu p_\mu. \tag{2.43}$$

The Hamiltonian is

$$H=\sum_s\int d^3p\,\omega(\boldsymbol{k})(a^\dagger(\boldsymbol{p},s)a(\boldsymbol{p},s)+b^\dagger(\boldsymbol{p},s)b(\boldsymbol{p},s)). \tag{2.44}$$

2.3 Local Symmetry Transformations

Consider a generalized Lagrangian density for an n-component field $\phi(x)$,

$$\mathcal{L}=(\partial_\mu\phi^\dagger)(\partial^\mu\phi)-V(\phi), \tag{2.45}$$

and an $m-$parameter symmetry group G whose elements depend on space-time coordinates x_μ. Call the generators of G in the representation as T^a, $a=1,\ldots,m$. It is easy to see that the Lagrangian density is not invariant under the action of G. To achieve invariance, a few adjustments to the Lagrangian density must be made [10](pp.28-29). For starters, a gauge vector field $A_\mu=A_\mu^aT^a$ must be introduced. The gauge-covariant derivative $\mathcal{D}_\mu$ replaces the derivative ∂_μ and is defined as

$$\mathcal{D}_\mu\phi=(\partial_\mu-ieA_\mu)\phi. \tag{2.46}$$

Finally, a term $-\frac{1}{4}F^a_{\mu\nu}F^{a\mu\nu}$ must be added to the Lagrangian density, with the definition

$$F^a_{\mu\nu}=\partial_\mu A^a_\nu-\partial_\nu A^a_\mu+ef_{abc}A^b_\mu A^c_\nu, \tag{2.47}$$

where e is the gauge coupling constant and f_{abc} are the structure constants of G. Another way to express this, using $F_{\mu\nu}=F^a_{\mu\nu}T^a$, is

$$F_{\mu\nu}=\partial_\mu A_\nu-\partial_\nu A_\mu-ie[A_\mu,A_\nu]. \tag{2.48}$$

This is called Yang-Mills theory. Note that if G is abelian, then $f_{abc}=0$.

Putting this all together, the generalized gauge-covariant Lagrangian density is

$$\mathcal{L} = (\mathcal{D}_\mu \phi)^\dagger (\mathcal{D}^\mu \phi) - V(\phi) - \frac{1}{4} F^a_{\mu\nu} F^{a\mu\nu}. \tag{2.49}$$

A gauge transformation $g(x) \in G$ represented by the matrix $D(g)$ induces the transformations

$$\phi \to D(g)\phi, \tag{2.50}$$

$$A_\mu \to D(g) A_\mu D^{-1}(g) + \frac{i}{e} D(g) \partial_\mu D(g), \tag{2.51}$$

$$\mathcal{D}_\mu \phi \to D(g) \mathcal{D}_\mu \phi, \tag{2.52}$$

$$F_{\mu\nu} \to D(g) F_{\mu\nu} D^{-1}(g). \tag{2.53}$$

Chapter 3

Spontaneous Symmetry Breaking and σ-Models

Spontaneous symmetry breaking [6](pp.351-352), [7](pp.187-208), [10](pp.23-30) occurs when a field has a non-zero vacuum expectation value. If the symmetry is global, spontaneous symmetry breaking results in massless Nambu-Goldstone bosons. If the symmetry is local, spontaneous symmetry breaking causes the gauge field to "eat" the Nambu-Goldstone bosons and become massive.

Chiral symmetry and its breaking [11](pp.123-155) is exhibited by σ-models. The linear σ-model involves global chiral symmetry. When this symmetry is spontaneously broken, the new set of ground states is called the chiral sphere. The chiral sphere gives a nonlinear realization of the σ-model, which can be expressed using an exponential parametrization. Gauged chiral symmetry breaking in the nonlinear σ-model [11](pp.261-283) leads to the Skyrme Lagrangian.

3.1 Global Spontaneous Symmetry Breaking

To understand spontaneous symmetry breaking, the Lagrangian density of the system in question must be analyzed. The generalized Lagrangian density for an n-component field $\phi(x)$ can be expressed as

$$\mathcal{L} = (\partial_\mu \phi^\dagger)(\partial^\mu \phi) - V(\phi), \tag{3.1}$$

where $V(\phi)$ is the potential of the field. Suppose the Lagrangian density is invariant under the action of an $m-$parameter Lie group G. It will initially be assumed that G is a global Lie group, meaning that its elements do not depend on space-time. A transformation under the action of an element $g \in G$ can be represented as

$$\phi_i \to \phi_i' = e^{-iw_a T^a_{ij}\phi_j} = D_{ij}(g)\phi_j, \tag{3.2}$$

where the w^a are the parameters of the Lie group and the T^a are its generators in the representation, $a = 1, \ldots, m$. The $n \times n$ matrix $D(g)$ represents g.

The set of ground states of the theory is called the vacuum. Suppose $\phi = \phi_+$ is a ground state. If there are values of $\phi \neq \phi_+$ that minimize the potential $V(\phi)$, then the vacuum expectation value, say ϕ_-, is not equal to ϕ_+. This means that ϕ_+ corresponds to a false vacuum, which is a state of unstable equilibrium.

When the vacuum transitions from the false vacuum to the stable, true vacuum, the symmetry under the action of G is spontaneously broken. This means that there are elements of G which do not leave ϕ_- invariant. The elements under which ϕ_- is invariant form a subgroup $H \subset G$, defined as

$$H = \{g \in G : D(g)\phi_- = \phi_-\}. \tag{3.3}$$

Call the generators of H in the representation as t^a, which can be chosen so that they are a subset of the T^a. The t^a are known as the unbroken generators and must satisfy $t^a\phi_- = 0$. The leftover generators, say they are represented by $\mathcal{T}^a$, are called the broken generators and do not annihilate the true vacuum, $\mathcal{T}^a\phi_- \neq 0$. The broken generators generate the coset space G/H, otherwise known as the vacuum manifold.

In a unitary representation of G, the kinetic term of the Lagrangian density is clearly invariant under the action of G. However, the potential term is invariant only if $V(\phi) = V(D(g)\phi)$.

Consider an infinitesimal transformation $\phi \to \phi' = \phi + \delta\phi$. For invariance, $V(\phi) = V(\phi + \delta\phi)$. Since

$$V(\phi + \delta\phi) = V(\phi) + \frac{\partial V(\phi)}{\partial \phi_i}\delta\phi_i + \dots, \tag{3.4}$$

invariance requires that

$$\frac{\partial V(\phi)}{\partial \phi_i}\delta\phi_i = 0. \tag{3.5}$$

Taking the second derivative yields

$$\frac{\partial^2 V}{\partial \phi_j \partial \phi_i}\delta\phi_i + \frac{\partial V}{\partial \phi_i}\frac{\partial(\delta\phi_i)}{\partial \phi_j} = 0. \tag{3.6}$$

Near a true vacuum state $\phi' = \phi_-$, there is an infinitesimal perturbation for each T^a so that $\delta\phi^a = T^a\phi_-$. Then for each T^a, Equation (3.6) becomes

$$\left.\frac{\partial^2 V}{\partial \phi_j \partial \phi_i}\right|_{\phi=\phi_-} T^a_{ij}\phi_{-j} = 0. \tag{3.7}$$

The potential can be expressed as

$$V(\phi) = V(\phi_-) + \frac{1}{2}\left.\frac{\partial^2 V}{\partial \phi_j \partial \phi_i}\right|_{\phi=\phi_-} (\phi - \phi_-)_i(\phi - \phi_-)_j + \dots, \tag{3.8}$$

which means the mass matrix elements are

$$\mu^2_{ij} = \left.\frac{\partial^2 V}{\partial \phi_j \partial \phi_i}\right|_{\phi=\phi_-}. \tag{3.9}$$

Note that the eigenvalues of μ^2_{ij} are non-negative because they correspond to the second derivative evaluated at a minimum. Equation (3.7) and the fact that $\mathcal{T}^a\phi_- \neq 0$ means that $\dim G - \dim H$ mass matrix eigenvalues, one for each broken generator, must be zero. Therefore, each broken generator has a corresponding massless boson called a Nambu-Goldstone boson. This result is called Goldstone's Theorem.

3.2 Gauged Symmetry Breaking

Instead of having global symmetry, let the symmetry group G now depend on space-time coordinates x_μ. Recall from Section 2.3 that the generalized gauge-covariant Lagrangian density is

$$\mathcal{L} = (\mathcal{D}_\mu\phi)^\dagger(\mathcal{D}^\mu\phi) - V(\phi) - \frac{1}{4}F^a_{\mu\nu}F^{a\mu\nu}. \tag{3.10}$$

Now tiny flucations $\phi = \phi_- + \phi'$ about a true vacuum expectation value ϕ_- yield a mass term in $(\mathcal{D}_\mu\phi)^\dagger(\mathcal{D}^\mu\phi)$ which is

$$M^2_{ab}A^{a*}_\mu A^{b\mu} = e^2(T^aT^b)_{ij}\phi_{-i}\phi_{-j}A^{a*}_\mu A^{b\mu}. \tag{3.11}$$

The gauge can be chosen such that the other mass matrix μ_{ij} from Equation (3.9) refers only to the unbroken subspace H. Looking at it this way then, the massless Nambu-Goldstone boson are gone, having been absorbed by the broken gauge fields as additional spin states. This is called the Anderson-Higgs mechanism and the fluctuation $\phi'(x)$ is called the Anderson-Higgs field.

3.2.1 Electroweak Symmetry Breaking

The use of the term "Anderson-Higgs field" generally refers to that of electroweak theory. In this case, the Anderson-Higgs field [7](pp.220-232), [6](pp.715-716) is a complex doublet

$$H(x) = \frac{1}{\sqrt{2}} \begin{pmatrix} H_1(x) + iH_2(x) \\ H_3(x) + iH_4(x) \end{pmatrix}. \tag{3.12}$$

The gauge can be chosen to be what is called the unitary gauge by choosing the right local $SU(2)$ transformation $U(x)$ such that

$$U(x)H(x) = \frac{1}{\sqrt{2}} \begin{pmatrix} 0 \\ v_h + h(x) \end{pmatrix} \tag{3.13}$$

where $h(x)$ is a real scalar field with vacuum expectation value

$$\langle h \rangle = 0. \tag{3.14}$$

It is easy to see now that

$$H^\dagger H = \frac{v_h^2}{2} + v_h h(x) + \frac{h^2(x)}{2}. \tag{3.15}$$

Note that v_h is related to the vacuum expectation value of $H^\dagger H$ by

$$\langle H^\dagger H \rangle = \frac{v_h^2(x)}{2}. \tag{3.16}$$

The potential can be shifted to reflect this true ground state state, resulting in

$$\begin{aligned} V(H^\dagger H) &= \mu^2 \Big(H^\dagger H - \frac{v_h^2}{2} \Big) - \frac{\lambda}{4} \Big(H^\dagger H - \frac{v_h^2}{2} \Big)^2 \\ &= \mu^2 \Big(v_h h(x) + \frac{h^2(x)}{2} \Big) - \frac{\lambda}{4} \Big(v_h h(x) + \frac{h^2(x)}{2} \Big)^2. \end{aligned} \tag{3.17}$$

The bosons that become massive in this case are the W^+,W^-, and Z bosons which mediate the weak force.

3.3 Topological Defects

The topology of the vacuum manifold involved in spontaneous symmetry breaking determines the type of topological defects [9], [10](pp.54-85), [11](pp.219-242) which can occur.

3.3.1 Homotopy

Consider two manifolds X and Y without boundary, and with points $x_0 \in X$ and $y_0 \in Y$. Also consider two continuous maps $f_1, f_2 : X \mapsto Y$ where $f_1(x_0) = f_2(x_0) = y_0$. The points x_0 and y_0 are called base points and the maps f_1 and f_2 are called based maps. The maps f_1 and f_2 are called homotopic if there exists a continuous map $\tilde{f} : X \times [0,1] \mapsto Y$ such that, for all $t \in [0,1]$ and $x \in X$, $\tilde{f}(t = 0; x) = f_1$, $\tilde{f}(t = 1; x) = f_2$, and $\tilde{f}(t; x = x_0) = y_0$. Maps such as $\tilde{f}$ are called continuous deformations.

Homotopy is a type of equivalence relation, so maps from X to Y can be sorted into equivalence classes. If X is the n-sphere S^n, these equivalence classes form a group under composition called $\pi_n(Y)$, the nth homotopy group of Y ($n = 1, 2, 3, \dots$). Different elements of $\pi_n(Y)$ have different topological charges. The topological charge is defined by how many times and the direction in which a mapping wraps around the base base point y_0. For $\pi_1(Y)$, the topological charge is called the winding number, but the term "winding number" is often used generally to mean the topological charge associated with mappings in any $\pi_n(Y)$.

Spontaneous symmetry breaking can cause topological defects, also known as topological solitons, to form when the homotopy group of the vacuum manifold, say $\mathcal{M}$, is non-trivial (recall that the trivial group is just the identity group). There is an associated topological current density W_μ for which the topological charge W is defined as

$$W = \int W_0 d^3x. \tag{3.18}$$

3.3.2 Types of Topological Defects

The types of topological defects that can form due to spontaneous symmetry breaking depend on the topology of the vacuum manifold $\mathcal{M}$. Domain walls, generally associated with discrete symmetry breaking, have dimension 2 and occur when $\mathcal{M}$ is disconnected, in which case $\pi_0(\mathcal{M}) \neq I$. If $\pi_1(\mathcal{M}) \neq I$ then $\mathcal{M}$ has unshrinkable loops and cannot be simply connected. This causes 1-D topological defects called strings. Zero-dimensional topological defects are called monopoles and occurs when $\mathcal{M}$ has unshrinkable surfaces, so that $\pi_2(\mathcal{M}) \neq I$. The relevant topological defect here is called a texture, which occurs for $\pi_3(\mathcal{M}) \neq I$.

3.4 The Linear σ-Model

Chiral transformations [12](pp.13-15) should include transformations that preserve parity and those that do not. Consider 3-rotations of a 3-component real field $\boldsymbol{\phi}$ generated by I_i, $i = 1, 2, 3$, which obey the commutation relations of Eq. (2.7). The commutation relations mean the I_i mix together the components of $\boldsymbol{\phi}$. Since these just generate rotations, they cannot violate parity. To include parity violation, add a 4th real component, ϕ_0, to $\boldsymbol{\phi}$ (note that the metric here is Euclidean), and three more generators K_j, $j = 1, 2, 3$. The K_j mix components of $\boldsymbol{\phi}$ with ϕ_0. The I_i remain having nothing to do with ϕ_0. The algebra of these six generators is

$$[I_i, I_j] = i\epsilon_{ijk} I_k, \quad [I_i, K_j] = i\epsilon_{ijk} K_k, \quad [K_i, K_j] = i\epsilon_{ijk} I_k. \tag{3.19}$$

This is the Lie algebra of the group of special orthogonal 4×4 matrices, $SO(4)$. However, these generators can be used to define the left-chiral and right-chiral generators,

$$L_i = \frac{1}{2}(I_i - K_i), \quad R_i = \frac{1}{2}(I_i + K_i). \tag{3.20}$$

Then,

$$\begin{aligned} [L_i, L_j] &= \frac{1}{4}[I_i - K_i, I_j - K_j] \\ &= \frac{1}{4}\Big([I_i, I_j] - [I_i, K_j] - [K_i, I_j] + [K_i, K_j]\Big) \\ &= \frac{1}{4}\Big(2i\epsilon_{ijk} I_k - i\epsilon_{ijk} K_k + i\epsilon_{jik} K_k\Big) \\ &= i\epsilon_{ijk} L_k, \end{aligned} \tag{3.21}$$

and similarly,

$$[R_i, R_j] = i\epsilon_{ijk} R_k, \quad [L_i, R_j] = 0. \tag{3.22}$$

Therefore both the R_i and L_i generate independent Lie algebras, each corresponding to $SU(2)$. In other words, $SO(4)$ is isomorphic to $SU(2)_L \times SU(2)_R$.

The above construction of $SU(2)_L \times SU(2)_R$ is called a (linear) σ-model. This is because traditionally $\boldsymbol{\phi}$ is the triplet of pions $\boldsymbol{\pi}$ under the action of 3-isorotations and the additional component ϕ_0 is usually called σ.

A simple Lagrangian density for the linear σ-model, where all the fields are massless is

$$\mathcal{L} = \frac{1}{2}\partial_\mu \phi_\alpha \partial^\mu \phi_\alpha = \frac{1}{2}\partial_\mu \phi_0 \partial^\mu \phi_0 + \frac{1}{2}\partial_\mu \phi_i \partial^\mu \phi_i. \tag{3.23}$$

A global infinitesimal chiral transformation corresponds to a global rotation by infinitesimal angles ϵ_i which transforms the ϕ_α as

$$\phi_i \to \phi_i + \phi_0 \epsilon_i, \tag{3.24}$$

$$\phi_0 \to \phi_0 - \phi_i \epsilon_i. \tag{3.25}$$

Therefore

$$\begin{aligned} \partial_\mu \phi_i \partial^\mu \phi_i \to &\partial_\mu(\phi_i + \phi_0\epsilon_i)\partial^\mu(\phi_i + \phi_0\epsilon_i) \\ &= \partial_\mu \phi_i \partial^\mu \phi_i + \epsilon_i \partial_\mu \phi_i \partial^\mu \phi_0 + \epsilon_i \partial_\mu \phi_0 \partial^\mu \phi_i + \epsilon_i \epsilon_i \partial_\mu \phi_0 \partial^\mu \phi_0, \end{aligned} \tag{3.26}$$

$$\begin{aligned}\partial_\mu\phi_0\partial^\mu\phi_0 \rightarrow &\partial_\mu(\phi_0-\phi_i\epsilon_i)\partial^\mu(\phi_0-\phi_j\epsilon_j)\\ &=\partial_\mu\phi_0\partial^\mu\phi_0-\epsilon_j\partial_\mu\phi_0\partial^\mu\phi_j-\epsilon_i\partial_\mu\phi_i\partial^\mu\phi_0+\epsilon_i\epsilon_j\partial_\mu\phi_i\partial^\mu\phi_j.\end{aligned} \tag{3.27}$$

Discarding the terms that are second order in ϵ_i, it is easy to see that

$$\mathcal{L}\rightarrow\mathcal{L}. \tag{3.28}$$

That is, the Lagrangian density (3.23) is invariant under chiral transformations.

3.4.1 Spontaneous Chiral Symmetry Breaking

Some mass and interaction terms can be added to the Lagrangian density of Eq. (3.23) so that it becomes

$$\mathcal{L}=\frac{1}{2}\partial_\mu\phi_0\partial^\mu\phi_0+\frac{1}{2}\partial_\mu\phi_i\partial^\mu\phi_i-\mu_1^2(\phi_0^2+\phi_i\phi_i-\mu_2)^2, \tag{3.29}$$

where μ_1 and μ_2 are constants. These new terms transform under Eqs. (3.24), (3.25) as

$$\begin{aligned}\phi_0^2\rightarrow&(\phi_0-\phi_i\epsilon_i)(\phi_0-\phi_j\epsilon_j)\\ &=\phi_0^2-2\phi_0\phi_i\epsilon_i+\epsilon_i\epsilon_j\phi_i\phi_j,\end{aligned} \tag{3.30}$$

$$\begin{aligned}\phi_i\phi_i\rightarrow&(\phi_i+\phi_0\epsilon_i)(\phi_i+\phi_0\epsilon_i)\\ &=\phi_i\phi_i+2\phi_0\phi_i\epsilon_i+\phi_0^2\epsilon_i\epsilon_i.\end{aligned} \tag{3.31}$$

Discarding the terms which are second order in ϵ_i, the Lagrangian density is still invariant under chiral transformations.

This new addition to the Lagrangian density is the potential whose extrema satisfy

$$\frac{\partial V}{\partial\phi_\alpha}=4\mu_1^2(\phi_0^2+\phi_i\phi_i-\mu_2)\phi_\alpha=0. \tag{3.32}$$

If $\mu_2<0$ then $\langle\phi_0\rangle=\langle\phi_i\rangle=0$ but if $\mu_2>0$ then the ground state satisfies

$$\langle\phi_0\rangle^2+\langle\phi_i\rangle\langle\phi_i\rangle=\mu_2. \tag{3.33}$$

The latter, broken, vacuum manifold is called the chiral sphere, which is a 3-sphere $S^3\cong SU(2)$. When the ϕ_i are identified as pions, μ_2 is identified as f_π^2, the pion decay constant. From this point, the general substition $\mu_2\equiv f^2$ is made, as well as $\mu_1\equiv\mu$.

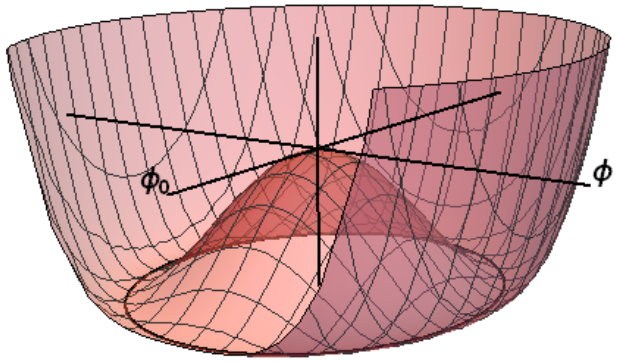

Figure 3.1: The linear σ-model potential $V(\phi_\alpha)$, with the coordinates centered at the false vacuum. The circle at the bottom of the potential is the chiral sphere. Note that $\boldsymbol{\phi}$ has been suppressed to one-dimension.

In the broken phase, the mass matrix elements are

$$\left.\frac{\partial^2 V}{\partial\phi_\alpha\partial\phi_\beta}\right|_{\langle\phi_\mu\rangle\langle\phi_\mu\rangle=f^2} = 8\mu^2\langle\phi_\alpha\rangle\langle\phi_\beta\rangle + 4\mu^2(\langle\phi_\alpha\rangle\langle\phi_\alpha\rangle - f^2)\delta_{\alpha\beta} = 8\mu^2\langle\phi_\mu\rangle\langle\phi_\mu\rangle\,. \tag{3.34}$$

No point on the vacuum manifold is preferred over the other. One possible ground state solution is

$$\langle\boldsymbol{\phi}\rangle = 0, \quad \langle\phi_0\rangle = -f. \tag{3.35}$$

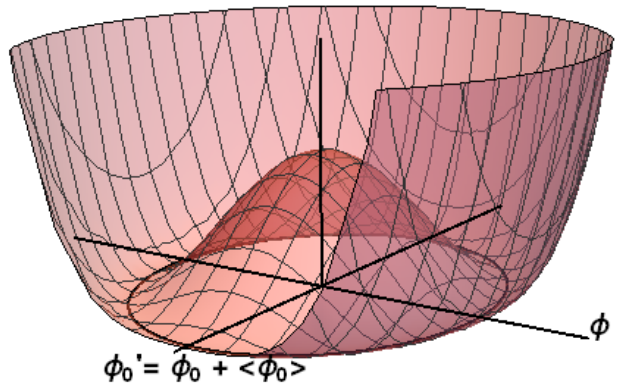

Figure 3.2: The linear σ-model potential $V(\phi_\alpha)$ in terms of the shifted field $\phi_0' = \phi_0 + \langle\phi_0\rangle$ for $\langle\phi_0\rangle = -f$. Note that $\boldsymbol{\phi}$ has been suppressed to one-dimension.

3.4.2 Explicit Chiral Symmetry Breaking

Another way to break the chiral symmetry is by adding a term that is first order in ϕ_0, say $a\phi_0$ where a is a constant so that the potential becomes

$$V(\phi) = \mu^2(\phi_0^2 + \phi_i\phi_i - f^2)^2 - a\phi_0, \tag{3.36}$$

in which case the extrema of the potential are found by

$$\frac{\partial V}{\partial\phi_i} = 4\mu^2(\phi_\alpha\phi_\alpha - f^2)\phi_i = 0, \tag{3.37}$$

$$\frac{\partial V}{\partial\phi_0} = 4\mu^2(\phi_\alpha\phi_\alpha - f^2)\phi_0 - a = 0. \tag{3.38}$$

The non-trivial ($a \neq 0$) solutions are

$$\langle\phi_i\rangle = 0, \qquad 4\mu^2(\langle\phi_0\rangle^2 - f^2)\langle\phi_0\rangle = a. \tag{3.39}$$

As before, if $f^2 < 0$ then the system is in the unbroken phase and $\langle\phi_0\rangle = 0$. The broken phase case, $f^2 > 0$, has mass matrix

$$\left.\frac{\partial^2 V}{\partial\phi_\alpha\partial\phi_\beta}\right|_{\text{broken ground}} = 8\mu^2\langle\phi_\alpha\rangle\langle\phi_\beta\rangle + \frac{a}{\langle\phi_0\rangle}\delta_{\alpha\beta}. \tag{3.40}$$

This means that after symmetry breaking the ϕ_i have mass

$$m_{\boldsymbol{\phi}}^2 = \frac{a}{\langle\phi_0\rangle} \tag{3.41}$$

and ϕ_0 has mass

$$m_{\phi_0}^2 = 8\mu^2\langle\phi_0\rangle^2 + m_{\boldsymbol{\phi}}^2. \tag{3.42}$$

In the limit that $a \to 0$ the ϕ_i are recovered as massless Nambu-Goldstone bosons.

3.5 The Nonlinear σ-Model

There exists a nonlinear realization of the σ-model which can be obtained by imposing that the broken phase is in the ground state. That is, ϕ_α must live in the chiral sphere. In other words,

$$\phi_0^2 + \phi_i^2 = f^2. \tag{3.43}$$

This means that the potential in Eq. (3.29) is simply zero.

The fields ϕ_0 and ϕ_i are now necessarily dependent so ϕ_0 can be expressed as,

$$\phi_0 = \sqrt{f^2 - \phi_i^2}. \tag{3.44}$$

The Lagrangian density can therefore be written as

$$\mathcal{L} = \frac{(\phi_i \partial_\mu \phi_i)^2}{f^2 - \phi_i^2} + (\partial_\mu \phi_i)^2. \tag{3.45}$$

There exists an exponential parametrization of the nonlinear σ-model which is

$$U = e^{i\boldsymbol{w}\cdot\boldsymbol{\tau}/f} = (\phi_0 + i\boldsymbol{\tau}\cdot\boldsymbol{\phi})/f, \tag{3.46}$$

where $\boldsymbol{w} = w\hat{\boldsymbol{w}}$ and w is called the chiral angle, and

$$\phi_0 = f\cos\Big(\frac{w}{f}\Big), \qquad \boldsymbol{\phi} = f\hat{\boldsymbol{w}}\sin\Big(\frac{w}{f}\Big). \tag{3.47}$$

To see how this can be, first notice that

$$\begin{aligned}
(\boldsymbol{w}\cdot\boldsymbol{\tau})^2 &= (w_1\tau_1 + w_2\tau_2 + w_3\tau_3)^2 \\
&= w_1^2\tau_1^2 + w_2^2\tau_2^2 + w_3\tau_3^2 + w_1w_2(\tau_1\tau_2 + \tau_2\tau_1) \\
&\quad + w_1w_3(\tau_1\tau_3 + \tau_3\tau_1) + w_2w_3(\tau_2\tau_3 + \tau_3\tau_2) \\
&= (w_1^2 + w_2^2 + w_3^2)I \\
&= w^2 I,
\end{aligned} \tag{3.48}$$

where I is the 2×2 identity matrix. So then

$$\begin{aligned}
e^{i\boldsymbol{w}\cdot\boldsymbol{\tau}/f} &= \sum_{k=0}^{\infty} \frac{(i\boldsymbol{w}\cdot\boldsymbol{\tau}/f)^k}{k!} \\
&= 1 + \frac{i\boldsymbol{w}\cdot\boldsymbol{\tau}}{f} - \frac{(\boldsymbol{w}\cdot\boldsymbol{\tau})^2}{2!f^2} - \frac{i(\boldsymbol{w}\cdot\boldsymbol{\tau})^3}{3!f^3} + \frac{(\boldsymbol{w}\cdot\boldsymbol{\tau})^4}{4!f^4} + \dots \\
&= 1 + \frac{iw\hat{\boldsymbol{w}}\cdot\boldsymbol{\tau}}{f} - \frac{w^2 I}{2!f^2} - \frac{iw^3\hat{\boldsymbol{w}}\cdot\boldsymbol{\tau}}{3!f^3} + \frac{w^4 I}{4!f^4} + \dots \\
&= \Big(1 - \frac{w^2}{2!f^2} + \frac{w^4}{4!f^4} + \dots\Big)I + i\hat{\boldsymbol{w}}\cdot\boldsymbol{\tau}\Big(\frac{w}{f} - \frac{w^3}{3!f^3} + \frac{w^5}{5!f^5} + \dots\Big) \\
&= \cos\Big(\frac{w}{f}\Big)I + i\hat{\boldsymbol{w}}\cdot\boldsymbol{\tau}\sin\Big(\frac{w}{f}\Big) \\
&= (\phi_0 I + i\boldsymbol{\tau}\cdot\boldsymbol{\phi})/f.
\end{aligned} \tag{3.49}$$

The Lagrangian density using the exponential parametrization is found by looking at

$$\begin{aligned}
\partial_\mu U^\dagger \partial^\mu U &= (\partial_\mu\phi_0 I - i\boldsymbol{\tau}\cdot\partial_\mu\boldsymbol{\phi})(\partial_\mu\phi_0 I + i\boldsymbol{\tau}\cdot\partial_\mu\boldsymbol{\phi})/f^2 \\
&= (\partial_\mu\phi_0 I)^2/f^2 + (\boldsymbol{\tau}\cdot\partial_\mu\boldsymbol{\phi})^2/f^2.
\end{aligned} \tag{3.50}$$

This is obviously not the desired kinetic term. However,

$$\mathrm{Tr}\,(\partial_\mu\phi_0 I)^2 = 2(\partial_\mu\phi_0)^2, \tag{3.51}$$

and

$$\begin{aligned}\operatorname{Tr}(\boldsymbol{\tau}\cdot\partial_\mu\boldsymbol{\phi})^2 &= \operatorname{Tr}(\tau_i\partial_\mu\phi_i\tau_j\partial^\mu\phi_j)\\ &= \partial_\mu\phi_i\partial^\mu\phi_j\operatorname{Tr}(\tau_i\tau_j)\\ &= 2\partial_\mu\phi_i\partial^\mu\phi_j\delta_{ij}\\ &= 2(\partial_\mu\boldsymbol{\phi})^2.\end{aligned} \tag{3.52}$$

Therefore

$$\frac{1}{2}\partial_\mu\phi_0\partial^\mu\phi_0+\frac{1}{2}\partial_\mu\phi_i\partial^\mu\phi_i=\frac{f^2}{4}\operatorname{Tr}(\partial_\mu U^\dagger\partial^\mu U), \tag{3.53}$$

giving the Lagrangian density of the nonlinear σ-model in the exponential parametrization.

3.5.1 Chiral Symmetry Breaking

An $SU(2)_L\times SU(2)_R$ transformation transforms U as

$$U\to LUR^\dagger, \tag{3.54}$$

where $L\in SU(2)_L$ and $R\in SU(2)_R$. The Lagrangian density of Eq. (3.53) is, at a glance, invariant under this action because it transforms as

$$\begin{aligned}\frac{f^2}{4}\operatorname{Tr}(\partial_\mu U^\dagger\partial^\mu U)\to&\frac{f^2}{4}\operatorname{Tr}(R\partial_\mu U^\dagger L^\dagger L\partial^\mu U R^\dagger)\\ =&\frac{f^2}{4}\operatorname{Tr}(\partial_\mu U^\dagger\partial^\mu U),\end{aligned} \tag{3.55}$$

where the cyclic nature of the trace has been invoked.

Symmetry breaking in the nonlinear σ-model can be seen be analyzing the energy [11](pg.294). The energy-momentum tensor is

$$\begin{aligned}T^{\mu\nu}&=\frac{\partial\mathcal{L}}{\partial(\partial_\mu U)}\partial^\nu U+\frac{\partial\mathcal{L}}{\partial(\partial_\mu U^\dagger)}\partial^\nu U^\dagger-g^{\mu\nu}\mathcal{L}\\ &=\frac{f^2}{4}\operatorname{Tr}(\partial^\mu U^\dagger\partial^\nu U+\partial^\mu U\partial^\nu U^\dagger-\eta^{\mu\nu}\partial_\alpha U^\dagger\partial^\alpha U).\end{aligned} \tag{3.56}$$

Then the energy density is

$$\begin{aligned}\mathcal{H}&=T^{00}\\ &=\frac{f^2}{4}\operatorname{Tr}(2\partial_0U^\dagger\partial^0U-\partial_\alpha U^\dagger\partial^\alpha U)\\ &=\frac{f^2}{4}\operatorname{Tr}(\partial_0U^\dagger\partial^0U-\partial_iU^\dagger\partial^iU)\end{aligned} \tag{3.57}$$

The energy

$$E=\int\mathcal{H}d^3x \tag{3.58}$$

should be finite and for it to also have a static solution, it must be that

$$\partial_0U^\dagger\partial^0U=0 \tag{3.59}$$

and

$$\lim_{|\boldsymbol{x}|\to\infty}\partial_iU^\dagger\partial^iU=0. \tag{3.60}$$

This, along with the unitarity of U, imposes the boundary condition

$$\lim_{|\boldsymbol{x}|\to\infty}U=1, \tag{3.61}$$

which is equivalent to saying

$$\lim_{|\boldsymbol{x}|\to\infty} \phi_0 = 1, \quad \lim_{|\boldsymbol{x}|\to\infty} \boldsymbol{\phi} = 0, \tag{3.62}$$

or

$$\lim_{|\boldsymbol{x}|\to\infty} \boldsymbol{w} = 2n\pi, \tag{3.63}$$

where n is an integer. This boundary condition is what breaks the $SU(2)_L \times SU(2)_R$ symmetry because the transformation

$$\lim_{|\boldsymbol{x}|\to\infty} (LUR^\dagger) = LR^\dagger \tag{3.64}$$

is only consistent with the boundary condition if $L = R$. Therefore only transformations

$$U \to VUV^\dagger \tag{3.65}$$

are allowed, where V is an element of $SU(2)_V$, the group of vector $SU(2)$ transformations.

Another way to see symmetry breaking in the nonlinear σ-model is by breaking the symmetry explicity with a mass term. First, note that the second term of

$$\begin{aligned} \frac{1}{2}\operatorname{Tr} U &= \cos\left(\frac{w}{f}\right) \\ &= 1 - \frac{w^2}{2!f^2} + \dots \end{aligned} \tag{3.66}$$

looks like a mass term. In this case, it is the mass of a w_i particle, so the identification $f = f_w$ is made. Discarding the higher order terms, the mass term in the nonlinear σ-model Lagrangian is

$$\frac{m_w^2 f_w^2}{2} \operatorname{Tr}(U - I) = -\frac{m_w^2}{2} w_i w_i. \tag{3.67}$$

This breaks the symmetry because this mass term must also obey the boundary conditions.

3.6 Gauged Nonlinear σ-Model

Now consider a local chiral transformation of the nonlinear σ-model. The boundary condition of the previous section is still necessary, so only local $SU(2)$ transformations are considered here. First, rewrite U as

$$U = U_L^\dagger U_R. \tag{3.68}$$

The U_L and U_R transform under local $SU(2)$ as

$$U_L \to h(x) U_L, \quad U_R \to h(x) U_R, \tag{3.69}$$

where $h(x)$ is an element of $SU(2)$. Therefore U transforms as

$$U \to U_L^\dagger h^\dagger(x) h(x) U_R = U. \tag{3.70}$$

Since U is special unitary, it must be that U_L and U_R are also special unitary. It is easy to see then how writing $U = U_L^\dagger U_R$ is justified via group closure. Now,

$$\begin{aligned} \partial_\mu(U_L U_L^\dagger) &= \partial_\mu(1) = 0 \\ &= \partial_\mu U_L U_L^\dagger + U_L \partial_\mu U_L^\dagger, \end{aligned} \tag{3.71}$$

meaning that

$$\partial_\mu U_L U_L^\dagger = -U_L \partial_\mu U_L^\dagger. \tag{3.72}$$

The same goes for U_R. This result will be useful right away.

Now, the Lagrangian density can be written as

$$\begin{aligned}\frac{4}{f_w^2}\mathcal{L}_0 &= \mathrm{Tr}\,(\partial_\mu U^\dagger \partial^\mu U) \\ &= \mathrm{Tr}[(\partial_\mu (U_R^\dagger U_L)\partial^\mu (U_L^\dagger U_R)] \\ &= \mathrm{Tr}[(\partial_\mu U_R^\dagger U_L + U_R^\dagger \partial_\mu U_L)(\partial^\mu U_L^\dagger U_R + U_L^\dagger \partial^\mu U_R)] \\ &= \mathrm{Tr}(\partial_\mu U_R^\dagger U_L \partial^\mu U_L^\dagger U_R + \partial_\mu U_R^\dagger U_L U_L^\dagger \partial^\mu U_R \\ &\quad + U_R^\dagger \partial_\mu U_L \partial^\mu U_L^\dagger U_R + U_R^\dagger \partial_\mu U_L U_L^\dagger \partial^\mu U_R).\end{aligned} \tag{3.73}$$

The first term is

$$\begin{aligned}\mathrm{Tr}(\partial_\mu U_R^\dagger U_L \partial^\mu U_L^\dagger U_R) &= \mathrm{Tr}(U_R \partial_\mu U_R^\dagger U_L \partial^\mu U_L^\dagger) \\ &= \mathrm{Tr}[(-\partial_\mu U_R U_R^\dagger)(-\partial^\mu U_L U_L^\dagger)] \\ &= \mathrm{Tr}(\partial^\mu U_L U_L^\dagger \partial_\mu U_R U_R^\dagger).\end{aligned} \tag{3.74}$$

The second term is

$$\begin{aligned}\mathrm{Tr}(\partial_\mu U_R^\dagger \partial^\mu U_R) &= \mathrm{Tr}(\partial^\mu U_R \partial_\mu U_R^\dagger) \\ &= \mathrm{Tr}(\partial^\mu U_R U_R^\dagger U_R \partial_\mu U_R^\dagger) \\ &= \mathrm{Tr}(-\partial^\mu U_R U_R^\dagger \partial_\mu U_R U_R^\dagger),\end{aligned} \tag{3.75}$$

and the third term is

$$\begin{aligned}\mathrm{Tr}(U_R^\dagger \partial_\mu U_L \partial^\mu U_L^\dagger U_R) &= \mathrm{Tr}(\partial_\mu U_L U_L^\dagger U_L \partial^\mu U_L^\dagger) \\ &= \mathrm{Tr}(-\partial_\mu U_L U_L^\dagger \partial^\mu U_L U_L^\dagger).\end{aligned} \tag{3.76}$$

Putting the pieces back together, the Lagrangian density is

$$\begin{aligned}\mathcal{L}_0 &= \frac{f_w^2}{4}\,\mathrm{Tr}[2\partial^\mu U_L U_L^\dagger \partial_\mu U_R U_R^\dagger - (\partial_\mu U_R U_R^\dagger)^2 - (\partial_\mu U_L U_L^\dagger)^2] \\ &= f_w^2\,\mathrm{Tr}\left(\frac{1}{2i}(\partial_\mu U_L U_L^\dagger - \partial_\mu U_R U_R^\dagger)\right)^2.\end{aligned} \tag{3.77}$$

Now, because $h(x)$ is a local transformation, a gauge field A_μ must be included, in which case

$$\begin{aligned}\mathcal{L}_0 &= f_w^2\,\mathrm{Tr}\left(\frac{1}{2i}(\mathcal{D}_\mu U_L U_L^\dagger - \mathcal{D}_\mu U_R U_R^\dagger)\right)^2 \\ &= f_w^2\,\mathrm{Tr}\left(\frac{1}{2i}[(\partial_\mu - igA_\mu)U_L U_L^\dagger - (\partial_\mu - igA_\mu)U_R U_R^\dagger]\right)^2 \\ &= f_w^2\,\mathrm{Tr}\left(\frac{1}{2i}(\partial_\mu U_L U_L^\dagger - \partial_\mu U_R U_R^\dagger)\right)^2.\end{aligned} \tag{3.78}$$

A term can be added to the Lagrangian density which describes the interactions between the gauge field and the U_L, U_R which looks like, for some constant α,

$$\begin{aligned}\mathcal{L}_I &= \alpha f_w^2\,\mathrm{Tr}\left(\frac{1}{2i}(\mathcal{D}_\mu U_L U_L^\dagger + \mathcal{D}_\mu U_R U_R^\dagger)\right)^2 \\ &= \alpha f_w^2\,\mathrm{Tr}\left(\frac{1}{2i}[(\partial_\mu - ig_V A_\mu)U_L U_L^\dagger + (\partial_\mu - igA_\mu)U_R U_R^\dagger]\right)^2 \\ &= \alpha g_V^2 f_w^2\,\mathrm{Tr}\left(A_\mu - \frac{1}{2ig}(\partial_\mu U_L U_L^\dagger + \partial_\mu U_R U_R^\dagger)\right)^2,\end{aligned} \tag{3.79}$$

where g_V is the gauge coupling constant (the subscript V indicates that this is related to the vector $SU(2)_V$ symmetry). The gauge is chosen to be

$$A_\mu = \frac{1}{2ig_V}(\partial_\mu U_L U_L^\dagger + \partial_\mu U_R U_R^\dagger) \tag{3.80}$$

so that $\mathcal{L}_I = 0$.

The Yang-Mills term of the Lagrangian density is

$$\begin{aligned}\mathcal{L}_{YM} &= -\frac{1}{4}F^a_{\mu\nu}F^{\mu\nu a} \\ &= -\frac{1}{2}F^a_{\mu\nu}F^{\mu\nu b}\frac{1}{2}\delta^{ab} \\ &= -\frac{1}{2}F^a_{\mu\nu}F^{\mu\nu b}\,\mathrm{Tr}(T^aT^b) \\ &= -\frac{1}{2}\,\mathrm{Tr}(F^a_{\mu\nu}T^aF^{\mu\nu b}T^b) \\ &= -\frac{1}{2}\,\mathrm{Tr}(F_{\mu\nu}F^{\mu\nu}).\end{aligned} \tag{3.81}$$

To put this in terms of A_μ first recall that

$$F_{\mu\nu} = \partial_\mu A_\nu - \partial_\nu A_\mu - ig[A_\mu, A_\nu]. \tag{3.82}$$

The first term is

$$\partial_\mu A_\nu = \frac{1}{2ig_V}(\partial_\mu\partial_\nu U_L U_L^\dagger + \partial_\nu U_L \partial_\mu U_L^\dagger + \partial_\mu\partial_\nu U_R U_R^\dagger + \partial_\nu U_R \partial_\mu U_R^\dagger). \tag{3.83}$$

Note that the terms symmetric under swapping the indices μ and ν cancel out with those in $-\partial_\nu A_\mu$ so that

$$\partial_\mu A_\nu - \partial_\nu A_\mu = \frac{1}{2ig_V}(\partial_\nu U_L \partial_\mu U_L^\dagger - \partial_\mu U_L \partial_\nu U_L^\dagger + \partial_\nu U_R \partial_\mu U_R^\dagger - \partial_\mu U_R \partial_\nu U_R^\dagger). \tag{3.84}$$

This can be further simplified using

$$\partial_\nu U_L \partial_\mu U_L^\dagger = \partial_\nu U_L U_L^\dagger U_L \partial_\mu U_L^\dagger = -\partial_\nu U_L U_L^\dagger \partial_\mu U_L U_L^\dagger \tag{3.85}$$

so that

$$\partial_\mu A_\nu - \partial_\nu A_\mu = \frac{1}{2ig_V}\Big([\partial_\mu U_L U_L^\dagger, \partial_\nu U_L U_L^\dagger] + [\partial_\mu U_R U_R^\dagger, \partial_\nu U_R U_R^\dagger]\Big). \tag{3.86}$$

Turning to the third term of $F_{\mu\nu}$, notice that

$$\begin{aligned}A_\mu A_\nu &= \frac{1}{(2ig_V)^2}(\partial_\mu U_L U_L^\dagger \partial_\nu U_L U_L^\dagger + \partial_\mu U_L U_L^\dagger \partial_\nu U_R U_R^\dagger \\ &\quad + \partial_\mu U_R U_R^\dagger \partial_\nu U_L U_L^\dagger + \partial_\mu U_R U_R^\dagger \partial_\nu U_R U_R^\dagger) \\ &= \frac{1}{(2ig_V)^2}(-\partial_\mu U_L \partial_\nu U_L^\dagger + \partial_\mu U_L U_L^\dagger \partial_\nu U_R U_R^\dagger \\ &\quad + \partial_\mu U_R U_R^\dagger \partial_\nu U_L U_L^\dagger - \partial_\mu U_R \partial_\nu U_R^\dagger),\end{aligned} \tag{3.87}$$

and so

$$\begin{aligned}[A_\mu, A_\nu] = \frac{1}{(2ig_V)^2}\Big([\partial_\mu U_L U_L^\dagger, \partial_\nu U_R U_R^\dagger] + [\partial_\mu U_R U_R^\dagger, \partial_\nu U_L U_L^\dagger] \\ + 2ig(\partial_\mu A_\nu - \partial_\nu A_\mu)\Big).\end{aligned} \tag{3.88}$$

Therefore,

$$\begin{aligned}F_{\mu\nu} &= \frac{1}{4ig_V}\Big([\partial_\mu U_L U_L^\dagger, \partial_\nu U_L U_L^\dagger] + [\partial_\mu U_R U_R^\dagger, \partial_\nu U_R U_R^\dagger] \\ &\quad - [\partial_\mu U_L U_L^\dagger, \partial_\nu U_R U_R^\dagger] - [\partial_\mu U_R U_R^\dagger, \partial_\nu U_L U_L^\dagger]\Big) \\ &= \frac{1}{4ig_V}[(\partial_\mu U_L U_L^\dagger - \partial_\mu U_R U_R^\dagger), (\partial_\nu U_L U_L^\dagger - \partial_\nu U_R U_R^\dagger)].\end{aligned} \tag{3.89}$$

The end result should be expressed in terms of U. First,

$$\begin{aligned}\partial_\mu U &= \partial_\mu U_L^\dagger U_R + U_L^\dagger \partial_\mu U_R \\ &= -U_L^\dagger \partial_\mu U_L U_L^\dagger U_R - U_L^\dagger U_R \partial_\mu U_R^\dagger U_R \\ &= -U_L^\dagger (\partial_\mu U_L U_L^\dagger - \partial_\mu U_R U_R^\dagger) U_R.\end{aligned} \tag{3.90}$$

To easily get a nice result, a factor of $U^\dagger$ will help:

$$U^\dagger \partial_\mu U = -U_R^\dagger (\partial_\mu U_L U_L^\dagger - \partial_\mu U_R U_R^\dagger) U_R \tag{3.91}$$

so that now

$$\begin{aligned}F_{\mu\nu} &= \frac{1}{4ig_V}[U_R U^\dagger \partial_\mu U U_R^\dagger, U_R U^\dagger \partial_\nu U U_R^\dagger] \\ &= \frac{1}{4ig_V} U_R [U^\dagger \partial_\mu U, U^\dagger \partial_\nu U] U_R^\dagger,\end{aligned} \tag{3.92}$$

and finally

$$\begin{aligned}\mathcal{L}_{YM} &= -\frac{1}{2}\,\mathrm{Tr}(F_{\mu\nu}F^{\mu\nu}) \\ &= \frac{1}{32g_V^2}\,\mathrm{Tr}[U^\dagger \partial_\mu U, U^\dagger \partial_\nu U]^2\end{aligned} \tag{3.93}$$

This is called the quartic term of the Skyrme Lagrangian.

Chapter 4

Skyrmions

To summarize, the Skyrme Lagrangian density comes from the nonlinear σ-model as described in the previous chapter and is

$$\mathcal{L}_S = \frac{f_w^2}{4}\,\mathrm{Tr}(\partial_\mu U \partial^\mu U^\dagger) + \frac{1}{32 g_V^2}\,\mathrm{Tr}[U^\dagger \partial_\mu U, U^\dagger \partial_\nu U]^2. \tag{4.1}$$

U lives in $SU(2)$ and looks like

$$U = e^{i\boldsymbol{w}\cdot\boldsymbol{\tau}/f_w} = \cos\left(\frac{w}{f_w}\right) + i\boldsymbol{\tau}\cdot\hat{\boldsymbol{w}}\sin\left(\frac{w}{f_w}\right) \tag{4.2}$$

where $\boldsymbol{w} = w\hat{\boldsymbol{w}}$. There exists a boundary condition

$$\lim_{|\boldsymbol{x}|\to\infty} U(x) = 1, \tag{4.3}$$

which causes spontaneous chiral symmetry breaking $SU(2)_L \times SU(2)_R \to SU(2)_V$. The vacuum manifold of this symmetry breaking is the chiral sphere

$$\frac{SU(2)_L \times SU(2)_R}{SU(2)_V} \cong SU(2) \cong S^3. \tag{4.4}$$

The boundary condition, and the fact that U is static, means that U is not a map from $\mathbb{R}^3$ into the vacuum manifold, but rather it is a map from S^3 into the vacuum manifold. This corresponds to $\pi_3(SU(2)) = \mathbb{Z} \neq I$, which results in textures called skyrmions [10](pp.65-66), [11](pp.287-298).

The associated topological current is defined as

$$W_\mu = \frac{1}{24\pi^2}\epsilon_{\mu\nu\alpha\beta}\,\mathrm{Tr}(U^\dagger\partial^\nu U U^\dagger \partial^\alpha U U^\dagger \partial^\beta U) \tag{4.5}$$

with winding number

$$W = \int W_0 d^3x, \tag{4.6}$$

where $\epsilon_{\mu\nu\alpha\beta}$ is equal to 1 if its indices are an even permutation of $(0,1,2,3)$, or equal to -1 otherwise. The winding number is the number of times that the mapping $U(x)$ wraps S^3 around S^3.

4.1 Stability

The boundary condition does not guarantee that the skyrmion is stable, and so the energy must be analysed further[11](pp.294-295). To make this easy, first remember that the soliton is static so

$$\partial_0 U = \partial_0 U^\dagger = 0. \tag{4.7}$$

Then

$$T^{00} = -\mathcal{L}. \tag{4.8}$$

For D spatial dimensions, the energy is

$$\begin{aligned} E &= \int T^{00} d^3x \\ &= -\int \Big(\frac{f_w^2}{4} \operatorname{Tr}(\partial_i U(\boldsymbol{x}) \partial^i U^\dagger(\boldsymbol{x})) \\ &\quad + \frac{1}{32 g_V^2} \operatorname{Tr}[U^\dagger(\boldsymbol{x}) \partial_i U(\boldsymbol{x}), U^\dagger(\boldsymbol{x}) \partial_j U(\boldsymbol{x})]^2 \Big) d^3x. \end{aligned} \tag{4.9}$$

Now consider the transformation

$$U(\boldsymbol{x}) \to U(\lambda \boldsymbol{x}) \tag{4.10}$$

for some number λ. This is called a scale transformation, under which the energy transforms as

$$\begin{aligned} E \to E(\lambda) = &- \frac{f_w^2}{4} \operatorname{Tr} \int \frac{\partial U(\lambda \boldsymbol{x})}{\partial x^i} \frac{\partial U^\dagger(\lambda \boldsymbol{x})}{\partial x_i} d^D x \\ &- \frac{1}{32 g_V^2} \operatorname{Tr} \int \Big[U^\dagger(\lambda \boldsymbol{x}) \frac{\partial U(\lambda \boldsymbol{x})}{\partial x^i}, U^\dagger(\lambda \boldsymbol{x}) \frac{\partial U(\lambda \boldsymbol{x})}{\partial x^j} \Big]^2 d^D x \\ = &-\lambda^{2-D} \frac{f_w^2}{4} \operatorname{Tr} \int \frac{\partial U(\lambda \boldsymbol{x})}{\partial (\lambda x^i)} \frac{\partial U^\dagger(\lambda \boldsymbol{x})}{\partial (\lambda x_i)} d^D(\lambda x) \\ &- \lambda^{4-D} \frac{1}{32 g_V^2} \operatorname{Tr} \int \Big[U^\dagger(\lambda \boldsymbol{x}) \frac{\partial U(\lambda \boldsymbol{x})}{\partial (\lambda x^i)}, U^\dagger(\lambda \boldsymbol{x}) \frac{\partial U(\lambda \boldsymbol{x})}{\partial (\lambda x^j)} \Big]^2 d^D(\lambda x). \end{aligned} \tag{4.11}$$

Call the integral of the second order term K_2 and that of the fourth order term K_4. These are independent of λ. Then

$$E(\lambda) = \lambda^{2-D} K_2 + \lambda^{4-D} K_4. \tag{4.12}$$

For stability, $\lambda = 1$ should minimize the energy (any finite value of λ would rescale g_V and f_w but $E(\lambda)$ would diverge if λ was 0 or infinite, depending on D). Therefore

$$\left. \frac{dE(\lambda)}{d\lambda} \right|_{\lambda=1} = (2-D) K_2 + (4-D) K_4 = 0, \tag{4.13}$$

$$\left. \frac{d^2 E(\lambda)}{d\lambda^2} \right|_{\lambda=1} = (2-D)(1-D) K_2 + (4-D)(3-D) K_4 > 0. \tag{4.14}$$

If $D = 1$, then $K_2 < 0$ which is no good. If $D = 2$, then K_4 must be equal to zero, but also larger than zero. Similarly, if $D = 4$, then K_2 must be zero while also being greater than zero. For $D \geq 5$, it must be that $K_4 < 0$. The only option that doesn't have any problems is $D = 3$. Hence stability of the soliton is achieved only for $D = 3$.

This is an extension of Derrick's theorem, which says that if $\mathcal{H}$ consists of a term like $\lambda^{2-D} K_2$ along with a potential term, the only dimension that allows for stability is $D = 1$. The stability of a skyrmion relies on its quartic term.

4.2 Hedgehog Skyrmions

The hedgehog ansatz [11](pp.298-300, 312-316), [12](pp.89-92), [13] is a static one, meaning that

$$\boldsymbol{w}(x) = \boldsymbol{w}(\boldsymbol{r}) \tag{4.15}$$

where

$$r = (x_i x_i)^{1/2}. \tag{4.16}$$

The hedgehog part of it is

$$\boldsymbol{w}(\boldsymbol{r}) = \hat{\boldsymbol{r}} w(r), \tag{4.17}$$

noting that

$$\hat{\boldsymbol{r}} = \hat{x}_k \frac{x_k}{r}. \tag{4.18}$$

In this case,

$$\begin{aligned} \mathrm{Tr}(\partial_\mu U \partial^\mu U^\dagger) &= -\mathrm{Tr}(\partial^i U \partial^i U^\dagger) \\ &= -\frac{1}{f_w^2}\mathrm{Tr}[(\partial^i\phi_0 I + i\tau_j\partial^i\phi_j)(\partial^i\phi_0 I - i\tau_k\partial^i\phi_k)] \\ &= -\frac{2}{f_w^2}(\partial^i\phi_0\partial^i\phi_0 + \partial^i\phi_j\partial^i\phi_j). \end{aligned} \tag{4.19}$$

Now

$$\begin{aligned} \partial^i\phi_0 &= f_w \frac{\partial}{\partial x_i}\cos\Big(\frac{w}{f_w}\Big) \\ &= -f_w \sin\Big(\frac{w}{f_w}\Big)\frac{1}{f_w}\frac{\partial w}{\partial x_i} \\ &= -\sin\Big(\frac{w}{f_w}\Big)\frac{dw}{dr}\frac{x_i}{r}, \end{aligned} \tag{4.20}$$

so that

$$\begin{aligned} \partial^i\phi_0\partial^i\phi_0 &= \Big(\frac{dw}{dr}\Big)^2 \frac{x_i x_i}{r^2}\sin^2\Big(\frac{w}{f_w}\Big) \\ &= \Big(\frac{dw}{dr}\Big)^2 \sin^2\Big(\frac{w}{f_w}\Big). \end{aligned} \tag{4.21}$$

Next up is

$$\begin{aligned} \partial^i\phi_j &= f_w \frac{\partial}{\partial x_i}\left(\hat{r}_j \sin\Big(\frac{w}{f_w}\Big)\right) \\ &= f_w\left(\frac{\partial \hat{r}_j}{\partial x_i}\sin\Big(\frac{w}{f_w}\Big) + \hat{r}_j\frac{1}{f_w}\frac{dw}{dr}\frac{x_i}{r}\cos\Big(\frac{w}{f_w}\Big)\right), \end{aligned} \tag{4.22}$$

where

$$\begin{aligned} \frac{\partial \hat{r}_j}{\partial x_i} &= \frac{\partial}{\partial x_i}\Big(\frac{x_j}{r}\Big) \\ &= \frac{\delta_{ij}}{r} - \frac{x_i x_j}{r^3}. \end{aligned} \tag{4.23}$$

Therefore

$$\begin{aligned} \partial^i\phi_j\partial^i\phi_j = f_w^2\Bigg(&\frac{3}{r^2}\sin^2\Big(\frac{w}{f_w}\Big) + \frac{x_i x_j x_i x_j}{r^6}\sin^2\Big(\frac{w}{f_w}\Big) \\ &+ \frac{x_i x_i}{f_w^2 r^2}\Big(\frac{dw}{dr}\Big)^2\cos^2\Big(\frac{w}{f_w}\Big) - 2\frac{x_i x_i}{r^4}\sin^2\Big(\frac{w}{f_w}\Big) \\ &+ 2\frac{\hat{r}_i x_i}{f_w r^2}\frac{dw}{dr}\cos\Big(\frac{w}{f_w}\Big)\sin\Big(\frac{w}{f_w}\Big) \\ &- 2\frac{x_i x_j x_i \hat{r}_j}{f_w r^4}\frac{dw}{dr}\cos\Big(\frac{w}{f_w}\Big)\sin\Big(\frac{w}{f_w}\Big)\Bigg) \\ = \frac{2f_w^2}{r^2}\sin^2\Big(\frac{w}{f_w}\Big) &+ \Big(\frac{dw}{dr}\Big)^2\cos^2\Big(\frac{w}{f_w}\Big). \end{aligned} \tag{4.24}$$

All of this results in

$$\mathrm{Tr}(\partial_\mu U \partial^\mu U^\dagger) = -2\left(\frac{1}{f_w^2}\Big(\frac{dw}{dr}\Big)^2 + 2\frac{\sin^2(\frac{w}{f_w})}{r^2}\right). \tag{4.25}$$

As for the quartic term in the Skyrme Lagrangian, first note that

$$\partial^\mu U^\dagger U = -U^\dagger \partial^\mu U \tag{4.26}$$

because

$$\partial^\mu (U^\dagger U) = 0. \tag{4.27}$$

Then

$$\begin{aligned}[U^\dagger \partial^\mu U, U^\dagger \partial^\nu U] &= U^\dagger \partial^\mu U U^\dagger \partial^\nu U - U^\dagger \partial_\nu U U^{\dagger\mu} U \\ &= -\partial^\mu U^\dagger \partial^\nu U + \partial^\nu U^\dagger \partial^\mu U \\ &= -\partial^i U^\dagger \partial^j U + \partial^j U^\dagger \partial^i U.\end{aligned} \tag{4.28}$$

The rest of the derivation is tedious but involves similar logic for the derivation of the first term. For this reason, only the result is shown here:

$$\mathrm{Tr}[U^\dagger \partial_\mu U, U^\dagger \partial_\nu U]^2 = -16\frac{\sin^2(\frac{w}{f_w})}{r^2}\left(\frac{2}{f_w^2}\Big(\frac{dw}{dr}\Big)^2 + \frac{\sin^2(\frac{w}{f_w})}{r^2}\right). \tag{4.29}$$

The entire hedgehog Skyrme Lagrangian is

$$\mathcal{L}_S = -\frac{1}{2}\Big(\frac{dw}{dr}\Big)^2 - f_w^2\frac{\sin^2(\frac{w}{f_w})}{r^2} - \frac{1}{g^2 f_w^2}\frac{\sin^2(\frac{w}{f_w})}{r^2}\Big(\frac{dw}{dr}\Big)^2 - \frac{1}{2g^2}\frac{\sin^4(\frac{w}{f_w})}{r^4}. \tag{4.30}$$

Looking towards the equation of motion for this Lagrangian now, the action to be minimized is

$$\begin{aligned}S &= \int \mathcal{L}_S d^4x \\ &= -\int E dt\end{aligned} \tag{4.31}$$

where the static nature of the soliton has been used (see Eqs. (4.7) and (4.8)). This means that to minimize the action, the energy must be minimized:

$$\begin{aligned}0 &= -\delta E \\ &= \delta \int \mathcal{L}_S d^3x \\ &= 4\pi\delta \int r^2 \mathcal{L}_S dr \\ &= 4\pi \int \left(\frac{\partial(r^2\mathcal{L}_S)}{\partial w} - \partial_r\Big(\frac{\partial(r^2\mathcal{L}_S)}{\partial(\partial_r w)}\Big)\right)\delta w dr.\end{aligned} \tag{4.32}$$

Note that $\delta w(r=0) = \delta w(r\to\infty) = 0$ has been imposed. This yields the equation of motion

$$\frac{\partial(r^2\mathcal{L}_S)}{\partial w} - \partial_r\Big(\frac{\partial(r^2\mathcal{L}_S)}{\partial(\partial_r w)}\Big) = 0. \tag{4.33}$$

Equivalently,

$$\begin{aligned}0 = \frac{d^2w}{dr^2}\left(r^2 + \frac{2}{g^2 f_w^2}\sin^2\Big(\frac{2w}{f_w}\Big)\right) + 2r\frac{dw}{dr} + \frac{1}{g^2 f_w^3}\Big(\frac{dw}{dr}\Big)^2 \sin\Big(\frac{2w}{f_w}\Big) \\ - f_w \sin\Big(\frac{2w}{f_w}\Big) - \frac{1}{g^2 f_w}\frac{1}{r^2}\sin^2\Big(\frac{2w}{f_w}\Big)\sin\Big(\frac{2w}{f_w}\Big).\end{aligned} \tag{4.34}$$

The solution $w_S(r)$, also known as the skyrmion profile function, has yet to be determined analytically but a semi-analytic approximation exists,

$$w_S(r) = \frac{2}{f_w} \arccos\left[1 - \exp\left(-\frac{\sqrt{2}}{0.94510062} g_V f_w r\right)\right], \tag{4.35}$$

which is plotted in Figure 4.1. Using approximations for the profile function in the energy functional, it is

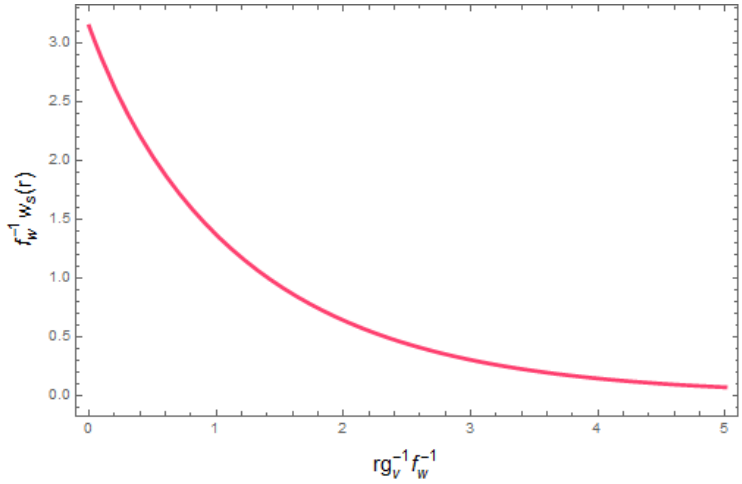

Figure 4.1: The hedgehog skyrmion profile function

possible to determine a natural length scale

$$L_S \simeq \frac{1.2}{g_V f_w} \tag{4.36}$$

and the skyrmion mass

$$M_S \simeq 73 \frac{f_w}{g_V}. \tag{4.37}$$

The hedgehog ansatz is a very helpful one because it makes it easy to find the equation of motion for a hedgehog skyrmion. This equation of motion, or profile function, may not have a known analytic solution but approximate solutions exist and provide helpful results.

Chapter 5

Phase Transitions

Spontaneous symmetry breaking marks a phase transition, which begins to occur at what is called the critical temperature. That is, the critical temperature corresponds to the formation of the true minimum of the potential. Before the potential can be properly analyzed, quantum corrections must first be taken into account. Depending on the shape of the potential, there may be a potential barrier between the false and true minima at the beginning of the phase transition. If this happens, the phase transition is called a First Order phase transition. On the other hand, if there is no potential barrier at the critical temperature, the phase transition is a Second Order, or continuous, phase transition.

5.1 Effective Potential

Before calculating the critical temperature, quantum corrections to the classical potential $V(\phi)$ must be taken into account [26](pp.195-259), [10](pp.37-53). The corrected potential is called the effective potential, $V_{\text{eff}}(\phi)$. It can be expressed as the sum of the classical potential and the contributions from Feynman diagrams with n loops, $V_n(\phi)$. That is,

$$V_{\text{eff}}(\phi) = V(\phi) + V_1(\phi) + V_2(\phi) + \dots \quad . \tag{5.1}$$

Replacing the Green's functions in $V_{\text{eff}}(\phi)$ with finite-temperature Green's functions yields the finite-temperature effective potential, $V_{\text{eff}}(\phi, T)$. The finite-temperature effective potential can be equated with the free energy density. This can be expressed to the lowest order (one-loop) as

$$V_{\text{eff}}(\phi, T) = V(\phi) + \sum_n F_n(\phi, T), \tag{5.2}$$

with summation over particle spin states. The free energy contribution is given by

$$F_n = \pm T \int \frac{d^3k}{(2\pi)^3} \ln\left[1 \mp \exp\left(-\sqrt{k^2 + m_n^2}/T\right)\right], \tag{5.3}$$

where the upper signs are for bosons and the lower signs are for fermions. Note that the free energy is defined as

$$F = E - TS, \tag{5.4}$$

where E is the energy and S is the entropy,

$$S = -\frac{\partial F}{\partial T}. \tag{5.5}$$

For temperatures $T \ll m_n$, a good approximation for the finite-temperature effective potential is [10](pg.41)

$$V_{\text{eff}}(\phi, T) = V(\phi) + \frac{1}{24}\left(\sum_B m_n^2 + \frac{1}{2}\sum_F m_n^2\right)T^2 - \frac{\pi^2}{90}\left(\mathcal{N}_B + \frac{7}{8}\mathcal{N}_F\right)T^4, \tag{5.6}$$

where $\mathcal{N}_B$ ($\mathcal{N}_F$) is the number of bosonic (fermionic) spin states and Σ_B (Σ_F) represents summation over bosonic (fermionic) states.

5.2 First and Second Order Phase Transitions

The key difference between First and Second Order phase transitions is whether or not a potential barrier exists between the false and true minima at the critical temperature. This barrier exists for First Order phase transitions. Second Order, or continuous, phase transitions have no such barrier.

For $T \gg T_c$ there is only the false minimum because the symmetry has not yet been broken, as seen in the red curve in Figure 5.1. In a First Order phase transition, when the temperature becomes closer to T_c a second critical point appears but is less energetically favourable than the symmetric minimum (orange curve in Figure 5.1). As the temperature decreases further, the potential at the second minimum drops until the two minima become degenerate (green curve). This degeneracy occurs at $T = T_c$, marking the beginning of the phase transition. Tunnelling through the barrier is the only way for the phase transition to actually occur at the point. Decreasing the temperature further, the value of the potential at the second minimum continues to decrease. That is, for temperatures $T < T_c$, the second minimum is the global minimum (blue curve). Eventually the potential barrier disappears completely and the transition can proceed classically (purple curve).

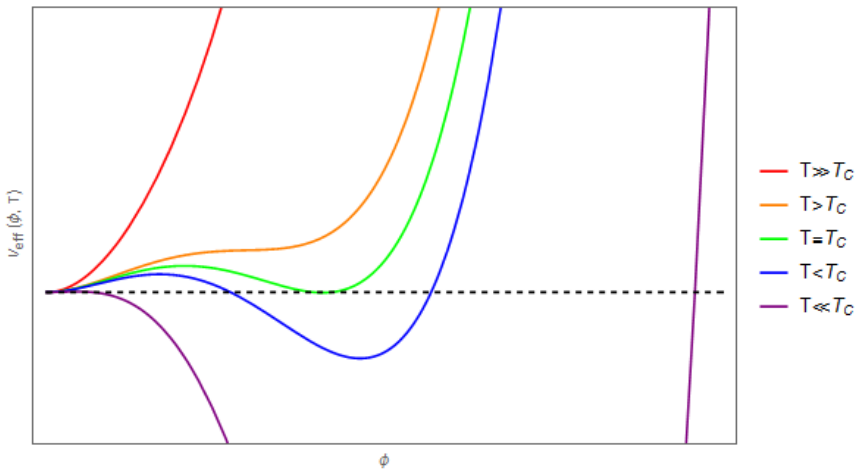

Figure 5.1: Temperature-dependent effective potential for a few temperatures, where $V_{eff}(\phi, T) = (T - 0.01)\phi^2 + 0.7(T - 5)\phi^3 + \phi^4$.

5.3 First Order Phase Transitions

First Order phase transitions [26](pp.195-259), [10](pp.37-53), [14], are characterized by a barrier between the false and true minima of the potential at the critical temperature, between which quantum tunnelling must occur for the phase transition to proceed. In 1977, S. Coleman and C.J. Callan developed a zero-temperature, field-theoretic, semiclassical description of First Order phase transitions [15], [16]. This description involves a "bounce": the system starts off in a false vacuum state, tunnels to a true vacuum state, but eventually returns to the initial state as time approaches infinity. Note that in this section, $\hbar = 1$ will NOT be used. This is because the semiclassical limit, where $\hbar$ is small, is used here.

5.3.1 Summary of Derivation

The bubble nucleation rate per volume is of the form

$$\Gamma/V = Ae^{-B/\hbar}[1 + O(\hbar)]. \tag{5.7}$$

To see this, consider a scalar field ϕ with the Lagrangian density

$$\begin{aligned}\mathcal{L} &= \frac{1}{2}\partial_\mu\phi\partial^\mu\phi - V(\phi) \\ &= \frac{1}{2}\Big(\frac{d\phi}{dt}\Big)^2 - \frac{1}{2}(\vec{\nabla}\phi)^2 - V(\phi),\end{aligned} \tag{5.8}$$

with the potential $V(\phi)$ having its relative (false) minimum at $\phi = \phi_+$ and its absolute (true) minimum at $\phi = \phi_-$. The corresponding equation of motion is

$$\partial_\mu\partial^\mu\phi + V'(\phi) = \frac{d^2\phi}{dt^2} - \nabla^2\phi + V'(\phi) = 0. \tag{5.9}$$

The first thing to do is to perform a Wick rotation which puts everything in Euclidean coordinates instead of Minkowskian coordinates. To do this, the substitution

$$t = -it_E \tag{5.10}$$

is made. This means the Euclidean Lagrangian density is

$$\mathcal{L}_E = \frac{1}{2}\Big(\frac{d\phi}{dt_E}\Big)^2 + \frac{1}{2}(\vec{\nabla}\phi)^2 + V(\phi) \tag{5.11}$$

and the Euclidean equation of motion is

$$\frac{d^2\phi}{dt_E^2} + \nabla^2\phi - V'(\phi) = 0. \tag{5.12}$$

The Euclidean action is

$$S_E(\phi) = \int\left(\frac{1}{2}\Big(\frac{d\phi}{dt_E}\Big)^2 + \frac{1}{2}(\vec{\nabla}\phi)^2 + V(\phi)\right)d^3x dt_E, \tag{5.13}$$

and is of particular important because the bounce is the action. The bounce boundary conditions are

$$\lim_{t_E\to\pm\infty}\phi(t_E,\vec{x}) = \phi_+, \tag{5.14}$$

$$\lim_{|\vec{x}|\to\infty}\phi(t_E,\vec{x}) = \phi_+, \tag{5.15}$$

and

$$\frac{d\phi(0,\vec{x})}{dt_E} = 0. \tag{5.16}$$

Assuming there is $O(4)$ symmetry to be taken advantage of, ϕ can be written in terms of a single variable r defined by

$$r^2 = t_E^2 + |\vec{x}|^2. \tag{5.17}$$

Now the Euclidean equation of motion takes the form

$$\frac{d^2\phi}{dr^2} + \frac{3}{r}\frac{d\phi}{dr} - V'(\phi) = 0, \tag{5.18}$$

along with the Euclidean action,

$$S_E(\phi) = 2\pi^2\int_0^\infty\Big[\frac{1}{2}\Big(\frac{d\phi}{dr}\Big)^2 + V(\phi)\Big]r^3dr. \tag{5.19}$$

The boundary conditions are now

$$\lim_{r\to\infty}\phi(r) = \phi_+ \tag{5.20}$$

and

$$\frac{d\phi(0)}{dr} = 0. \tag{5.21}$$

This is the final form of the action that will be used for the bounce action.

Eq. (5.18) can provide decent insight. The initial field configuration is released from rest at $r = 0$ via the boundary condition. Several things can happen depending on what the initial field configuration is. If $\phi(r = 0)$ is to the right of but still close to ϕ_-, it will overshoot and pass ϕ_+. If $\phi(r = 0)$ is far enough to the left, it will undershoot and never reach the configuration $\phi = \phi_+$. There must be some point in between where the field eventually comes to rest at ϕ_+. This point is called the escape point ϕ_e. Note also the Eq. (5.18) has a viscous damping term which has a significant effect on the "motion" when r is small.

The exponential factor in Eq. (5.7) is the dominant factor. The other, less important, factor A is somewhat more difficult to derive. The idea is to use the path integral corresponding to the transition from ϕ_+ back to ϕ_+. Since this model is semiclassical, $\hbar$ is small and so the integrand $e^{-S_E/\hbar}$ is dominated when the Euclidean action, S_E, is minimized. Only as far as the second order terms of the Euclidean action's Taylor expansion about its zeros need be considered, as the higher order terms are higher order in $\hbar$.

Suppose that $\bar{\phi}$ minimizes S_E. The zeroth order term $S_E(\bar{\phi})/\hbar$ is a constant of path integration. The first order terms are zero by definition. Finally, the second order terms yield an eigenvalue problem. Most of these eigevalues are positive and contribute to a product of Gaussian integrals. Nonetheless, translational invariance at the centre of the bounce removes four degrees of freedom from the system and so there are four zero eigenvalues there. An eigenvalue with a zero is an eigenvalue with a node. Then the ground state (nodeless) energy eigenvalues must be negative.

Indeed, the bounce must be a saddle point of the action rather than a minimum. Analytic continuation using the steepest descent approximation method can handle this. Comparing the imaginary part of the result to what the bounce solution is expected to look like gives the bubble nucleation rate per volume

$$\Gamma/V = \left(\frac{B}{2\pi}\right)^2 \left(\frac{\det'[-\partial_{t_E}^2 - \nabla^2 + V''(\bar{\phi})]}{\det[-\partial_{t_E}^2 - \nabla^2 + V''(\phi_-)]}\right)^{-1/2} e^{-B/\hbar}, \tag{5.22}$$

where the determinant prime means the zero eigenvalues are omitted and the bounce action is given by $B = S_E(\bar{\phi})$. Eq. (5.7) now has its pieces put together.

5.3.2 Thin Wall Approximation

The bounce action must often be solved for numerically. The thin wall approximation is a method that has a closed form solution. It assumes that the energy density difference ΔV between the true and false vacua is small. This means that the initial configuration $\bar{\phi}(r = 0)$ has to be close to ϕ_- so that not much energy is lost.

This approximation assumes $\bar{\phi}(r)$ continues to stay close to ϕ_- until large $r = R$ at which time a bubble of radius R nucleates, containing phase space that can classically transition. The bubble expands outwards at the speed of light as the tunnelling phase transition occurs rapidly; this means the bubble wall doesn't have much time to grow, hence the name "thin wall approximation". Only for this short period of time is the thin wall solution $\bar{\phi}(r) = \phi^{TW}(r)$ valid. Afterwards, the field gradually returns to ϕ_+ at infinity.

The damping term in Eq. (5.18) can be ignored because $r \approx R$ is large. Define $V_+(\phi) = V(\phi) + \Delta V$. Keeping in mind that ΔV is essentially constant during the short bounce period, the resulting equation of motion is

$$\frac{d^2\bar{\phi}}{dr^2} = V_+^{'}(\bar{\phi}) \tag{5.23}$$

which means that

$$\frac{d\bar{\phi}}{dr} = \sqrt{2V_+(\bar{\phi})}. \tag{5.24}$$

Substituting this into the bounce action Eq. (5.19) yields

$$\begin{aligned} S_E(\bar{\phi}) &= 2\pi^2 \int (2V_+(\bar{\phi}) - \Delta V) r^3 dr \\ &= -\frac{1}{2}\pi^2 R^4 \Delta V + 2\pi^2 R^3 \int_{\phi_-}^{\phi_+} \sqrt{2V_+(\phi)} d\phi. \end{aligned} \tag{5.25}$$

Note that the R^3 term is the contribution from inside the bubble and the R^4 term is the contribution from the bubble surface. The bubble radius R can be found by minimizing the variation with respect to R:

$$\begin{aligned} 0 &= \frac{dS_E}{dR} \\ &= -2\pi^2 R^3 \Delta V + 6\pi^2 R^2 \int_{\phi_-}^{\phi_+} \sqrt{2V_+(\phi)} d\phi \end{aligned} \tag{5.26}$$

so

$$R = \frac{3}{\Delta V} \int_{\phi_-}^{\phi_+} \sqrt{2V_+(\phi)} d\phi. \tag{5.27}$$

And finally, substituting this back into the bounce action yields

$$B = S_E = \frac{27\pi^2}{2(\Delta V)^3} \left(\int_{\phi_-}^{\phi_+} \sqrt{2V_+(\phi)} d\phi \right)^4. \tag{5.28}$$

This is the desired closed form solution of the bounce action in the thin wall approximation.

5.3.3 Finite Temperature

The above discussion is restricted to the case of the potential at zero temperature. If the temperature is high enough that thermal fluctuations must be taken into consideration, the bubble nucleation rate per volume is [17]

$$\Gamma/V = \frac{\omega_-}{\pi} \left(\frac{S_3}{2\pi\mathcal{T}} \right)^{3/2} \left(\frac{\det'[-\nabla^2 + V''(\bar{\phi}, T)]}{\det[-\nabla^2 + V''(0, T)]} \right)^{-1/2} e^{-S_3/\mathcal{T}}, \tag{5.29}$$

where S_3 is the 3-D Euclidean action, $\mathcal{T}^{-1}$ is the period from integration over imaginary time, $V(\phi, T)$ is the temperature-dependent potential, and ω_- is the unstable mode frequency. Explicitly the 3-D Euclidean action is

$$S_3(\phi) = \int \Big[\frac{1}{2} (\nabla^2 \phi)^2 + V(\phi, T) \Big] d^3x. \tag{5.30}$$

When the temperature is high enough, the equation of motion has $O(3)$ symmetry so the spatial coordinates can be replaced by $s^2 = \boldsymbol{x}^2$. The equation of motion takes the form

$$\frac{d^2\phi}{ds^2} + \frac{2}{s}\frac{d\phi}{ds} - \frac{\partial V(\phi, T)}{\partial \phi} = 0, \tag{5.31}$$

the action becomes

$$S_3 = 4\pi \int \Big[\frac{1}{2} \Big(\frac{d\phi}{ds} \Big)^2 + V(\phi, T) \Big] d^3x, \tag{5.32}$$

and the boundary conditions are

$$\lim_{s \to \infty} \phi(s) = \phi_+, \tag{5.33}$$

and

$$\frac{d\phi(s=0)}{ds} = 0. \tag{5.34}$$

5.4 Second Order Phase Transitions

Second order, or continuous, phase transitions do not have any potential barriers and are described by the Kibble-Zurek mechanism [18], [19], [20], [21], [22]. Topological defects form because uncorrelated patches of the system (the universe) have different vacuum expecation values, as no point on the vacuum manifold is preferred over another. The correlation length ξ determines how far apart topological defects form. The skyrmion number density produced due to a continuous phase transition would be $n_S \sim 1/\xi^3$. Causality requires that the correlation length is bounded by the horizon distance. The correlation time, or relaxation time, τ is the temporal equivalent of the correlation length and determines how much time is available for the vacuum expectation value to smooth itself out. Both the correlation length and relaxation time diverge at the critical temperature.

The temperature parameter ϵ is used to describe how close the temperature is to the critical temperature T_c and is given by

$$\epsilon = \frac{T_c - T}{T_c}. \tag{5.35}$$

This is used to express both the correlation length and relaxation time:

$$\xi = \xi_0 |\epsilon|^{-\nu}, \tag{5.36}$$

$$\tau = \tau_0 |\epsilon|^{-\mu}, \tag{5.37}$$

where μ and ν are critical exponents. As discussed by Murayama and Shu [23], $\mu = \nu = 2/3$ is appropriate for pointlike topological defects such as skyrmions.

It is assumed that the temperature parameter changes linearly with time over a timescale τ_Q called the quench time. That is,

$$\epsilon = \frac{t}{\tau_Q}. \tag{5.38}$$

Note that $t = 0$ corresponds to the critical temperature.

Once the critical temperature has been reached, the correlation length becomes fixed after the freeze-out time $\hat{t}$ has elapsed. Before the freeze-out time, the relaxation time is large enough that there is time for fluctuations in the vacuum expectation value to smooth out. After the freeze-out time, the relaxation time is too small for fluctuations to smooth out. Therefore, the topological defects are frozen with number density corresponding to the correlation length at the freeze-out time.

To determine the freeze-out time, note that it must be equal to the relaxation time at the freeze-out time. That is,

$$\tau(\hat{t}) = \tau_0 \Big(\frac{\hat{t}}{\tau_Q} \Big)^{-\mu} = \hat{t}, \tag{5.39}$$

as seen in Figure 5.2. Therefore, the freeze-out time is

$$\hat{t} = (\tau_0 \tau_Q^{\mu})^{\frac{1}{1+\mu}}. \tag{5.40}$$

This means the correlation length determining the number density of defects formed is

$$\begin{aligned} \xi(\hat{t}) &= \xi_0 \Big(\frac{\hat{t}}{\tau_Q} \Big)^{-\nu} \\ &= \xi_0 \Big(\tau_0^{\frac{1}{1+\mu}} \tau_Q^{\frac{\mu}{1+\mu} - 1} \Big)^{-\nu} \\ &= \xi_0 \Big(\frac{\tau_Q}{\tau_0} \Big)^{\frac{\nu}{1+\mu}}. \end{aligned} \tag{5.41}$$

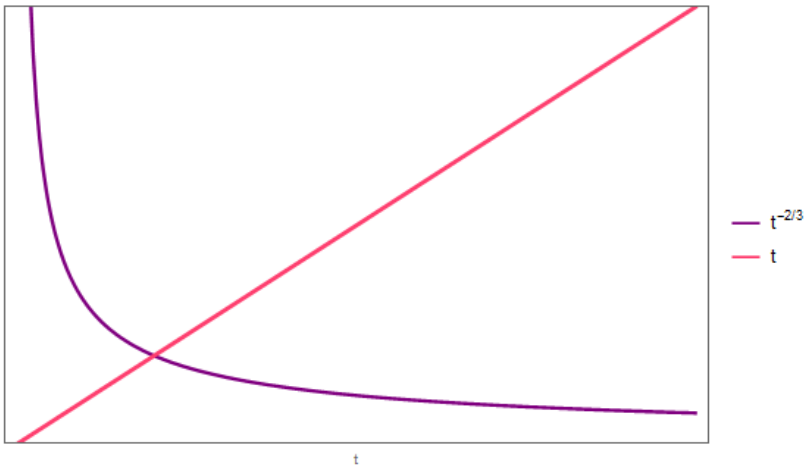

Figure 5.2: The relaxation time is equal to the linear function t at the critical temperature. Here $\tau(t) = t^{-2/3}$ is used.

Chapter 6

Dark Matter

Dark matter is the most abundant type of matter in the universe. It is nonbaryonic and does not interact with light but it is known to exist due to its gravitational effects. It could have been created in the early universe either thermally or non-thermally. Thermally created dark matter would have had to decouple from the early universe heat bath in a process called freeze-out. Non-thermal dark matter would have been created as topological defects from an early universe phase transition.

6.1 Cosmology

To adequately discuss dark matter, the context must first be laid out. This context is our universe [24](pp.1-100), [25](pp.49-101), [26](pp.29-86), [4]. It is isotropic and homogeneous so its geometry can be described using the Robertson-Walker metric,

$$\begin{aligned} d\tau^2 &= g_{\mu\nu}dx^\mu dx^\nu \\ &= dt^2 - a^2(t)\Big(\frac{dr^2}{1-\kappa r^2} + r^2 d\Omega\Big), \end{aligned} \tag{6.1}$$

where $a(t)$ is the scale factor and κ is the curvature. The Planck satellite data suggests that this metric provides a good description of our universe [27]. Positive curvature means the universe is spherical (closed), negative curvature means the universe is hyperbolic (open), and $\kappa = 0$ means the universe is flat. The scale factor describes how the universe expands or contracts over time.

The gravitational field equations are

$$R_{\mu\nu} - \frac{1}{2}g_{\mu\nu}g^{\lambda\kappa}R_{\lambda\kappa} = -8\pi G T_{\mu\nu}. \tag{6.2}$$

In this equation, $R_{\mu\nu}$ is the Ricci tensor, $T_{\mu\nu}$ is the energy-momentum tensor, and G is the gravitational constant. This implies the Friedmann equation,

$$\Big(\frac{\dot{a}}{a}\Big)^2 = \frac{8\pi G\rho}{3} - \frac{\kappa}{a^2}, \tag{6.3}$$

where $\rho = \rho(t)$ is the proper energy density. The Friedmann equation describes the expansion of the universe. The expansion rate of the universe is called the Hubble parameter H, given by

$$H(t) = \frac{\dot{a}(t)}{a(t)}. \tag{6.4}$$

The Hubble parameter evaluated right now, $t = t_0$, is called the Hubble constant, $H_0 \equiv H(t_0)$. It is often convenient to use the dimensionless quantity h defined by

$$H_0 = 100h\text{kms}^{-1}\text{Mpc}^{-1}. \tag{6.5}$$

The critical energy density is

$$\rho_{cr} = \frac{3H^2}{8\pi G} \tag{6.6}$$

which, when compared with the energy density $\rho(t)$, dictates the curvature of the universe via the Friedmann equation. Defining the dimensionless density parameter

$$\Omega(t) = \frac{\rho(t)}{\rho_{cr}(t)}, \tag{6.7}$$

gives the Friedmann equation the following form:

$$\Omega(t) - 1 = \frac{\kappa}{a^2(t)H^2(t)}. \tag{6.8}$$

However, observations indicate that the universe is flat, or at least very close to it, so that it is safe to put $\kappa = 0$. Therefore, the density parameters of all constituents of the universe add to unity. The largest density parameter is that of the cosmological constant Λ which is responsible for the accelerated expansion of the universe with $\Omega_\Lambda \approx 0.70$. The next largest contributor is cold dark matter with $\Omega_c \approx 0.25$. Baryonic matter contributes the third largest amount with $\Omega_b \approx 0.05$. The remaining constituents contribute even less.

Another equation relating $\rho(t)$ and $a(t)$, along with the proper pressure $p(t)$, is the fluid equation

$$\dot{\rho} + 3H(p + \rho) = 0, \tag{6.9}$$

which is a conservation law that comes from the gravitational field equations. There is also the equation of state that relates the pressure and energy density,

$$p = w\rho, \tag{6.10}$$

where radiation has $w = 1/3$, matter is pressureless so has $w = 0$, and vacuum energy has $w = -1$. Combining the equation of state with the fluid equation yields

$$\int_\rho^{\rho_0} \frac{1}{\rho} d\rho = -3(1 + w) \int_a^{a_0} \frac{1}{a} da, \tag{6.11}$$

which implies

$$\frac{\rho}{\rho_0} = \Big(\frac{a}{a_0}\Big)^{-3(1+w)}. \tag{6.12}$$

This is only the case for a universe that is dominated by a single component. The early universe was very hot, and thus, radiation-dominated so that

$$\rho = \rho_{0,r}\Big(\frac{a}{a_{0,r}}\Big)^{-4}. \tag{6.13}$$

The r in the subscripts is there as a reminder that these would be the present values for a radiation dominated universe. Putting this into the Friedmann equation for a spatially flat universe yields

$$\frac{\dot{a}^2}{a^2} = H_{0,r}^2\Big(\frac{a_{0,r}}{a}\Big)^4 \tag{6.14}$$

and so

$$\int_0^a \frac{a}{a_{0,r}^2} da = \int_0^t H_{0,r} dt, \tag{6.15}$$

resulting in

$$a(t) = a_{0,r}\sqrt{2H_{0,r}t}. \tag{6.16}$$

This has time derivative

$$\dot{a}(t) = \frac{1}{2} a_{0,r}\sqrt{\frac{2H_{0,r}}{t}} \tag{6.17}$$

which means

$$\begin{aligned} H_{0,r} &= \frac{\dot{a}(t_{0,r})}{a(t_{0,r})} \\ &= \frac{1}{2t_{0,r}}. \end{aligned} \tag{6.18}$$

Putting this back into the scale factor equation gives

$$a(t) = a_{0,r}\sqrt{\frac{t}{t_{0,r}}}. \tag{6.19}$$

During radiation domination, the time and temperature were related by the equation, [10](pg.12),

$$tT^2 = \frac{3}{4\pi} m_{Pl}\sqrt{\frac{5}{\pi g_*(T)}}, \tag{6.20}$$

where m_{Pl} is the Planck mass, and $g_*(T)$ is the number of relativistic degrees of freedom which is given by

$$g_* = \sum_{b=bosons} g_b\Big(\frac{T_b}{T}\Big)^4 + \frac{7}{8}\sum_{f=fermions} g_f\Big(\frac{T_f}{T}\Big)^4. \tag{6.21}$$

Another important quantity is the entropy,

$$S = a^3\frac{\rho + p}{T}. \tag{6.22}$$

It is used to define the entropy density,

$$s = \frac{S}{a^3} = \frac{\rho + p}{T}, \tag{6.23}$$

which is dominated by relativistic particles. Taking advantage of this gives the very good approximation

$$s = \frac{2\pi^2}{45} g_{*S} T^3, \tag{6.24}$$

where g_{*S} is the degrees of freedom counted in the above expressed for the entropy density. Specifically,

$$g_{*S} = \sum_{b=bosons} g_b\Big(\frac{T_b}{T}\Big)^3 + \frac{7}{8}\sum_{f=fermions} g_f\Big(\frac{T_f}{T}\Big)^3. \tag{6.25}$$

The universe is observed to be expanding. Suppose a wave crest of light emitted from r_e at time t_e along the radial direction reaches an observer at $r = 0$ at time t_0. Light has $d\tau^2 = 0$ and if it is travelling along the radial direction then $d\Omega = 0$ and Eq. (6.1) becomes

$$dt = -a(t)\frac{dr}{\sqrt{1 - \kappa r^2}}. \tag{6.26}$$

When taking the square root of dt^2, the negative root is taken because as the time increases, the distance between the observer and the wave crest decreases. Therefore

$$\int_{t_e}^{t_0} \frac{dt}{a(t)} = \int_0^{r_e} \frac{dr}{\sqrt{1 - \kappa r^2}}. \tag{6.27}$$

If the light source has wavelength λ_e, then a second wave crest will be emitted at $t_e + \lambda_e$. It will reach the observer at $t_0 + \lambda_0$. If the size of the universe is not constant, then $\lambda_e \neq \lambda_0$. The equation corresponding to this second wave crest is

$$\int_{t_e+\lambda_e}^{t_0+\lambda_0} \frac{dt}{a(t)} = \int_0^{r_e} \frac{dr}{\sqrt{1 - \kappa r^2}}. \tag{6.28}$$

The right hand sides of Eqs. (6.27) and (6.28) indicate that the two equations are equal. Therefore

$$\int_{t_e}^{t_0} \frac{dt}{a(t)} + \int_{t_0}^{t_e+\lambda_e} \frac{dt}{a(t)} = -\int_{t_0+\lambda_0}^{t_e+\lambda_e} \frac{dt}{a(t)} - \int_{t_e+\lambda_e}^{t_0} \frac{dt}{a(t)}, \tag{6.29}$$

which simplifies to

$$\int_{t_e}^{t_e+\lambda_e} \frac{dt}{a(t)} = \int_{t_0}^{t_0+\lambda_0} \frac{dt}{a(t)}. \tag{6.30}$$

The time between wave crest emissions is very small compared to the age of the universe so $a(t_e) \approx a(t_e) + \lambda_e$ and $a(t_0) \approx a(t_0) + \lambda_0$. It is safe to take the scale factor to be constant between emissions. Eq. (6.30) becomes

$$\frac{\lambda_e}{a(t_e)} = \frac{\lambda_0}{a(t_0)}. \tag{6.31}$$

Define the redshift z as

$$z \equiv \frac{\lambda_0 - \lambda_e}{\lambda_e} \tag{6.32}$$

so that Eq. (6.31) can be expressed as

$$1 + z = \frac{a(t_0)}{a(t_e)} \tag{6.33}$$

The frequency of light from a distant source should be shifted one way or the other, depending on whether $a(t)$ is increasing or decreasing. If the universe is contracting, then light that reaches an observer will be more blue than when it was emitted. The universe is expanding, so red shifts are observed. Hubble's law states

$$H_0 d = z + \frac{1}{2}\Big(1 + \frac{\ddot{a}_0}{\dot{a}_0^2} a_0\Big) z^2 + \dots \tag{6.34}$$

and accordingly, nearby objects have a roughly linear relation between redshift and distance.

6.2 Evidence for Dark Matter

There are a variety of sources that provide evidence for dark matter [25](pp.123-141), [26](pp.16-21). Observations of the motion of galaxies and galaxy clusters as well as gravitational lensing strongly indicate the presence of something that interacts only gravitationally.

Kepler's 3rd Law describes orbital motion and can be used to detect dark matter in spiral galaxies. A star of mass m with orbital speed v whose distance is R from the galactic centre experiences the centripetal force

$$F_c = m\frac{v^2}{R}. \tag{6.35}$$

The gravitational force between the star and the mass $M(R)$ contained within the star's orbit is approximately

$$F_g = \frac{GmM(R)}{R^2} \tag{6.36}$$

and is responsible for the centripetal force. Therefore

$$v = \sqrt{\frac{GM(R)}{R}}. \tag{6.37}$$

For sufficiently large R, most of the galaxy's stars are contained within that radius. Assuming that the galaxy's mass comes primarily from its stars, $M(R)$ becomes close to constant far from the galactic centre. This means that the orbital velocity of stars on the galaxy's visible outskirts should decrease like $v \propto R^{-1/2}$. However, this has not been observed to be the case. Instead, measured orbital speeds indicate that $M(R)$ continues to increase past the visible region of stars in most or all spiral galaxies.

The effects of dark matter can also be observed in clusters of galaxies [24](pp.66-69). F. Zwicky used the term "dunkle Materie", which means "dark matter" in English, to account for what was holding the Coma

cluster together in his work on galaxy clusters in 1933 [1]. A system of gravitionally bound point masses, in this case galaxies in a cluster, is called virialized if it obeys the virial theorem,

$$2T + V = 0. \tag{6.38}$$

Irregular clusters such as the Virgo cluster do not seem to meet the virialized conidition. If the total mass of the system is M, then the kinetic energy of the system is

$$T = \frac{1}{2} M \langle v^2 \rangle \tag{6.39}$$

in terms of the mass-weighted mean square velocity $\langle v^2 \rangle$. The potential energy, in terms of the mean inverse separation $\langle r^{-1} \rangle$, is

$$V = -\frac{1}{2} G M^2 \langle r^{-1} \rangle . \tag{6.40}$$

The virial theorem may therefore be expressed as

$$M = \frac{2 \langle v^2 \rangle}{G \langle r^{-1} \rangle}. \tag{6.41}$$

The mass-to-light ratio of galaxy clusters including the Coma cluster determined using the virial theorem is much greater than that of individual galaxies in the clusters. Mass estimates of clusters determined by how much gravitational lensing a cluster causes generally agree with estimates using the virial theorem.

The existence of the bullet cluster [24](pg.186), [28] is excellent evidence for dark matter. It consists of two subclusters that had previously collided but continue on their original paths. In between the subclusters is a cloud of hot X-ray emitting gas, left over from the collision. The gravitational lensing effects of the bullet cluster indicates that most of its mass is concentrated in two subclusters and not the centre. Therefore most of the mass of the colliding galaxy clusters did not interact, other than gravitationally. An image of the bullet cluster can be seen in Figure 6.1.

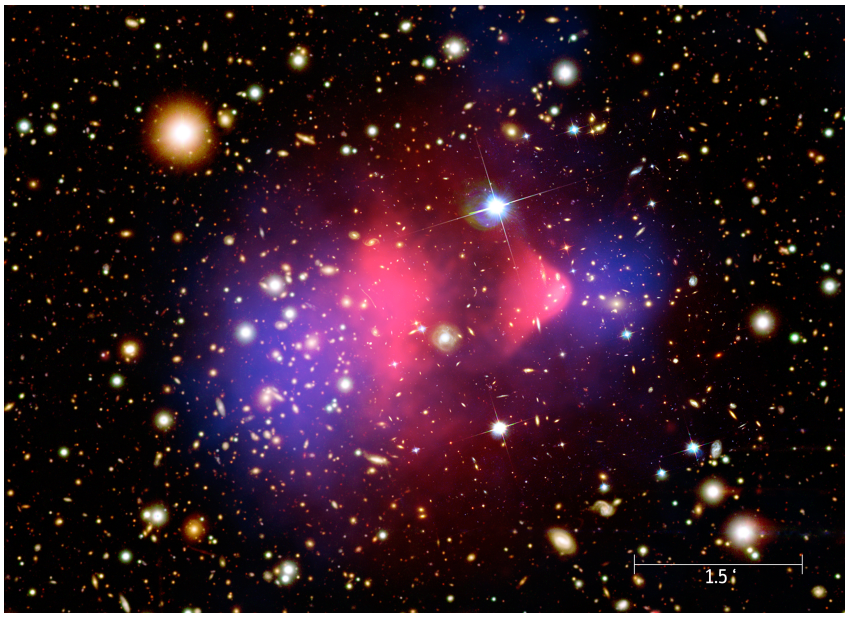

Figure 6.1: X-ray image (pink) and matter distribution (blue) of the bullet cluster over visible light image (NASA/CXC/M. Weiss, https://chandra.harvard.edu/photo/2006/1e0657/more.html).

6.3 Freeze-Out Thermodynamics

The very early universe was in thermal equilibrium[26](pp.60-64). As it cooled off, particle species decoupled from the thermal equilibrium soup in a process called freeze-out [26](pp.115-156), [29]. Freeze-out occurs when the Hubble parameter becomes greater than a particles interaction rate with other particles in thermal equilbrium,

$$\Gamma = n \langle \sigma v \rangle , \tag{6.42}$$

where n is the number density of the particle and $\langle \sigma v \rangle$ is its velocity-weighted scattering cross section.

The distribution function f describes the phase space distribution of particles. For Fermi-Dirac and Bose-Einstein statistics, the distribution function for a particle species with mass m, temperature T, and chemical potential μ is

$$f(\boldsymbol{p}) = \frac{1}{e^{(E-\mu)/T} \pm 1}, \tag{6.43}$$

where the $+$ sign is for fermions and the $-$ sign is for bosons. Particles with g internal degrees of freedom have number density

$$n = \frac{g}{(2\pi)^3} \int f d^3p. \tag{6.44}$$

The number density of relativistic particles ($m \ll T$) with $\mu \ll T$ in thermal equilibrium is

$$n = \frac{\zeta(3)}{\pi^2} g_{eff} T^3, \tag{6.45}$$

where $\zeta(s)$ is the Riemann-zeta function and the effective degrees of freedom g_{eff} is equal to the degrees of freedom g for bosons or $3g/4$ for fermions. Non-relativistic particles ($m \gg T$) in thermal equilibrium have number density

$$g\Big(\frac{mT}{2\pi}\Big)^{3/2} e^{-(m-\mu)/T}. \tag{6.46}$$

To properly discuss the thermodynamics of freeze-out, equilibrium thermodynamics cannot be used. The Boltzmann equation describes non-equilibrium thermodynamics, and is given by,

$$\hat{\boldsymbol{L}}[f] = \boldsymbol{C}[f], \tag{6.47}$$

where $\hat{\boldsymbol{L}}$ is the Liouville operator and $\boldsymbol{C}$ is the collision operator. The relativistic covariant Liouville operator is

$$\hat{\boldsymbol{L}} = p^\alpha \frac{\partial}{\partial x^\alpha} - \Gamma^\alpha_{\beta\gamma} p^\beta p^\gamma \frac{\partial}{\partial p^\alpha}. \tag{6.48}$$

The FRW model is spatially homogeneous and isotropic, so the distribution of particles should depend only on $x^0 = t$ and $p^0 = E$. This reduces the Liouville operator to

$$\hat{\boldsymbol{L}} = E\frac{\partial}{\partial t} - H|\boldsymbol{p}|^2 \frac{\partial}{\partial E}. \tag{6.49}$$

where H is the Hubble parameter. The next step is to divide the the Boltzmann equation by E and integrate over the 3-momentum portion of the phase space, then multiply by the number of internal degrees of freedom g. This is simplified by $E^2 = \boldsymbol{p}^2 + m^2$. In spherical coordinates, there is radial symmetry, where the radius is $|\boldsymbol{p}|$. Additionally, $E\partial E = |\boldsymbol{p}|\partial|\boldsymbol{p}|$. Then

$$\begin{aligned}
\frac{g}{(2\pi)^3} \int \frac{1}{E} \boldsymbol{C}[f] d^3p &= \frac{g}{(2\pi)^3} \int \frac{\partial f}{\partial t} d^3p - H \frac{g}{(2\pi)^3} \int |\boldsymbol{p}|^2 \frac{1}{E} \frac{\partial f}{\partial E} d^3p \\
&= \dot{n} - H \frac{g}{(2\pi)^3} \int |\boldsymbol{p}|^4 \frac{1}{E} \frac{\partial f}{\partial E} d|\boldsymbol{p}| d\Omega \\
&= \dot{n} - 4\pi H \frac{g}{(2\pi)^3} \int |\boldsymbol{p}|^3 \frac{\partial f}{\partial |\boldsymbol{p}|} d|\boldsymbol{p}| \\
&= \dot{n} + 3Hn,
\end{aligned} \tag{6.50}$$

where, in the last step, integration by parts was used.

Now consider a process where the particle species ψ is one of the initial particles. Then the collision term is

$$\begin{aligned}\frac{g}{(2\pi)^3}\int \boldsymbol{C}[f]\frac{d^3p_\psi}{E_\psi} = &-\int\left(\prod_{j=i,f} d\Pi_j\right)(2\pi)^4\delta^4\left(\sum_{initial} p_i - \sum_{final} p_f\right)\\ &\times\left(|\mathcal{M}|^2_{initial\to final}\prod_{initial} f_i\prod_{final}(1\pm f_f)\right.\\ &\left.-|\mathcal{M}|^2_{final\to initial}\prod_{final} f_f\prod_{initial}(1\pm f_i)\right),\end{aligned} \tag{6.51}$$

where $+$ is for bosons, $-$ is for fermions, and

$$d\Pi = \frac{g}{(2\pi)^{3/2}}\frac{d^3p}{2E}. \tag{6.52}$$

Note that the matrix element squared, $|\mathcal{M}|^2$, is the same regardless of the direction of the process. In other words, invariance under time reversal is assumed. Another helpful simplification is that the temperature is high enough that there is no Bose-Einstein condensate nor Fermi degeneracy. This means that the distribution function is small compared to unity and Maxwell-Boltzmann statistics can be used. The Maxwell-Boltzmann distribution function is simply

$$f_i(E_i) = \exp\Big(-\frac{E_i-\mu_i}{T}\Big). \tag{6.53}$$

The Boltzmann equation therefore reduces to

$$\begin{aligned}\dot{n}_\psi + 3Hn_\psi = &-\int\left(\prod_{j=i,f} d\Pi_j\right)(2\pi)^4\delta^4\left(\sum_{initial} p_i - \sum_{final} p_f\right)\\ &\times|\mathcal{M}|^2\left(\prod_{initial} f_i - \prod_{final} f_f\right).\end{aligned} \tag{6.54}$$

At this point, consider a massive stable particle species ψ. Because it is stable, the only reaction to consider is ψ annihilating with its antiparticle $\bar{\psi}$ into another particle-antiparticle pair, say X and $\bar{X}$ (as well as the inverse reaction). That is, in a comoving volume, only

$$\psi\bar{\psi} \rightleftharpoons X\bar{X} \tag{6.55}$$

changes the number of ψ and $\bar{\psi}$.

It is assumed that even when ψ freezes out, X and $\bar{X}$ remain in equilibrium via other interactions. Furthermore, the principle of detailed balance states that $f_X^{EQ}f_{\bar{X}}^{EQ} = f_\psi^{EQ}f_{\bar{\psi}}^{EQ}$. Then the Boltzmann equation becomes

$$\begin{aligned}\dot{n}_\psi + 3Hn_\psi = &-\int d\Pi_\psi d\Pi_{\bar{\psi}} d\Pi_X d\Pi_{\bar{X}}(2\pi)^4\\ &\times\delta^4(p_\psi + p_{\bar{\psi}} - p_X - p_{\bar{X}})|\mathcal{M}|^2(f_\psi f_{\bar{\psi}} - f_\psi^{EQ}f_{\bar{\psi}}^{EQ}).\end{aligned} \tag{6.56}$$

The non-thermal-equilibrium distribution function for ψ ($\bar{\psi}$) has a factor of $e^{\mu_\psi/T}$ ($e^{\mu_{\bar{\psi}}/T}$) which is independent of the momentum. For the sake of simplicity, it is assumed here that these species have zero chemical potential in thermal equilibrium. In other words,

$$\begin{aligned}f_\psi &= e^{\mu_\psi/T}f_\psi^{EQ}\\ &= \frac{n_\psi}{n_\psi^{EQ}}f_\psi^{EQ},\end{aligned} \tag{6.57}$$

and

$$\begin{aligned} f_{\bar{\psi}} &= e^{\mu_{\bar{\psi}}/T} f_{\bar{\psi}}^{EQ} \\ &= \frac{n_{\bar{\psi}}}{n_{\bar{\psi}}^{EQ}} f_{\bar{\psi}}^{EQ} \\ &= \frac{n_{\psi}}{n_{\psi}^{EQ}} f_{\bar{\psi}}^{EQ}. \end{aligned} \tag{6.58}$$

The Boltzmann equation can now be rewritten as

$$\dot{n}_{\psi} + 3Hn_{\psi} = -\langle \sigma_{\psi\bar{\psi}\to X\bar{X}} v \rangle [n_{\psi}^2 - (n_{\psi}^{EQ})^2], \tag{6.59}$$

where

$$\begin{aligned} \langle \sigma_{\psi\bar{\psi}\to X\bar{X}} v \rangle &= \frac{\int d^3p_1 d^3p_2 \sigma v e^{-E_1/T} e^{-E_2/T}}{\int d^3p_1 d^3p_2 e^{-E_1/T} e^{-E_2/T}} \\ &= \frac{1}{(n_{\psi}^{EQ})^2} \int d\Pi_{\psi} d\Pi_{\bar{\psi}} d\Pi_X d\Pi_{\bar{X}} (2\pi)^4 \\ &\quad \times \delta^4(p_{\psi} + p_{\bar{\psi}} - p_X - p_{\bar{X}}) |\mathcal{M}|^2 f_{\psi}^{EQ} f_{\bar{\psi}}^{EQ} \end{aligned} \tag{6.60}$$

is the velocity-weighted annihilation cross section for $\psi\bar{\psi} \to X\bar{X}$. If there is more than one annihilation channel, then the velocity-weighted cross section is the sum of the individual velocity-weighted cross sections over all annihilation channels. The thermally averaged velocity-weighted annihilation cross section for a particle with mass m at temperature T is

$$\langle \sigma v \rangle (T) = \frac{1}{8m^4 T K_2^2(m/T)} \int_{4m^2}^{\infty} ds \sigma(s) \sqrt{s} (s - 4m^2) K_1(\sqrt{s}/T), \tag{6.61}$$

where K_1 and K_2 are modified Bessel functions of the second kind.

To find the number density of a frozen-out particle species ψ, the Boltzmann equation must be solved. The number density can then be used to determine the density parameter Ω_{ψ}.

6.4 Dark Matter Detection

Dark matter can be detected [24](pp.194-196) either directly or indirectly. Indirect dark matter detection involves observing gamma rays produced from dark matter annihilation. Direct detection [30](pp.347-466),[31], [32] is the method focused on here and involves looking for nuclear recoils caused by dark matter particles scattering elastically off of a nucleus.

Consider a target of mass m_{total} in kilograms whose nuclei each have A nucleons. The total number of target nuclei is

$$K = \frac{6.02 \times 10^{26} \text{kg}^{-1} m_{total}}{A}. \tag{6.62}$$

The expected measured nucleon recoil rate is then

$$R = K \frac{\rho_D}{M} v_0 \sigma_{eff}, \tag{6.63}$$

for dark matter with mass M, average velocity v_0, and effective nucleon recoil cross section σ_{eff}. The local dark matter density depends on the local dark matter distribution. Assuming a spherical dark halo, $0.2\text{GeVcm}^{-3} \leq \rho_D \leq 0.4\text{GeVcm}^{-3}$. The local average dark matter velocity is $v_0 = 220\text{km/s}$ [4]. Constraints on the nucleon recoil rate determined from direct detection experiments therefore constrain σ_{eff}/M.

When the momentum transfer between the nucleon and the dark matter particle becomes too large, the cross section decreases. The cross section σ determined by perturbation theory does not account for this and the effective cross section must be used:

$$\sigma_{eff}(q) = \sigma F^2(q). \tag{6.64}$$

The factor $F(q)$ is called the form factor and depends on the momentum transfer

$$q = \sqrt{2m_N E_R}, \tag{6.65}$$

where m_N is the nucleon mass and E_R is the recoil energy. The recoil energy is given by

$$E_R = \frac{\mu_N^2 v^2 (1 - \cos\theta^*)}{m_N}, \tag{6.66}$$

where θ^* is the scattering angle in the centre of mass frame, v is the dark matter speed, and the reduced mass is

$$\mu_N = \frac{M m_N}{M + m_N}. \tag{6.67}$$

The effective cross section is summed over its spin-independent contributions and its spin-dependent contributions. The spin-independent contribution has the analytic Helm form factor

$$F(q) = 3\frac{j_1(qr)}{qr} e^{-q^2 s^2/2}, \tag{6.68}$$

where j_1 is the first spherical Bessel function, r is the effective nuclear radius, and $s \simeq 1$fm is the nuclear skin thickness.

One possible method for detecting dark matter is by the use of liquid noble gases such as xenon or argon [30](pp.413-436). A particle hitting the detector will cause ionization and scintillation. Scintillation is an emission of light from liquids and solids caused by the de-excitation of an ionized electron [30](pp.392-393). In two-phase detectors, the scintillation signal S_1 from the recoil is detected and the ionization electrons are moved by an electric field to the noble gas in a gaseous phase, which causes a second scintillation S_2. The ratio of S_2/S_1 is different for nuclear recoil compared to electron recoil.

Chapter 7

PeV Scale Dark Skyrmions

The results of dark matter search data can be extended to include very high masses [35]. This is because dark matter particles could lose too much kinetic energy from scattering off of particles in the Earth and the Earth's atmosphere to be detected. The kinetic energy lost decreases with mass, while it increases with scattering cross section and number of possible scattering partners. Therefore, any observed dark matter flux is dependent on the angle that it hits the detector, which is related to the dark matter mass. However, the Griest-Kamionkowski bound gives the upper limit on the mass of thermally created dark matter to be about 100TeV [36]. This limit is not a problem for non-thermally created topological defects as dark matter. Dark skyrmions created from a First Order phase transition are a possibility and could have very high masses [33]. It has been shown that dark pointlike topological defects created from a Second Order phase transition could have mass up to 10PeV or even higher [23]. This chapter follows Reference [37].

7.1 Anderson-Higgs Portal Model

The model used here is based on the one in Reference [34], where the spherically symmetric hedgehog $\boldsymbol{w}(x)$ mesons are coupled to Standard Model particles through an Anderson-Higgs portal. The Lagrangian density is

$$\mathcal{L} = \mathcal{L}_S + \mathcal{L}^{(h)}_{DSM} \tag{7.1}$$

where

$$\mathcal{L}_{\mathcal{S}} = \frac{1}{16 g_V^2} \operatorname{Tr}\Big(\partial^\mu U \partial^\nu U^\dagger (\partial_\mu U \partial_\nu U^\dagger - \partial_\nu U \partial_\mu U^\dagger)\Big) + \frac{f_w^2}{2} \operatorname{Tr}(\partial_\mu U \partial^\mu U^\dagger) \tag{7.2}$$

is the Skyrme Lagrangian and

$$\begin{aligned} \mathcal{L}^{(h)}_{DSM} &= \frac{g_{wh} f_w^2}{2} (2H^\dagger(x)H(x) - v_h^2) \operatorname{Tr}(U(x) - I_2) \\ &= g_{wh} f_w^2 v_h \Big(h(x) + \frac{h^2(x)}{2v_h}\Big) \operatorname{Tr}(U(x) - I_2) \end{aligned} \tag{7.3}$$

describes the coupling between the Anderson-Higgs field and the dark $\boldsymbol{w}(x)$ field, where g_{wh} is the coupling strength. Through this Anderson-Higgs portal, the $\boldsymbol{w}(x)$ field couples to Standard Model fields. From [34], the velocity-weighted annihilation cross sections for $\boldsymbol{w}$ mesons (with mass much greater than Standard Model masses) with center of mass energy $\sqrt{s_w}$ annihilating into Standard Model states are

$$v\sigma_{ww\to hh} = v\sigma_{ww\to ZZ} = \frac{1}{2} v\sigma_{ww\to W^+W^-} = \frac{g_{wh}^2}{4\pi s_w} \tag{7.4}$$

and

$$v\sigma_{ww\to f\overline{f}} = N_c \frac{g_{wh}^2 m_f^2}{\pi s_w^2}, \tag{7.5}$$

where N_c is the number of possible colour charges (leptons have $N_c = 1$ and quarks have $N_c = 3$). The fermionic contribution can be ignored because $\sqrt{s_w} \geq 2m_w$ and $m_w \gg m_{top}$. Adding up the remaining contributions, the total velocity-weighted annihilation cross section, to leading order, is

$$v\sigma_{ww} = \frac{g_{wh}^2}{\pi s_w}. \tag{7.6}$$

7.2 Relic Skyrmion Density

Before discussing the relic skyrmion abundance, it is necessary to determine the creation mechanisms involved. Numerical simulations of antiskyrmion-skyrmion annihilation [38], [39] and observations of antiproton-proton annihilation into pions [40] indicate that that skyrmions and antiskyrmions annihilate with the classical cross section

$$\sigma_{S\bar{S}} = \pi L_S^2 \tag{7.7}$$

into a number of $\boldsymbol{w}$ particles $2 < \langle N_w \rangle \lesssim 7$. The large number of $\boldsymbol{w}$ particles involved suppresses the reverse process. Therefore, the dark skyrmions would have had to have been created non-thermally. They would not have been created in thermal equilibrium with the heat bath because bubble nucleation and quenching would have delayed the completion of the phase transition such that the heat bath would be too cold. This must necessarily be the case for skyrmions to be a good dark matter candidate due to the supression of $S\bar{S}$ creation in thermal equilibrium. No assumption is made as to whether the phase transition is First or Second Order.

To determine the present relic Skyrmion abundance,

$$\Omega_S h^2 = \frac{M_S n_S(t_0)}{\rho_{cr}} h^2, \tag{7.8}$$

the balance equation

$$\frac{d}{dt}(n_S a^3) = -\frac{1}{2} n_S^2 a^3 \langle v\sigma_{S\bar{S}} \rangle \tag{7.9}$$

must be solved to find $n_S(t_0)$ [24](pp.187-188), [26](pg.124). This equation does not contain an equilibrium term. The number density n_S includes both skyrmions as well as antiskyrmions, whose number densities are assumed to be approximately equal, hence the factor of $1/2$. Rearranging the balance equation gives

$$\frac{1}{(n_S a^3)^2} \frac{d}{dt}(n_S a^3) = -\frac{1}{2} \frac{1}{a^3} \langle v\sigma_{S\bar{S}} \rangle \tag{7.10}$$

and so

$$\int_{t_c}^{t} \frac{1}{(n_S a^3)^2} d(n_S a^3) = -\frac{1}{2} \int_{t_c}^{t} \frac{\langle v\sigma_{S\bar{S}} \rangle}{a^3} d\tau. \tag{7.11}$$

The left-hand side of the equation is

$$\int_{t_c}^{t} \frac{1}{(n_S a^3)^2} d(n_S a^3) = \frac{-1}{n_S(t) a^3(t)} + \frac{1}{n_S(t_c) a^3(t_c)}. \tag{7.12}$$

Therefore

$$n_S(t) = \frac{n_S(t_c)}{1 + \frac{1}{2} n_S(t_c) a^3(t_c) \int_{t_c}^{t} \langle v\sigma_{S\bar{S}} \rangle \, a^{-3} d\tau} \left(\frac{a(t_c)}{a(t)} \right)^3. \tag{7.13}$$

As for the time integral, first note that $|v|\sigma \propto v^{2\beta}$, where $\beta = 0$ for s-wave annihilation, and $\beta = 1$ for p-wave annihilation. This, along with the fact that $\langle v \rangle \sim T^{1/2}$, means that $\langle v\sigma \rangle \propto T^{\beta}$ and

$$\frac{\langle v\sigma \rangle}{\langle v\sigma \rangle_c} = \left(\frac{T}{T_c} \right)^{\beta}. \tag{7.14}$$

Since during radiation domination $T \propto t^{-1/2}$, the velocity-weighted annihilation cross section can be expressed as

$$\langle v\sigma \rangle = \langle v\sigma \rangle_c \left(\frac{t_c}{t}\right)^{\beta/2}. \tag{7.15}$$

And now

$$\begin{aligned}
\int_{t_c}^{t} \frac{\langle v\sigma_{S\bar{S}} \rangle}{a^3} dt' &= \langle v\sigma_{S\bar{S}} \rangle_c \, t_c^{\beta/2} \int_{t_c}^{t} \tau^{-\beta/2} a^{-3} d\tau \\
&= \langle v\sigma_{S\bar{S}} \rangle_c \, t_c^{\beta/2} a_{0,r}^{-3} \int_{t_c}^{t} \tau^{-\beta/2} \Big(\frac{\tau}{t_{0,r}}\Big)^{-3/2} d\tau \\
&= \langle v\sigma_{S\bar{S}} \rangle_c \, t_c^{\beta/2} a_{0,r}^{-3} t_{0,r}^{3/2} \Big(-\frac{\beta}{2} - \frac{1}{2}\Big)^{-1} \tau^{-\beta/2-1/2} \Big|_{t_c}^{t} \\
&\simeq 2 \langle v\sigma_{S\bar{S}} \rangle_c \, a_{0,r}^{-3} t_{0,r}^{3/2} (\beta+1)^{-1} t_c^{-1/2},
\end{aligned} \tag{7.16}$$

where in the last line $t_c \ll t$ is used. This is done because by the time of radiation-matter equality $t_{rm} \gg t_c$, $S\bar{S}$ annihilations were negligible.

Putting this all together yields

$$n_S(t) = \frac{n_S(t_c)}{1 + n_S(t_c) \langle v\sigma_{S\bar{S}} \rangle_c (\beta+1)^{-1} t_c} \left(\frac{a(t_c)}{a(t)}\right)^3. \tag{7.17}$$

Since $a(t) \gg a(t_c)$, the redshift corresponding to the start of the phase transition is

$$z_c^{-3}(t) \simeq \frac{a^3(t_c)}{a^3(t)}. \tag{7.18}$$

Furthermore, this can be put in terms of entropy,

$$\frac{a^3(t_c)}{a^3(t)} = \frac{s(t)}{s_c}. \tag{7.19}$$

Recall that the entropy density at the time of the phase transition was

$$s_c = \frac{2\pi^2}{45} g_{*S}(T_c) T_c^3. \tag{7.20}$$

The present relic number density can now be expressed as

$$n_S(t_0) = \frac{n_S(t_c)}{1 + n_S(t_c) \langle v\sigma_{S\bar{S}} \rangle_c (\beta+1)^{-1} t_c} \frac{45 s_0}{2\pi^2 g_{*S}(T_c) T_c^3}. \tag{7.21}$$

As for the annihilation term in the denominator, note that

$$n_S(t_c) \langle v\sigma_{S\bar{S}} \rangle_c \, t_c = \frac{\Gamma_S(t_c)}{2H(t_c)}. \tag{7.22}$$

At the phase transition, $\Gamma_S(t_c) \gg H(t_c)$ meaning that

$$n_S(t_0) \simeq \frac{(1+\beta)}{\langle v\sigma_{S\bar{S}} \rangle_c \, t_c} \frac{45 s_0}{2\pi^2 g_{*S}(T_c) T_c^3}. \tag{7.23}$$

Because the number density at the critical time has cancelled out and no longer appears in the equation for the present number density, the order of the phase transition does not matter. Also recall the relation between the (critical) time and (critical) temperature during radiation domination,

$$t_c T_c^2 = \frac{3}{4\pi} m_{Pl} \sqrt{\frac{5}{\pi g_*(T_c)}}. \tag{7.24}$$

Turning back now to the relic Skyrmion abundance, it can be written as

$$\Omega_S h^2 = \frac{6s_0}{m_{Pl} g_{*S}(T_c)} \frac{h^2}{\rho_{cr}} \sqrt{\frac{5}{\pi} g_*(T_c)} \frac{\beta+1}{\langle v\sigma_{S\bar{S}} \rangle_c} \frac{M_S}{T_c}. \tag{7.25}$$

Several further simplifications can be made. First, the ratio

$$x_c = \frac{M_S}{T_c} \tag{7.26}$$

can be bounded. The QCD chiral phase transition is expected to have occurred at a critical temperature of about $100 - 200$MeV [41], [42] and the nucleon mass is about 1GeV [4]. It is assumed that these values will have the same ratio x_c as the dark skyrmions from the dark chiral phase transition discussed here which gives $5 \lesssim x_c \lesssim 10$.

The non-relativistic approximation for the kinetic energy

$$\frac{1}{2} M_S v^2 = \frac{3}{2} T \tag{7.27}$$

implies

$$v^2 = \frac{3}{x}. \tag{7.28}$$

This, along with the classical cross section, gives the non-relativistic approximation

$$\langle v\sigma_{S\bar{S}} \rangle_c \simeq \pi L_S^2 \sqrt{\frac{3}{x_c}}. \tag{7.29}$$

Recall that

$$M_S \simeq 73 \frac{f_w}{g_V}, \tag{7.30}$$

and so

$$\begin{aligned} L_S &= \frac{1.2}{g_V f_w} \\ &= \frac{87.6}{g_V^2 M_S}. \end{aligned} \tag{7.31}$$

Another useful approximation is $\beta = 1/2$, meaning that s-wave and p-wave annihilations are equally possible.

Because all relativistic particles were in thermal equilibrium at the chiral phase transition,

$$\begin{aligned} g_*(T_c) &= g_{*S}(T_c) \\ &= \sum_{b=bosons} g_b + \frac{7}{8} \sum_{f=fermions} g_f \\ &= 112, \end{aligned} \tag{7.32}$$

where in the last step, the degrees of freedom for each type of elementary particle that was relativistic at that times have been summed together [7](pp.12-18), [4]. For example, all quarks were relativistic in the very early universe. There are 6 quark flavors and each has an antiquark, 2 spin states, and 3 colors each so the quark contribution to $g*(T_c)$ is $6 \times 2 \times 2 \times 3 = 72$.

Putting all of this together now,

$$\Omega_S h^2 = \frac{3s_0}{m_{Pl}} \frac{h^2}{\rho_{cr}} \sqrt{\frac{15x_c^3}{\pi^3 g_*(T_c)}} \Big(\frac{g_V^2 M_S}{87.6} \Big)^2. \tag{7.33}$$

To numerically constrain the skyrmion parameter $g_V^2 M_S$ from this expression for $\Omega_S h^2 \leq \Omega_{CDM} h^2$, particle group data [4] is referred to which says

$$s_0 = 2891.2\text{cm}^{-3}, \tag{7.34}$$

$$m_{Pl} = 1.220910 \times 10^{19}\text{GeV}, \tag{7.35}$$

$$\frac{\rho_{cr}}{h^2} = 1.05371 \times 10^{-5}\text{GeVcm}^{-3}, \tag{7.36}$$

and

$$\Omega_{CDM}h^2 = 0.1186. \tag{7.37}$$

If the dark skyrmions constitute all of dark matter then

$$g_V^2 M_S = 14.3316\text{PeV} \times x_c^{-3/4}, \tag{7.38}$$

so allowed values for the skyrmion parameter must be on or below this curve, as seen in Figure 7.1.

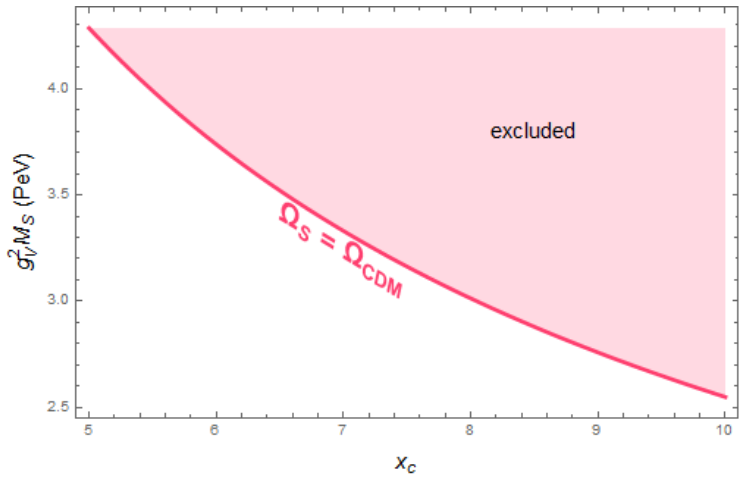

Figure 7.1: Possible values of the skyrmion parameter for $5 \leq x_c \leq 10$.

Therefore, for $5 \lesssim x_c \lesssim 10$, dark skyrmions can be PeV scale for $g_V^2 \simeq 1$ or even multi-PeV scale for $g_V^2 < 1$.

7.3 Constraints on the Heavy Dark Mesons

The $\boldsymbol{w}$ particles should not contribute much to dark matter compared to the skyrmions. For this to happen, g_{wh} must be large enough so that the $\boldsymbol{w}$ mesons are coupled strongly enough to thermal Standard Model particles in order to prevent freeze-out which would contribute significantly to the abundance of dark matter. However, $g_{wh} < 4\pi$ is also necessary so that the corresponding scattering cross sections can still be calculated using perturbation theory. The g_{wh} dependence on m_w is determined [34] using the fact that the scattering cross section determined from cosmology must be equal to the scattering cross section determined from quantum field theory. The thermally averaged annihilation cross section $\langle v\sigma_{ww}\rangle_G (m_w, T)$ from Eq. 6.61 is determined using quantum field theory while $\langle v\sigma_{ww}\rangle_r (T_f)$ is the cross section required for the $\boldsymbol{w}$ mesons to freeze out at T_f. They are related by

$$g_{wh}^2 = \frac{\langle v\sigma_{ww}\rangle_r (T_f)}{\langle v\sigma_{ww}\rangle_G (m_w, T_f)|_{g=1}}. \tag{7.39}$$

If $\Omega_w \leq 0.01\Omega_{CDM}$ then $m_w \lesssim 4$TeV and if $0.01\Omega_{CDM} < \Omega_w < 0.1\Omega_{CDM}$ then $m_w \lesssim 12$TeV, as seen in Figure 7.2. The case where $0.1\Omega_{CDM} < \Omega_w < \Omega_{CDM}$ is also indicated in Figure 7.2. Note that the bumps around $m_w = 4.2$TeV come from the fact that the top quarks do not contribute to the effective relativistic degrees of freedom once they have frozen out.

The rate at which the number density of a w_i particle changes is going to be the rate due to their annihilation into Standard Model particles subtracted from the rate due to their production via antiskyrmion-skyrmion annihilation. The w_i number density change rate due to their annihilation is half the number

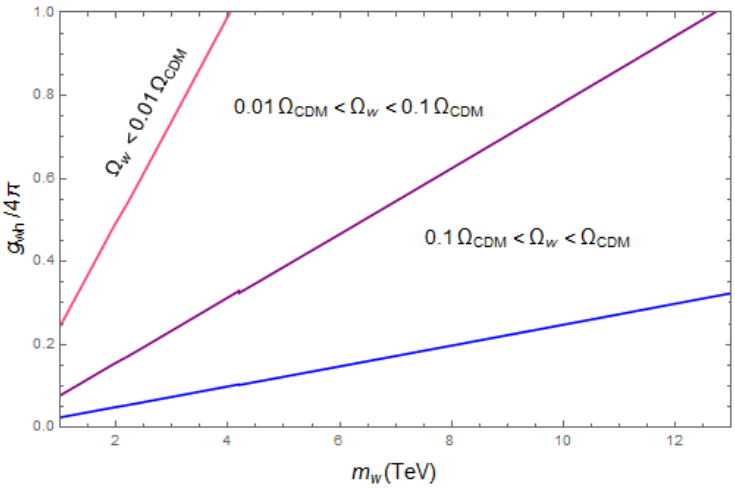

Figure 7.2: Possible values for m_w and g_{wh} where g_{wh} is perturbative and thermally created $\boldsymbol{w}$ mesons do not contribute significantly to dark matter.

density of w_i's (because they are their own antiparticle) multiplied by their annihilation rate multiplied by 2 (because each annihilation results in the loss of 2 w_i's). The number density change rate due to production is equal to the number density of skyrmions multiplied by the antiskyrmion-skyrmion annihilation rate multiplied by 1/3 the average number of $\boldsymbol{w}$ particles produced from this annihilation. That is,

$$\frac{dn_{w_i}}{dt} = \frac{1}{3}\langle N_w\rangle\left(\frac{n_S}{2}\right)^2 v_{S\overline{S}}\pi L_S^2 - 2\left(\frac{n_{w_i}}{2}\right)^2\frac{g_{wh}^2}{\pi}\langle s_w^{-1}\rangle\,. \tag{7.40}$$

Since $n_w = 3n_{w_i}$, the change rate of n_w can be found using

$$\frac{1}{3}\frac{dn_w}{dt} = \frac{1}{3}\langle N_w\rangle\left(\frac{n_S}{2}\right)^2 v_{S\overline{S}}\pi L_S^2 - 2\left(\frac{n_w}{6}\right)^2\frac{g_{wh}^2}{\pi}\langle s_w^{-1}\rangle \tag{7.41}$$

which means

$$\frac{dn_w}{dt} = \langle N_w\rangle\frac{n_S^2}{4}v_{S\overline{S}}\pi L_S^2 - n_w^2\frac{g_{wh}^2}{6\pi}\langle s_w^{-1}\rangle\,. \tag{7.42}$$

Detailed balance, $\dot{n}_w = 0$, gives

$$\frac{n_w^2}{n_S^2} = \frac{3}{2}\pi^2\frac{\langle N_w\rangle}{\langle s_w^{-1}\rangle}\frac{v_{S\overline{S}}L_S^2}{g_{wh}^2}. \tag{7.43}$$

The conservation of energy says that

$$2M_S \approx \langle N_w\rangle\, m_w \tag{7.44}$$

and

$$s_w \approx (2m_w)^2, \tag{7.45}$$

so

$$\frac{\langle N_w\rangle}{\langle s_w^{-1}\rangle} \simeq 16\frac{M_S^2}{\langle N_w\rangle}. \tag{7.46}$$

The ratio of number densities is therefore

$$\frac{n_w}{n_S} \simeq \frac{\sqrt{24}\pi}{g_{wh}\sqrt{\langle N_w\rangle}}M_S L_S\sqrt{v_{S\overline{S}}} \tag{7.47}$$

which is used to determine the relation between the dark skyrmion and dark $\boldsymbol{w}$ meson density parameters,

$$\begin{aligned}\frac{\Omega_w}{\Omega_S} &= \frac{n_w m_w}{n_S M_S}\\ &\simeq 4\times 10^2\times\frac{\pi v_{S\overline{S}}}{g_{wh}\sqrt{\langle N_w\rangle}}\frac{m_w}{g_V^2 M_S}.\end{aligned} \tag{7.48}$$

Figure 7.1 indicates that $M_S g_V^2$ is of the order PeV. Figure 7.2 indicates that $g_{wh} \sim 1$ and for $\Omega_w < 0.1\Omega_{CDM}$, the $\boldsymbol{w}$ meson mass must be of the order TeV. Therefore $m_w g_V^{-2} M_S^{-1} \sim \text{TeV} \times \text{PeV}^{-1} = 10^{-3}$. Since the dark skyrmions in question are very heavy, it is safe to say that $v_{S\overline{S}} \ll 1$. Therefore the skyrmions, and not the $\boldsymbol{w}$ mesons, constitute most of the dark matter in this model.

7.4 Direct Signals from the Dark Skyrmions

The skyrmion $\boldsymbol{w}_S$ is now considered to be a coherent superposition [8] (pp.112-118, 392-394) of the $\boldsymbol{w}$ particles. For this to happen, the skyrmion state in the interaction picture

$$|S(t)\rangle = \exp\Big(-\frac{1}{2}\int |\boldsymbol{\zeta}(\boldsymbol{k}',t)|^2 d^3k'\Big) \exp\Big(\int \boldsymbol{\zeta}(\boldsymbol{k}',t)\cdot \boldsymbol{a}_w^\dagger(\boldsymbol{k}')d^3k'\Big)|0\rangle \tag{7.49}$$

must be an eigenstate of the the the annihilation operator $\boldsymbol{a}_w(\boldsymbol{k})$ with eigenvalue

$$\boldsymbol{\zeta}(\boldsymbol{k},t) = \sqrt{\frac{\omega(\boldsymbol{k})}{2}}\boldsymbol{w}_S(\boldsymbol{k})e^{i\omega(\boldsymbol{k})t}, \tag{7.50}$$

where

$$\omega^2(\boldsymbol{k}) = \boldsymbol{k}^2 + m_w^2. \tag{7.51}$$

The skyrmion profile function $w_s(r)$ of Eq. 4.35 is used here. The skyrmion in $\boldsymbol{k}$ space is

$$\begin{aligned}
\boldsymbol{w}_S(\boldsymbol{k}) &= \int \frac{d^3x}{(2\pi)^{3/2}} w_S(r)\hat{\boldsymbol{r}}e^{-i\boldsymbol{k}\cdot\boldsymbol{x}} \\
&= \frac{1}{(2\pi)^{3/2}}\int_0^{2\pi} d\phi \int_0^{\pi} d\theta \int_0^{\infty} dr r^2 \sin\theta w_S(r) \begin{pmatrix} \sin\theta\cos\phi \\ \sin\theta\sin\phi \\ \cos\theta \end{pmatrix} e^{-ikr\cos\theta} \\
&= \sqrt{\frac{2}{\pi}}\hat{\boldsymbol{k}}\int_0^{\infty} dr \frac{r}{k} w_S(r)\sin(kr) \\
&= \hat{\boldsymbol{k}} w_S(k)
\end{aligned} \tag{7.52}$$

as seen in Figure 7.3. Note that the factor of $e^{i\omega(\boldsymbol{k})t}$ in $\boldsymbol{\zeta}(\boldsymbol{k},t)$ was absorbed from

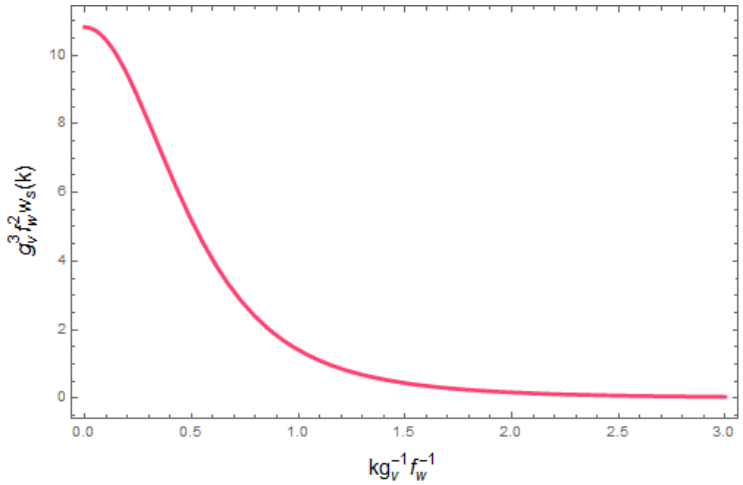

Figure 7.3: The hedgehog skyrmion profile function in k space.

$$\boldsymbol{a}_w(\boldsymbol{k},t) = \boldsymbol{a}_w(\boldsymbol{k})e^{i\omega(\boldsymbol{k})t}. \tag{7.53}$$

The $\boldsymbol{w}$ meson operator is

$$\boldsymbol{w}(x) = \int \frac{d^3k}{(2\pi)^{3/2}\sqrt{2\omega_w(\boldsymbol{k})}}\Big(\boldsymbol{a}_w(\boldsymbol{k})e^{-ikx} + \boldsymbol{a}_w^\dagger(\boldsymbol{k})e^{ikx}\Big), \tag{7.54}$$

Its expectation value in the skyrmion state,

$$\begin{aligned}
\langle S(t)|\,\boldsymbol{w}(x)\,|S(t)\rangle &= \frac{1}{2}\int \frac{d^3k}{(2\pi)^{3/2}}\Big(\boldsymbol{w}_s(\boldsymbol{k})e^{i\boldsymbol{k}\cdot\boldsymbol{x}} + \boldsymbol{w}_s^\dagger(\boldsymbol{k})e^{-i\boldsymbol{k}\cdot\boldsymbol{x}}\Big) \\
&= \frac{1}{2}\int \frac{d^3k}{(2\pi)^{3/2}}\Big(\boldsymbol{w}_s(\boldsymbol{k})e^{i\boldsymbol{k}\cdot\boldsymbol{x}} + \boldsymbol{w}_s(-\boldsymbol{k})e^{-i\boldsymbol{k}\cdot\boldsymbol{x}}\Big) \\
&= \int \frac{d^3k}{(2\pi)^{3/2}}\boldsymbol{w}_s(\boldsymbol{k})e^{i\boldsymbol{k}\cdot\boldsymbol{x}} \\
&= w_S(r)\hat{\boldsymbol{r}},
\end{aligned} \tag{7.55}$$

is the skyrmion solution to the equations of motion corresponding to the hedgehog Skyrme Lagrangian density.

The scattering amplitudes for coherent states are added up, so the amplitude for skyrmion-nucleon scattering is the amplitude for $\boldsymbol{w}$ meson-nucleon scattering multiplied by the number of $\boldsymbol{w}$ mesons in the skyrmion state. This means the cross sections are related by

$$\sigma_{SN} = \langle N_w\rangle_S^2\,\sigma_{wN}. \tag{7.56}$$

The average number [7](pg.128) of $\boldsymbol{w}$ mesons in the skyrmion state is

$$\begin{aligned}
\langle N_w\rangle_S &= \langle S(t)|\,\hat{N}\,|S(t)\rangle \\
&= \langle S(t)|\int d^3k\boldsymbol{a}_w^\dagger(\boldsymbol{k})\cdot\boldsymbol{a}_w(\boldsymbol{k})\,|S(t)\rangle \\
&= \int d^3k|\boldsymbol{\zeta}(\boldsymbol{k},t)|^2 \\
&= \frac{1}{2}\int d^3k\omega(\boldsymbol{k})w_S^2(\boldsymbol{k}) \\
&= 2\pi\int_0^\infty dk k^2\omega(k)w_S^2(k),
\end{aligned} \tag{7.57}$$

which is plotted in Figure 7.4. Comparing this with

$$\langle N_w\rangle_S \simeq \frac{M_S}{m_w} \simeq 73\frac{1}{m_w}f_w g_V^{-1} \tag{7.58}$$

using a linear fit yields $\langle N_w\rangle_S \simeq 47g_V^{-2}$ and $m_w \simeq 1.3g_V f_w$. Analysing the intersection of the two expressions for the meson count yields the approximations $\langle N_w\rangle_S \simeq 50.05g_V^{-2}$, $m_w \simeq 1.46g_V f_w$. The linear fit approximation is used here.

The $\boldsymbol{w}$ meson-nucleon recoil cross section in the limit $m_N \ll m_w$ is

$$\sigma_{wN} = \frac{1}{\pi}\Big(\frac{g_{wh}g_{hN}v_h m_N}{m_h^2 m_w}\Big)^2, \tag{7.59}$$

(see Appendix A for the calculation) where the Anderson-Higgs particle mass is $m_h = 125.18\text{GeV}$ [4], g_hN is the effective Anderson-Higgs-nucleon coupling constant [44] which has a modern value given by $g_{hN}v_h = 289\text{MeV}$ [45], and m_N is the nucleon mass. Here it is determined from stable and long-lived Xenon isotopes weighted by abundance:

$$\begin{aligned}
m_N &= \sum_i p_i\frac{(m_i - 54m_e)}{A_i} \\
&= 903.6\text{MeV}
\end{aligned} \tag{7.60}$$

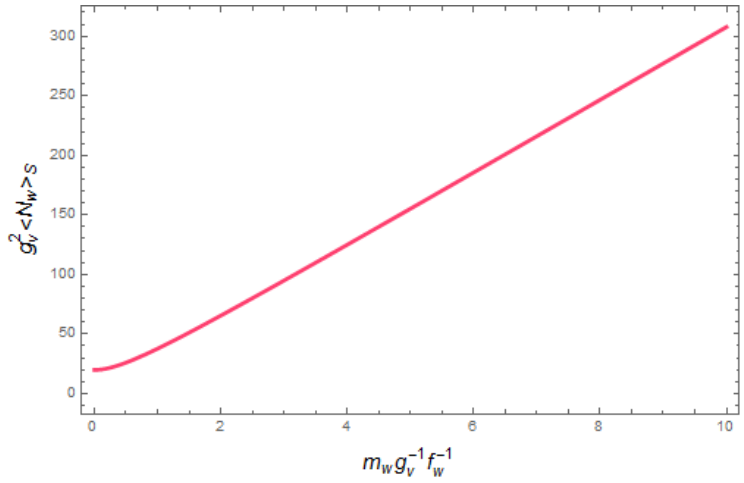

Figure 7.4: The $\boldsymbol{w}$ meson number in the coherent skyrmion state.

where, for the ith stable or long-lived isotope [43], p_i is its abundance, m_i is its mass, A_i is its number of nucleons , and m_e is the electron mass [4].

Now, the dark skyrmion-nucleon recoil cross section can be expressed as

$$\begin{aligned} \sigma_{SN} &= \frac{1}{\pi}\Big(\frac{47 g_{hN} v_h m_N}{m_h^2}\Big)^2 \Big(\frac{g_{wh}}{g_V^2 m_w}\Big)^2 \\ &= 2.071 \times 10^{-7} \times \Big(\frac{g_{wh}}{g_V^2 m_w}\Big)^2, \end{aligned} \tag{7.61}$$

as seen in Figure 7.5. In terms of the dark skyrmion mass, the nucleon-recoil cross section is

$$\begin{aligned} \sigma_{SN} &= \frac{1}{\pi}\Big(\frac{47^2 g_{hN} v_h m_N}{m_h^2}\Big)^2 \Big(\frac{g_{wh}}{g_V^2 M_S}\Big)^2 \\ &= 4.575 \times 10^{-4} \times \Big(\frac{g_{wh}}{g_V^4 M_S}\Big)^2, \end{aligned} \tag{7.62}$$

which is plotted in Figure 7.6.

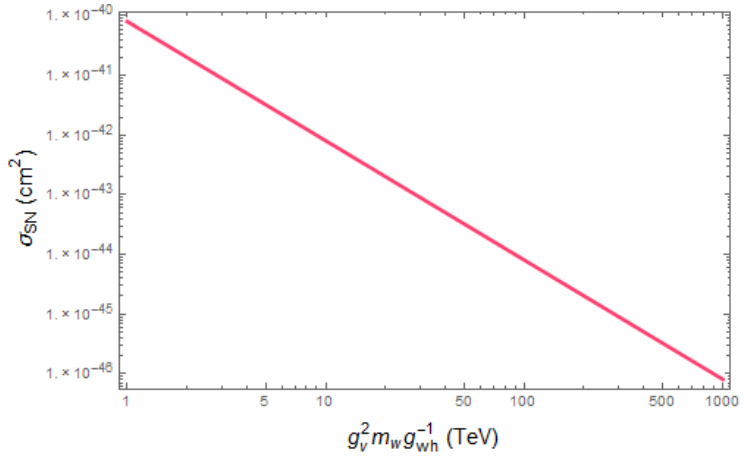

Figure 7.5: The skyrmion-nucleon recoil cross section for 1TeV $\leq g_V^2 m_w g_{wh}^{-1} \leq$ 1PeV

The XENON1T 1 ton year exposure [46] found no recoils that could be attributed to dark matter. This gave an upper limit on the possible ratio of nucleon recoil cross section to dark matter mass for a mass range

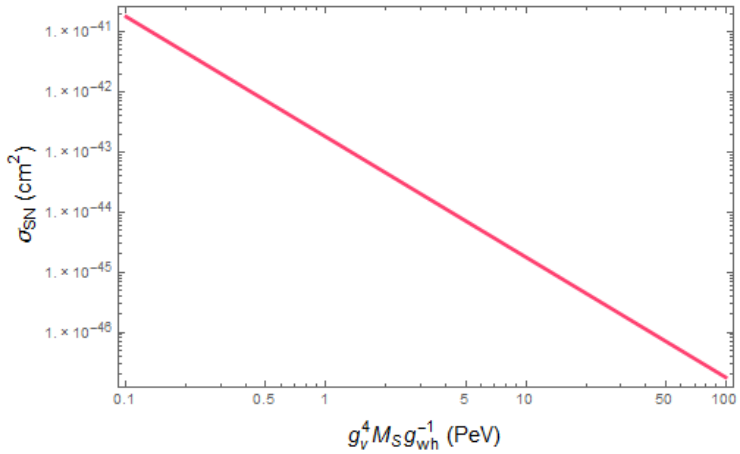

Figure 7.6: The skyrmion-nucleon recoil cross section for 100TeV $\leq g_V^4 M_S g_{wh}^{-1} \leq$ 100PeV

of 1GeV to 1TeV, as seen in Figure 7.7. The results indicate that $\sigma(m = 1\text{TeV}) \lesssim 8.3 \times 10^{-46}\text{cm}^2$. It is possible to extrapolate from these results an upper limit on the recoil cross section for even higher masses. This is because the maximum cross section increases approximately linearly with mass for large masses, as seen in the XENON1T 1 ton year results.

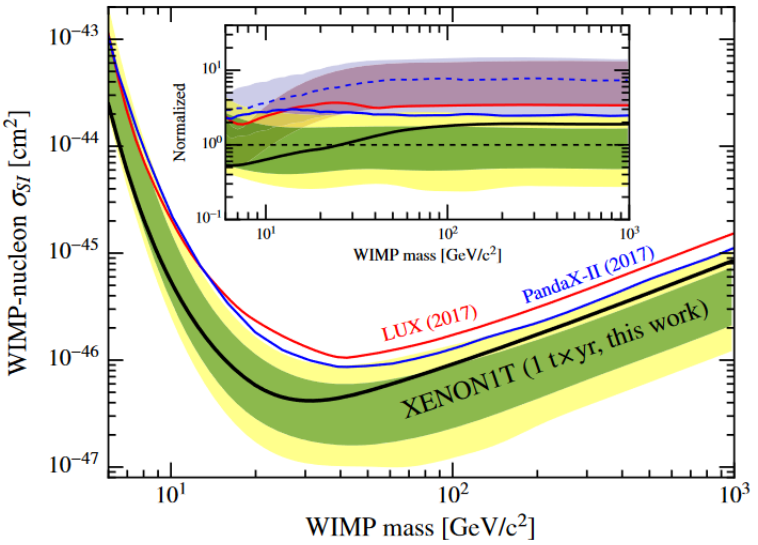

Figure 7.7: The XENON1T 1 ton year results. Figure from Reference [46].

The upper bound on the recoil cross section $\sigma_{max}(m)$ for large mass m is related to the upper bound for 1TeV by

$$\sigma_{max}(m) = \sigma_{max}(1\text{TeV}) \frac{\sigma_{eff,max}(m)}{\sigma_{eff,max}(1\text{TeV})} \frac{F^2(1\text{TeV})}{F^2(m)}, \tag{7.63}$$

where F is the Helm structure factor (see Eq. 6.68). The ratio of square Helm structure factors has very little dependence on mass for high masses. Therefore, the mass dependence comes primarily from the factor $\sigma_{eff,max}(m)$. Extrapolating, cross section constraints should continue to increase approximately linearly with m for masses above 1TeV so

$$\frac{\sigma_{eff,max}(m)}{m} = \frac{\sigma_{eff,max}(1\text{TeV})}{1\text{TeV}}. \tag{7.64}$$

The dark skyrmion-nucleon recoil section is therefore constrained by

$$\sigma_{SN} \lesssim 8.3 \times 10^{-46}\text{cm}^2 \frac{M_S}{1\text{TeV}} \frac{F^2(1\text{TeV})}{F^2(M_S)}. \tag{7.65}$$

Then

$$\left(\frac{g_{wh}}{g_v^4}\right)^2 \lesssim 3.8 \times 10^{-41}\text{cm}^2 \frac{M_S^3}{1\text{TeV}} \frac{F^2(1\text{TeV})}{F^2(M_S)}. \tag{7.66}$$

For $M_S = 100$TeV, the coupling strength g_V is constrained to be $g_V \gtrsim 1.8 g_{wh}^{1/4}$. This means that g_V could possibly be of non-perturbative strength, while g_{wh} would still be perturbative. However $g_V \gtrsim 0.32 g_{wh}^{1/4}$ for $M_S = 10$PeV. This coupling strength could be quite weak for higher skyrmion masses, as seen in Figure 7.8.

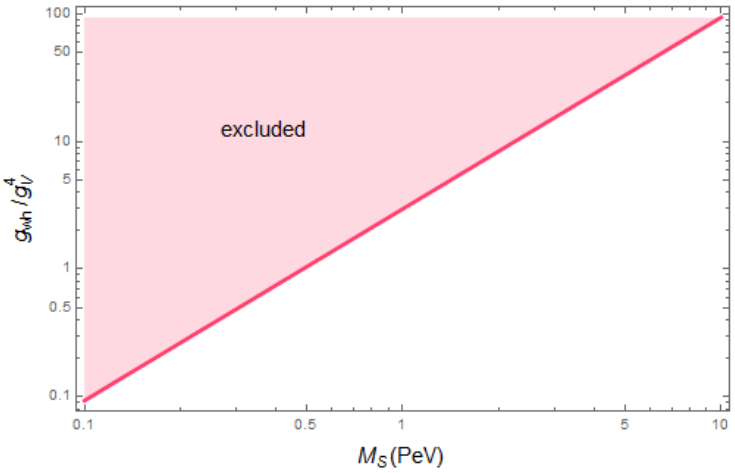

Figure 7.8: Direct search constraints on dark skyrmions of mass 100TeV to 10PeV from the XENON1T 1 ton year results.

The higher sensitivities of future direct detection xenon experiments such as XENONnT [47], LUX-ZEPLIN [48], PandaX-4T [49], and DARWIN [50] will allow for further constraints on dark matter candidates including PeV scale dark skyrmions.

Chapter 8

Conclusion

Skyrmions of a chiral $SU(2)_L \times SU(2)_R \to SU(2)_V$ phase transition with PeV scale mass have been analyzed here as dark matter candidates, where the heavy dark mesons of the corresponding nonlinear σ-model are coupled to the Standard Model by an Anderson-Higgs portal. The results are as follows.

The skyrmions would have had to have been created non-thermally via the chiral phase transition. This conclusion was reached here because it has already been determined from simulations that skyrmions annihilate with antiskyrmions into a large number of their dark mesons, which means the reverse process in thermal equilibrium is severely suppressed. Because the creation is not through thermal freeze-out, this is consistent with the Griest-Kamionkowski bound.

The present dark skyrmion number density was determined to be independent from the order of the phase transition, which allowed for the skyrmion parameter $g_V^2 M_S$ to be constrained, where g_V is the Skyrme coupling and M_S is the skyrmion mass. This was done by using the present total cold dark matter abundance as an upper bound for the present dark skyrmion abundance. The resuls of these constraints lead to the conclusion that it is possible for the dark skyrmion mass to be of the order PeV or higher if $g_V^2 \lesssim 1$.

Constraints were put on the dark mesons by assuming that they constitute at most a small fraction of all cold dark matter and by demanding that the Anderson-Higgs portal coupling be of perturbative strength, $g_{wh} < 4\pi$. It was determined that the dark mesons should be TeV scale and that most of the cold dark matter abundance in this model is due to the dark skyrmions.

Considering the dark skyrmions to be spherically symmetric coherent states of the dark mesons allowed for the dark skyrmion-nucleon recoil cross section to be expressed in terms of the dark meson-nucleon recoil cross section. The XENON1T 1 ton year experiment's results were extrapolated to higher masses, which allowed for g_V to be constrained in terms of g_{wh} and M_S. The results of doing so is that on the lower end of very heavy dark skyrmion mass, $M_S = 100$TeV, it is possible that g_V could be of non-perturbative strength. However, higher masses like $M_S = 10$PeV allow for g_V to be quite small.

Several future direct dark matter detection experiments are being planned, including XENONnT, LUX-ZEPLIN, PandaX-4T, and DARWIN. These experiments will have even higher sensitivities. Their results will further constrain the dark matter-nucleon recoil cross section. This, in turn, will allow for even stricter constraints to be placed on g_V in the same manner as done in this thesis.

Appendix A

Nucleon-Dark Meson Scattering Cross Section

The calculation for the nucleon-dark meson scattering cross section σ_{wN} [37] is as follows. Perturbation theory is used to find the scattering matrix element whose square is used in the definition of the differential scattering cross section [6](pp.77-130), [8](pp.241-282). The initial state is a w_i boson with momentum $\boldsymbol{k}_a$ and a nucleon with momentum $\boldsymbol{p}_b$ and spin s_b, denoted by $|\boldsymbol{k}_a;\boldsymbol{p}_b,s_b\rangle$. The subscript i indicates that no assumption is made as to which of the three w bosons is involved. The w_i boson bounces off the nucleon and they interact via the exchange of a virtual Anderson-Higgs boson. The final state is $|\boldsymbol{k}_c;\boldsymbol{p}_d,s_d\rangle$, defined in the same way as the initial state.

The $\boldsymbol{w}$ field is defined as

$$\boldsymbol{w}(x)=\int\frac{d^3k}{(2\pi)^{3/2}\sqrt{2\omega_w(\boldsymbol{k})}}\Big(\boldsymbol{a}_w(\boldsymbol{k})e^{-ikx}+\boldsymbol{a}_w^\dagger(\boldsymbol{k})e^{ikx}\Big), \tag{A.1}$$

and the Anderson-Higgs field is

$$h(x)=\int\frac{d^3k}{(2\pi)^{3/2}\sqrt{2\omega_h(\boldsymbol{k})}}\Big(a_h(\boldsymbol{k})e^{-ikx}+a_h^\dagger(\boldsymbol{k})e^{ikx}\Big), \tag{A.2}$$

where

$$\omega^2(\boldsymbol{k})=\boldsymbol{k}^2+m^2. \tag{A.3}$$

The interaction between these fields is described by the interaction Hamiltonian

$$H_{hww}=g_{wh}v_h h(x)\boldsymbol{w}^2(x). \tag{A.4}$$

The nucleon field is

$$N(x)=\sum_{s=\uparrow,\downarrow}\int\frac{d^3k}{(2\pi)^{3/2}\sqrt{2\omega_N(\boldsymbol{k})}}\Big(a_N(\boldsymbol{k},s)u(\boldsymbol{k},s)e^{-ikx}+b_N^\dagger(\boldsymbol{k},s)v(\boldsymbol{k},s)e^{ikx}\Big), \tag{A.5}$$

and its adjoint $\overline{N}(x)=N^\dagger(x)\gamma^0$ is

$$\overline{N}(x)=\sum_{s=\uparrow,\downarrow}\int\frac{d^3k}{(2\pi)^{3/2}\sqrt{2\omega_N(\boldsymbol{k})}}\Big(b_N(\boldsymbol{k},s)\overline{v}(\boldsymbol{k},s)e^{-ikx}+a_N^\dagger(\boldsymbol{k},s)\overline{u}(\boldsymbol{k},s)e^{ikx}\Big). \tag{A.6}$$

The interaction Hamltonian that describes the interaction between the Anderson-Higgs field and the nucleon field is [44]

$$H_{hNN}=g_{hN}h(x)\overline{N}(x)N(x). \tag{A.7}$$

A.1 First Order S Matrix

The relevant scattering matrix element, to first order, for this calculation is

$$\begin{aligned} S_{wN} &= \langle \boldsymbol{k}_c; \boldsymbol{p}_d, s_d | \, T\left((-i)^2 \int H_{hww}(x) d^4x \int H_{hNN}(x') d^4x' \right) | \boldsymbol{k}_a; \boldsymbol{p}_b, s_b \rangle \\ &= - \langle \boldsymbol{k}_c; \boldsymbol{p}_d, s_d | \int d^4x \int d^4x' \Big(N H_{hww}(x) N H_{hNN}(x') \Theta(t - t') \\ &\quad + N H_{hNN}(x') N H_{hww}(x) \Theta(t' - t) \Big) | \boldsymbol{k}_a; \boldsymbol{p}_b, s_b \rangle \, , \end{aligned} \tag{A.8}$$

where T is the time ordering operator and N is the normal ordering operator. The time ordering operator puts operators with later time arguments to the left. The normal ordering operator puts creation operators to the left of annihilation operators.

As neither the initial nor final states have any anti-nucleons, any terms involving b_N and $b_N^\dagger$ will necessarily be 0. As for the other terms, most involve vacuum annihilation or the wrong number of creation and annihilation operators, so (anti-)commutation relations would make these terms 0. For the $t > t'$ case, the first surviving term involves

$$\begin{aligned} &\sum_l \langle \boldsymbol{k}_c; \boldsymbol{p}_d, s_d | \, N\Big(a_h(\boldsymbol{q}_1) a^\dagger_{w_l}(\boldsymbol{k}_1) a_{w_l}(\boldsymbol{k}_2) \Big) N\Big(a^\dagger_h(\boldsymbol{q}_2) a^\dagger_N(\boldsymbol{p}_1, s_1) \overline{u}(\boldsymbol{p}_1, s_1) \\ &\qquad \times a_N(\boldsymbol{p}_2, s_2) u(\boldsymbol{p}_2, s_2) \Big) | \boldsymbol{k}_a; \boldsymbol{p}_b, s_b \rangle \\ &= \sum_l \langle 0 | \, a_{w_i}(\boldsymbol{k}_c) a_N(\boldsymbol{p}_d, s_d) a^\dagger_{w_l}(\boldsymbol{k}_1) a_h(\boldsymbol{q}_1) a_{w_l}(\boldsymbol{k}_2) a^\dagger_h(\boldsymbol{q}_2) a^\dagger_N(\boldsymbol{p}_1, s_1) \\ &\qquad \times \overline{u}(\boldsymbol{p}_1, s_1) a_N(\boldsymbol{p}_2, s_2) u(\boldsymbol{p}_2, s_2) a^\dagger_N(\boldsymbol{p}_b, s_b) a^\dagger_{w_i}(\boldsymbol{k}_a) | 0 \rangle \, . \end{aligned} \tag{A.9}$$

To evaluate this, commutation and anti-commutation relations are necessary. For example,

$$\begin{aligned} a_N(\boldsymbol{p}_2, s_2) a^\dagger_N(\boldsymbol{p}_b, s_b) | 0 \rangle &= \{ a_N(\boldsymbol{p}_2, s_2), a^\dagger_N(\boldsymbol{p}_b, s_b) \} | 0 \rangle - a^\dagger_N(\boldsymbol{p}_b, s_b) a_N(\boldsymbol{p}_2, s_2) | 0 \rangle \\ &= \delta^{(3)}(\boldsymbol{p}_2 - \boldsymbol{p}_b) \delta_{s_2, s_b} | 0 \rangle \end{aligned} \tag{A.10}$$

and

$$\begin{aligned} a_{w_l}(\boldsymbol{k}_2) a^\dagger_{w_i}(\boldsymbol{k}_a) | 0 \rangle &= [a_{w_l}(\boldsymbol{k}_2), a^\dagger_{w_i}(\boldsymbol{k}_a)] | 0 \rangle + a^\dagger_{w_i}(\boldsymbol{k}_a) a_{w_l}(\boldsymbol{k}_2) | 0 \rangle \\ &= \delta^{(3)}(\boldsymbol{k}_2 - \boldsymbol{k}_a) \delta_{w_i, w_l} | 0 \rangle \, . \end{aligned} \tag{A.11}$$

Similarly,

$$a_h(\boldsymbol{q}_1) a^\dagger_h(\boldsymbol{q}_2) | 0 \rangle = \delta^{(3)}(\boldsymbol{q}_1 - \boldsymbol{q_2}) | 0 \rangle \, , \tag{A.12}$$

$$a_N(\boldsymbol{p}_d, s_d) a^\dagger_N(\boldsymbol{p}_1, s_1) | 0 \rangle = \delta^{(3)}(\boldsymbol{p}_d - \boldsymbol{p}_1) \delta_{s_d, s_1} | 0 \rangle \, , \tag{A.13}$$

and

$$a_{w_i}(\boldsymbol{k}_c) a^\dagger_{w_i}(\boldsymbol{k}_1) | 0 \rangle = \delta^{(3)}(\boldsymbol{k}_c - \boldsymbol{k}_1). \tag{A.14}$$

Therefore Equation (A.9) is equal to

$$\begin{aligned} &\overline{u}(\boldsymbol{p}_1, s_1) u(\boldsymbol{p}_2, s_2) \delta^{(3)}(\boldsymbol{p}_2 - \boldsymbol{p}_b) \delta_{s_2, s_b} \delta^{(3)}(\boldsymbol{p}_d - \boldsymbol{p}_1) \delta_{s_d, s_1} \\ &\qquad \times \delta^{(3)}(\boldsymbol{k}_2 - \boldsymbol{k}_a) \delta^{(3)}(\boldsymbol{k}_c - \boldsymbol{k}_1) \delta^{(3)}(\boldsymbol{q}_1 - \boldsymbol{q_2}). \end{aligned} \tag{A.15}$$

The second non-vanishing $t > t'$ term is

$$\begin{aligned}
&\sum_l \langle \boldsymbol{k}_c; \boldsymbol{p}_d, s_d| \, N\Big(a_h(\boldsymbol{q}_1) a_{w_l}(\boldsymbol{k}_1) a^\dagger_{w_l}(\boldsymbol{k}_2)\Big) N\Big(a^\dagger_h(\boldsymbol{q}_2) a^\dagger_N(\boldsymbol{p}_1, s_1) \overline{u}(\boldsymbol{p}_1, s_1) \\
&\qquad \times a_N(\boldsymbol{p}_2, s_2) u(\boldsymbol{p}_2, s_2)\Big) \, |\boldsymbol{k}_a; \boldsymbol{p}_b, s_b\rangle \\
&= \sum_l \langle 0| \, a_{w_i}(\boldsymbol{k}_c) a_N(\boldsymbol{p}_d, s_d) a^\dagger_{w_l}(\boldsymbol{k}_2) a_h(\boldsymbol{q}_1) a_{w_l}(\boldsymbol{k}_1) a^\dagger_h(\boldsymbol{q}_2) a^\dagger_N(\boldsymbol{p}_1, s_1) \\
&\qquad \times \overline{u}(\boldsymbol{p}_1, s_1) a_N(\boldsymbol{p}_2, s_2) u(\boldsymbol{p}_2, s_2) a^\dagger_N(\boldsymbol{p}_b, s_b) a^\dagger_{w_i}(\boldsymbol{k}_a) \, |0\rangle \\
&= \overline{u}(\boldsymbol{p}_1, s_1) u(\boldsymbol{p}_2, s_2) \delta^{(3)}(\boldsymbol{p}_2 - \boldsymbol{p}_b) \delta_{s_2, s_b} \delta^{(3)}(\boldsymbol{p}_d - \boldsymbol{p}_1) \delta_{s_d, s_1} \\
&\qquad \times \delta^{(3)}(\boldsymbol{k}_1 - \boldsymbol{k}_a) \delta^{(3)}(\boldsymbol{k}_c - \boldsymbol{k}_2) \delta^{(3)}(\boldsymbol{q}_1 - \boldsymbol{q_2})
\end{aligned} \tag{A.16}$$

The $t < t'$ case has

$$\begin{aligned}
&\sum_l \langle \boldsymbol{k}_c; \boldsymbol{p}_d, s_d| \, N\Big(a_h(\boldsymbol{q}_2) a^\dagger_N(\boldsymbol{p}_1, s_1) \overline{u}(\boldsymbol{p}_1, s_1) a_N(\boldsymbol{p}_2, s_2) u(\boldsymbol{p}_2, s_2)\Big) \\
&\qquad \times N\Big(a^\dagger_h(\boldsymbol{q}_1) a^\dagger_{w_l}(\boldsymbol{k}_1) a_{w_l}(\boldsymbol{k}_2)\Big) \, |\boldsymbol{k}_a; \boldsymbol{p}_b, s_b\rangle \\
&= \langle 0| \, a_{w_i}(\boldsymbol{k}_c) a_N(\boldsymbol{p}_d, s_d) a^\dagger_N(\boldsymbol{p}_1, s_1) \overline{u}(\boldsymbol{p}_1, s_1) a_h(\boldsymbol{q}_2) a_N(\boldsymbol{p}_2, s_2) u(\boldsymbol{p_2} s_2) \\
&\qquad \times a^\dagger_h(\boldsymbol{q}_1) a^\dagger_{w_l}(\boldsymbol{k}_1) a_{w_l}(\boldsymbol{k}_2) a^\dagger_N(\boldsymbol{p}_b, s_b) a^\dagger_{w_i}(\boldsymbol{k}_a) \, |0\rangle \\
&= \overline{u}(\boldsymbol{p}_1, s_1) u(\boldsymbol{p}_2, s_2) \delta^{(3)}(\boldsymbol{p}_2 - \boldsymbol{p}_b) \delta_{s_2, s_b} \delta^{(3)}(\boldsymbol{p}_d - \boldsymbol{p}_1) \delta_{s_d, s_1} \\
&\qquad \times \delta^{(3)}(\boldsymbol{k}_2 - \boldsymbol{k}_a) \delta^{(3)}(\boldsymbol{k}_c - \boldsymbol{k}_1) \delta^{(3)}(\boldsymbol{q}_2 - \boldsymbol{q}_1)
\end{aligned} \tag{A.17}$$

and

$$\begin{aligned}
&\sum_l \langle \boldsymbol{k}_c; \boldsymbol{p}_d, s_d| \, N\Big(a_h(\boldsymbol{q}_2) a^\dagger_N(\boldsymbol{p}_1, s_1) \overline{u}(\boldsymbol{p}_1, s_1) a_N(\boldsymbol{p}_2, s_2) u(\boldsymbol{p}_2, s_2)\Big) \\
&\qquad \times N\Big(a^\dagger_h(\boldsymbol{q}_1) a_{w_l}(\boldsymbol{k}_1) a^\dagger_{w_l}(\boldsymbol{k}_2)\Big) \, |\boldsymbol{k}_a; \boldsymbol{p}_b, s_b\rangle \\
&= \langle 0| \, a_{w_i}(\boldsymbol{k}_c) a_N(\boldsymbol{p}_d, s_d) a_h(\boldsymbol{q}_2) a^\dagger_N(\boldsymbol{p}_1, s_1) \overline{u}(\boldsymbol{p}_1, s_1) a_N(\boldsymbol{p}_2, s_2) u(\boldsymbol{p_2} s_2) \\
&\qquad \times a^\dagger_h(\boldsymbol{q}_1) a^\dagger_{w_l}(\boldsymbol{k}_2) a_{w_l}(\boldsymbol{k}_1) a^\dagger_N(\boldsymbol{p}_b, s_b) a^\dagger_{w_i}(\boldsymbol{k}_a) \, |0\rangle \\
&= \overline{u}(\boldsymbol{p}_1, s_1) u(\boldsymbol{p}_2, s_2) \delta^{(3)}(\boldsymbol{p}_2 - \boldsymbol{p}_b) \delta_{s_2, s_b} \delta^{(3)}(\boldsymbol{p}_d - \boldsymbol{p}_1) \delta_{s_d, s_1} \\
&\qquad \times \delta^{(3)}(\boldsymbol{k}_1 - \boldsymbol{k}_a) \delta^{(3)}(\boldsymbol{k}_c - \boldsymbol{k}_2) \delta^{(3)}(\boldsymbol{q}_2 - \boldsymbol{q}_1).
\end{aligned} \tag{A.18}$$

This means the scattering matrix element is

$$
\begin{aligned}
S_{wN} = &\sum_{s_1}\sum_{s_2}(-i)^2\int d^4x\int d^4x'\frac{1}{(2\pi)^9}\int d^3p_1\int d^3p_2\int d^3q_1\int d^3q_2\\
&\times\int d^3k_1\int d^3k_2\frac{g_{wh}g_{hN}v_h}{\sqrt{2^6\omega_N(\boldsymbol{p}_1)\omega_N(\boldsymbol{p}_2)\omega_h(\boldsymbol{q}_1)\omega_h(\boldsymbol{q}_2)\omega_w(\boldsymbol{k}_1)\omega_w(\boldsymbol{k}_2)}}\\
&\times\overline{u}(\boldsymbol{p}_1,s_1)u(\boldsymbol{p}_2,s_2)\delta^{(3)}(\boldsymbol{p}_2-\boldsymbol{p}_b)\delta_{s_2,s_b}\delta^{(3)}(\boldsymbol{p}_d-\boldsymbol{p}_1)\delta_{s_d,s_1}\\
&\times\Bigg(\Theta(t-t')\Big(\delta^{(3)}(\boldsymbol{k}_2-\boldsymbol{k}_a)\delta^{(3)}(\boldsymbol{k}_c-\boldsymbol{k}_1)e^{i(-q_1+k_1-k_2)x}e^{i(q_2+p_1-p_2)x'}\\
&+\delta^{(3)}(\boldsymbol{k}_1-\boldsymbol{k}_a)\delta^{(3)}(\boldsymbol{k}_c-\boldsymbol{k}_2)e^{i(-q_1-k_1+k_2)x}e^{i(q_2+p_1-p_2)x'}\Big)\\
&+\Theta(t'-t)\Big(\delta^{(3)}(\boldsymbol{k}_2-\boldsymbol{k}_a)\delta^{(3)}(\boldsymbol{k}_c-\boldsymbol{k}_1)e^{i(q_1+k_1-k_2)x}e^{i(-q_2+p_1-p_2)x'}\\
&+\delta^{(3)}(\boldsymbol{k}_1-\boldsymbol{k}_a)\delta^{(3)}(\boldsymbol{k}_c-\boldsymbol{k}_2)e^{i(q_1-k_1+k_2)x}e^{i(-q_2+p_1-p_2)x'}\Big)\Bigg)\\
=&(-i)^2\int d^4x\int d^4x'\frac{1}{(2\pi)^9}\frac{g_{wh}g_{hN}v_h}{\sqrt{2^4\omega_N(\boldsymbol{p}_d)\omega_N(\boldsymbol{p}_b)\omega_w(\boldsymbol{k}_a)\omega_w(\boldsymbol{k}_c)}}\\
&\times\overline{u}(\boldsymbol{p}_d,s_d)u(\boldsymbol{p}_b,s_b)2e^{i(k_c-k_a)x}e^{i(p_d-p_b)x'}\int\frac{d^3q}{2\omega_h(\boldsymbol{q})}\\
&\times\Big(\Theta(t-t')e^{-iq(x-x')}+\Theta(t'-t)e^{-iq(x'-x)}\Big)\\
=&\frac{(-i)^3}{\pi}\int d^4x\int d^4x'\frac{1}{(2\pi)^9}\frac{g_{wh}g_{hN}v_h}{\sqrt{2^4\omega_N(\boldsymbol{p}_d)\omega_N(\boldsymbol{p}_b)\omega_w(\boldsymbol{k}_a)\omega_w(\boldsymbol{k}_c)}}\\
&\times\overline{u}(\boldsymbol{p}_d,s_d)u(\boldsymbol{p}_b,s_b)e^{i(k_c-k_a)x}e^{i(p_d-p_b)x'}\int\frac{d^4q}{-q^2+m_h^2-i\epsilon}e^{-iq(x-x')}\\
=&\frac{(-i)^3}{2(2\pi)^2}\frac{g_{wh}g_{hN}v_h}{\sqrt{\omega_N(\boldsymbol{p}_d)\omega_N(\boldsymbol{p}_b)\omega_w(\boldsymbol{k}_a)\omega_w(\boldsymbol{k}_c)}}\overline{u}(\boldsymbol{p}_d,s_d)u(\boldsymbol{p}_b,s_b)\\
&\times\int\frac{d^4q}{-q^2+m_h^2-i\epsilon}\delta^{(4)}(p_d-p_b-q)\delta^{(4)}(q-k_a+k_c)\\
=&\frac{(-i)^3}{2(2\pi)^2}\frac{g_{wh}g_{hN}v_h\overline{u}(\boldsymbol{p}_d,s_d)u(\boldsymbol{p}_b,s_b)}{\sqrt{\omega_N(\boldsymbol{p}_d)\omega_N(\boldsymbol{p}_b)\omega_w(\boldsymbol{k}_a)\omega_w(\boldsymbol{k}_c)}}\frac{\delta^{(4)}(p_d-p_b+k_c-k_a)}{-(p_d-p_b)^2+m_h^2-i\epsilon}.
\end{aligned}
\tag{A.19}
$$

A.2 Scattering Cross Section

The scattering cross section (multiplied by the velocity) is

$$
\begin{aligned}
v\sigma_{wN} = &\frac{1}{2}\sum_{s_d,s_b}\int d^3p_d\int d^3k_c(2\pi)^2\frac{1}{2^2(2\pi)^4}\frac{(g_{wh}g_{hN}v_h)^2}{\omega_N(\boldsymbol{p}_d)\omega_N(\boldsymbol{p}_b)\omega_w(\boldsymbol{k}_a)\omega_w(\boldsymbol{k}_c)}\\
&\times\left|\frac{\overline{u}(\boldsymbol{p}_d,s_d)u(\boldsymbol{p}_b,s_b)}{-(p_d-p_b)^2+m_h^2-i\epsilon}\right|^2\delta^{(4)}(p_d-p_b+k_c-k_a),
\end{aligned}
\tag{A.20}
$$

where the velocity is

$$
v=\left|\frac{\boldsymbol{k}_a}{\omega_w(\boldsymbol{k}_a)}-\frac{\boldsymbol{p}_b}{\omega_N(\boldsymbol{p}_b)}\right|. \tag{A.21}
$$

First note that

$$\begin{aligned}
\sum_{s_d,s_b} |\overline{u}(\boldsymbol{p}_d,s_d)u(\boldsymbol{p}_b,s_b)|^2 &= \sum_{s_d,s_b} \overline{u}(\boldsymbol{p}_d,s_d)u(\boldsymbol{p}_b,s_b)u^\dagger(\boldsymbol{p}_b,s_b)\gamma^0 u(\boldsymbol{p}_d,s_d) \\
&= \sum_{s_d,s_b} \overline{u}(\boldsymbol{p}_d,s_d)u(\boldsymbol{p}_b,s_b)\overline{u}(\boldsymbol{p}_b,s_b)u(\boldsymbol{p}_d,s_d) \\
&= \sum_{s_d} \overline{u}(\boldsymbol{p}_d,s_d)(m_N I + \gamma_\mu p_b^\mu)u(\boldsymbol{p}_d,s_d) \\
&= 4m_N^2 + \sum_{s_d} u_j(\boldsymbol{p}_d,s_d)\overline{u}_i(\boldsymbol{p}_d,s_d)(\gamma_\mu)_{ij}p_b^\mu \\
&= 4m_N^2 + \sum_{s_d} (m_N I + \gamma_\nu p_d^\nu)_{ji}(\gamma_\mu)_{ij}p_b^\mu \\
&= 4m_N^2 + \mathrm{Tr}(m_N\gamma_\mu p_b^\mu + \gamma_\nu\gamma_\mu p_b^\mu p_d^\nu) \\
&= 4m_N^2 + 4\eta_{\mu\nu}p_b^\mu p_d^\nu \\
&= 4m_N^2 + 4p_b\cdot p_d
\end{aligned} \tag{A.22}$$

Now,

$$\begin{aligned}
v\sigma_{wN} = \frac{1}{2(2\pi)^2}\int d^3p_d \int d^3k_c \frac{(g_{wh}g_{hN}v_h)^2}{\omega_N(\boldsymbol{p}_d)\omega_N(\boldsymbol{p}_b)\omega_w(\boldsymbol{k}_a)\omega_w(\boldsymbol{k}_c)} \\
\times \frac{m_N^2 + p_b\cdot p_d}{(-(p_d-p_b)^2 + m_h^2)^2 + \epsilon^2}\delta^{(4)}(p_d - p_b + k_c - k_a).
\end{aligned} \tag{A.23}$$

The coordinates can be switched to the center-of-mass coordinates of the initial state so that

$$\boldsymbol{k}_a = -\boldsymbol{p}_b \equiv \boldsymbol{k}. \tag{A.24}$$

The integration variables can be switched using the substitution

$$\boldsymbol{P} = \boldsymbol{p}_d + \boldsymbol{k}_c \tag{A.25}$$

and

$$\boldsymbol{p} = \frac{m_w}{M}\boldsymbol{p}_d - \frac{m_N}{M}\boldsymbol{k}_c, \tag{A.26}$$

where $M = m_N + m_w$. The inverse of this is

$$\boldsymbol{p}_d = \frac{m_N}{M}\boldsymbol{P} + \boldsymbol{p}, \tag{A.27}$$

$$\boldsymbol{k}_c = \frac{m_w}{M}\boldsymbol{P} - \boldsymbol{p}. \tag{A.28}$$

Also note that

$$d^3P d^3p = d^3p_d d^3k_c \tag{A.29}$$

Therefore

$$\begin{aligned}
v\sigma_{wN} &= \frac{1}{2(2\pi)^2}\int d^3P d^3p \frac{(g_{wh}g_{hN}v_h)^2}{\omega_N(\boldsymbol{p}_d)\omega_w(\boldsymbol{k}_c)\omega_N(\boldsymbol{k})\omega_w(\boldsymbol{k})} \\
&\quad\times \frac{m_N^2 + p_b\cdot p_d}{(-(p_d-p_b)^2 + m_h^2)^2 + \epsilon^2}\delta^{(3)}(\boldsymbol{P}) \\
&\quad\times \delta^{(1)}\big(\omega_N(\boldsymbol{p}_d) + \omega_w(\boldsymbol{k}_c) - \omega_N(\boldsymbol{k}) - \omega_w(\boldsymbol{k})\big) \\
&= \frac{1}{2(2\pi)^2}\int d^3p \frac{(g_{wh}g_{hN}v_h)^2}{\omega_N(\boldsymbol{p})\omega_w(\boldsymbol{p})\omega_N(\boldsymbol{k})\omega_w(\boldsymbol{k})} \\
&\quad\times \frac{m_N^2 + \omega_N(\boldsymbol{p})\omega_N(\boldsymbol{k}) - \boldsymbol{p}\cdot\boldsymbol{k}}{\Big(-\big(\omega_N(\boldsymbol{p}) - \omega_N(\boldsymbol{k})\big)^2 + (\boldsymbol{p}-\boldsymbol{k})^2 + m_h^2\Big)^2 + \epsilon^2} \\
&\quad\times \delta^{(1)}\big(\omega_N(\boldsymbol{p}) + \omega_w(\boldsymbol{p}) - \omega_N(\boldsymbol{k}) - \omega_w(\boldsymbol{k})\big).
\end{aligned} \tag{A.30}$$

Making the substitutions

$$E'(\boldsymbol{p}) = \omega_N(\boldsymbol{p}) + \omega_w(\boldsymbol{p}) \tag{A.31}$$

and

$$E = \omega_N(\boldsymbol{k}) + \omega_w(\boldsymbol{k}) \tag{A.32}$$

along with the change of variables

$$\begin{aligned} d^3p &= d\Omega d|\boldsymbol{p}||\boldsymbol{p}|^2 \\ &= d\Omega dE' \frac{d|\boldsymbol{p}|}{dE'}|\boldsymbol{p}|^2 \\ &= d\Omega dE' \frac{|\boldsymbol{p}|}{E'}\omega_N(\boldsymbol{p})\omega_w(\boldsymbol{p}) \end{aligned} \tag{A.33}$$

yields

$$\begin{aligned} v\sigma_{wN} = \frac{1}{2(2\pi)^3}\frac{(g_{wh}g_{hN}v_h)^2}{\omega_N(\boldsymbol{k})\omega_w(\boldsymbol{k})}\int d\Omega dE' \frac{|\boldsymbol{p}|}{E'}\delta^{(1)}(E'-E) \\ \times \frac{m_N^2 + \omega_N(\boldsymbol{p})\omega_N(\boldsymbol{k}) - \boldsymbol{p}\cdot\boldsymbol{k}}{\Big(-\big(\omega_N(\boldsymbol{p}) - \omega_N(\boldsymbol{k})\big)^2 + (\boldsymbol{p}-\boldsymbol{k})^2 + m_h^2\Big)^2 + \epsilon^2}, \end{aligned} \tag{A.34}$$

keeping in mind that $|\boldsymbol{p}| = |\boldsymbol{p}|(E')$. Because $|\boldsymbol{p}|(E) = |\boldsymbol{k}|$, it must be that

$$\begin{aligned} v\sigma_{wN} &= \frac{1}{2(2\pi)^2}\frac{(g_{wh}g_{hN}v_h)^2}{\omega_N(\boldsymbol{k})\omega_w(\boldsymbol{k})}\int d\Omega \frac{|\boldsymbol{k}|}{E}\frac{2m_N^2}{m_h^4+\epsilon^2} \\ &= \frac{1}{\pi}\frac{(g_{wh}g_{hN}v_h)^2}{\omega_N(\boldsymbol{k})\omega_w(\boldsymbol{k})}\frac{|\boldsymbol{k}|}{E}\frac{m_N^2}{m_h^4+\epsilon^2}. \end{aligned} \tag{A.35}$$

Using the velocity,

$$v = |\boldsymbol{k}|\left|\frac{\omega_N(\boldsymbol{k}) - \omega_w(\boldsymbol{k})}{\omega_w(\boldsymbol{k})\omega_N(\boldsymbol{k})}\right|, \tag{A.36}$$

the cross section can be expressed as

$$\begin{aligned} \sigma_{wN} &= \frac{(g_{wh}g_{hN}v_h)^2 m_N^2}{\pi\big|\omega_N(\boldsymbol{k}) - \omega_w(\boldsymbol{k})\big|\big(\omega_N(\boldsymbol{k}) - \omega_w(\boldsymbol{k})\big)\big(m_h^4 + e^2\big)} \\ &= \frac{(g_{wh}g_{hN}v_h)^2 m_N^2}{\pi|m_N^2 - m_w^2|(m_h^4+\epsilon^2)}. \end{aligned} \tag{A.37}$$

However, taking $\epsilon \to 0$ and since $m_N \ll m_w$, it is safe to say that

$$\sigma_{wN} = \frac{1}{\pi}\left(\frac{g_{wh}g_{hN}v_h m_N}{m_w m_h^2}\right)^2. \tag{A.38}$$

Bibliography

[1] F. Zwicky, Helv. Phys. Acta **6**, 110 (1933)

[2] T.H.R. Skymre, Proc. Roy. Soc. (London) A **260**, 127 (1961)

[3] T.H.R. Skyrme, Nucl. Phys. **31**, 556 (1962)

[4] M. Tanabashi *et al.* (Particle Group Data), Phys. Rev. D **98**, 030001 (2018)

[5] W. Greiner and B. Müller, *Quantum Mechanics: Symmetries, Second Edition* (Springer-Verlag, New York, 1994) pp.81-83

[6] M. Peskin and D. Schroeder, *An Introduction to Quantum Field Theory* (CRC Press, Boca Raton, 1995)

[7] D. McMahon, *Quantum Field Theory Demystified* (The McGraw Hill Company, Inc., New York, 2008)

[8] R. Dick, *Advanced Quantum Mechanics: Materials and Photons, Second Edition* (Springer International Publishing, Switzerland, 2016)

[9] N. Manton and P. Sutcliffe, *Topological Solitons* (Cambridge University Press, Cambridge, 2004) pp.45-74

[10] A. Vilenkin and E.P.S. Shellard, *Cosmic Strings and other Topological Defects* (Cambridge University Press, Cambridge, 1994)

[11] R.K. Bhaduri, *Models of the Nucleon: From Quarks to Soliton* (Addison-Wesley Publishing Co., Redwood City, 1988)

[12] V.G. Makhankov, Y.P. Rybakov, and V.I. Sanyuk, *The Skyrme Model: Fundamentals, Methods, Applications* (Spinger-Verlag, Berlin, 1993)

[13] J.F. Donoghue, E. Golowich, and B.R. Holstein, *Dynamics of the Standard Model* (Cambridge University Press, Cambridge, 1992) pp.292-312

[14] J.I. Kapusta and C. Gale, *Finite-Temperature Field Theory Principles and Applications* (Cambridge University Press, Cambridge, 2006) pp.289-316

[15] S. Coleman, Phys. Rev. D **15**, 2929 (1977)

[16] C.G. Callan, Jr. and S. Coleman, Phys. Rev. D **16**, 1762 (1977)

[17] A.D. Linde, Nucl. Phys. B **216**, 421 (1983)

[18] T.W.B. Kibble, J. Phys. A **9**, 1387 (1976)

[19] T.W.B. Kibble, Phys. Rep. **67**, 183 (1980)

[20] W.H. Zurek, Nature **317**, 505 (1985)

[21] P. Laguna and W.H. Zurek, Phys. Rev. D **58**, 085021 (1998)

[22] A. del Campo and W.H. Zurek, Int. J. Mod. Phys. A **29**, 1430018 (2014)

[23] H. Murayama and J. Shu, Phys. Lett. B **686**, 162 (2010)

[24] S. Weinberg, *Cosmology* (Oxford University Press Inc., Oxford, 2008)

[25] B. Ryden, *Introduction to Cosmology: Second Edition* (Cambridge University Press, Cambridge, 2019)

[26] E.W. Kolb and M.S. Turner, *The Early Universe* (Addison-Wesley Publishing Co., Reading, Massachusetts, 1990)

[27] Planck Collaboration (Y. Akrami *et al.*), *Planck 2018 results. I. Overview and the cosmological legacy of Planck*. arXiv:1807.06205 [astro-ph.CO]

[28] D. Clowe *et al.* Astrophys. J. **648**, L109 (2006)

[29] P. Gondolo and G. Gelmini, Nucl. Phys. B **360**, 145 (1991)

[30] G. Bertone (Eds.), *Particle Dark Matter: Observations, Models and Searches* (Cambridge University Press, Cambridge, 2010)

[31] M.W. Goodman and E. Witten, Phys. Rev. D **31**, 3059 (1985)

[32] J.D. Lewin and P.F. Smith, Astropart. Phys. **6**, 87 (1996)

[33] B.A. Campbell, J. Ellis, and K.A. Olive, JHEP **1203**, 026 (2012)

[34] R. Dick, Eur. Phys. J. C **77**, 841 (2017)

[35] J. Bramante, B. Broerman, R.F. Lang, and N. Raj, JHEP **98**, 083516 (2018)

[36] K. Griest and M. Kamionkowski, Phys. Rev. Lett. **64**, 615 (1990).

[37] M. Berezowski and R. Dick, Euro. Phys. J. C **79**, 763 (2019)

[38] H.M. Sommermann, R. Seki, S. Larson, and S.E. Koonin, Phys. Rev. D **45**, 4303 (1992)

[39] B. Shao, N.R. Walet, and R.D. Amado, Phys. Lett. B **303**, 1 (1993)

[40] E. Klempt, C. Batty, and J.-M. Richard, Phys. Rep. **413**, 197 (2005)

[41] F. Karsch, E. Laermann, and A. Peikert, Nucl. Phys. B **605**, 579 (2001)

[42] A. Ali Khan *et al.* (CP-PACS Collaboration), Phys. Rev. D **63**, 034502 (2001)

[43] S.T. Thornton and A. Rex, *Modern Physics for Scientists and Engineers, Fourth Edition* (Cengage Learning, Boston, 2013) pg.A-23

[44] M.A. Shifman, A.I. Vainshtein, and V.I. Zakharov, Phys. Lett. B **78**, 443 (1978)

[45] M. Hoferichter, P. Klos, J. Menéndez, and A. Schwenk, Phys. Rev. Lett. **119**, 181803 (2017)

[46] E. Aprile *et al.* (XENON Collaboration), Phys. Rev. Lett. **121**, 111302 (2018)

[47] XENON Collaboration (E. Aprile *et al.*), JCAP **1604**, 027 (2016)

[48] LUX-ZEPLIN (LZ) Collaboration (D.S. Akerib *et al.*), *Projected WIMP sensitivity of the LUX-ZEPLIN (LZ) dark matter experiment*. arXiv:1802.06039 [astro-ph.IM]

[49] PandaX Collaboration (Hongguang Zhang *et al.*), Sci. China Phys. Mech. Astron. **62**, 31011 (2019)

[50] DARWIN Collaboration (J. Aalbers *et al.*), JCAP **1611**, 017 (2016)